UNIVERSITÀ DEGLI STUDI DI MILANO
PhD School in Biological and Molecular Sciences
XXV Cycle

Phospho-regulation of ACA8, a plasma membrane Ca^{2+}-ATPase of *Arabidopsis thaliana*

Claudia Adriana Marrano
PhD Thesis

Scientific tutor: Professor M. I. De Michelis

Academic year: 2011-2012

SSD: BIO/04

Thesis performed at Department of Life Sciences, University of Milan

Contents

Contents

PART I

Abstract pg. 5

Introduction pg. 7
1. Cytosolic Ca^{2+} pg. 9
2. Plant Ca^{2+}-ATPases pg.13
3. ACA8 pg.18
4. Decoding Ca^{2+} signal pg.22
5. Aim of the project pg.28

Main Results pg.31
1. Analysis of the effect of phosphorylation on ACA8 activity pg.33
2. *In vitro* phosphorylation of the ACA8 N-terminus by CDPKs pg.35
3. ACA8 is a target of CBL-Interacting Protein Kinases pg.36

Discussion pg.39

References pg.47

PART II

Published paper pg.59

Phosphorylation of serine residues in the N-terminus modulates the activity of ACA8, a plasma membrane Ca^{2+}-ATPase of *Arabidopsis thaliana*.
Giacometti* S, Marrano* CA, Bonza MC, Luoni L, Limonta M and De Michelis MI.
Journal of Experimental Botany; (2012) **63**: 1215–1224.

Work in progress pg.71

The *Arabidopsis thaliana* Ca^{2+} pump ACA8 is a target of CBL Interacting Protein Kinases.
Marrano CA, Giacometti S, Bonza MC and De Michelis MI.

In collaboration with professor group of J Kudla, Institut für Biologie und Biotechnologie der Pflanzen, Universität Münster, Germany.

PART I

Abstract

ACA8 is a plasma membrane-localized isoform of calmodulin (CaM)-regulated Ca^{2+}-ATPase of *Arabidopsis thaliana*. Phospho-proteomic studies identified several phosphopeptides corresponding to portions of its regulatory N-terminus. Each of the Ser found to be phosphorylated in those studies (S19, S22, S27, S29, S57, and S99) has been mutated to Asp, to mimic phosphorylation of the ACA8 N-terminus, and to Ala to prevent phosphorylation. Mutants have been expressed in *Saccharomyces cerevisiae* and characterized: as shown by the low activation by CaM, mutants S19D, S57D, S22D and S27D are deregulated. Moreover, the low response to CaM of ACA8 mutants S22A, S27A, and S29A points the relevance of these serine residues *per se* in determining the amplitude of the response of ACA8 to CaM. To analyse the effect of S to D mutation on the kinetic of CaM binding, His-tagged N-termini of wild-type and mutant ACA8 (6His-^{1}M-I^{116}) were expressed in *Escherichia coli*, affinity-purified and used in surface plasmon resonance experiments. All the analysed mutations affect the kinetics of interaction with CaM to some extent: in most cases, the altered kinetics result in marginal changes in affinity, with the exception of mutants S57D (KD 10-fold higher than wild-type ACA8) and S99D (KD about half that of wild-type ACA8). Since S19 is in a consensus motive for calcium-dependent protein kinases (CDPKs) the ACA8 N-terminus has been subjected to *in vitro* phosphorylation assays with two isoforms of *A. thaliana* CDPKs: CDPK1, that phosphorylates ACA2 (an endoplasmic reticulum localised isoform of *A. thaliana* ACA) and CDPK16, a plasma membrane localised isoform of CDPK. Results show that both kinases are able to phosphorylate ACA8 N-terminus, but CDPK16 with higher extent. Phosphorylation of mutant 6His-^{1}M-I^{116} peptides mapped CDPK16 phosphorylation site at S19 and at S22. Furthermore, we identified by two-hybrid screening two isoforms of CBL-interacting protein kinases (CIPKs) as putative interactors of ACA8 N-terminus region: CIPK9 and CIPK14. BiFC analysis in *Nicotiana benthamiana* confirmed the two-hybrid results, showing that interaction between ACA8 full length and CIPK9 or CIPK14 occurs *in planta* at the plasma membrane. Moreover, phosphorylation assay demonstrate that both kinases phosphorylate ACA8 N-terminus *in vitro*. Implications of these results are discussed.

Introduction

1. Ca^{2+} in plants

A change in the cytosolic free Ca^{2+} concentration ($[Ca^{2+}]_c$) is known to be a crucial step in the signalling networks by which plant cells respond to a wide range of stimuli: biotic stimuli as those induced by hormones, such as abscisic acid (ABA) and gibberellins, nodulation factors (NodF), bacterial and fungal elicitors; abiotic stimuli induced by red, blue and UV/B light (all acting on different receptors and triggering different physiological responses), salt and drought signals, oxidative stress, cold and hot stress [Sanders et al., 2002; McAinsh and Pittman, 2009].

The low solubility of $Ca_3(PO_4)_2$ is one of the peculiar characteristics that elect Ca^{2+} as one of the most important second messengers in plants. The cellular metabolism indeed requires orthophosphate (Pi) and phosphorylated organic compounds for all the cytosolic reactions associated to transduction of free energy. In order to avoid the precipitation of Pi in the cytoplasm, the cell must maintain a very low $[Ca^{2+}]$, around 200 nM, despite a 0.1-0.5 mM external Ca^{2+} concentration and a membrane potential less than -150 mV [Sanders et al., 2002; Spalding and Harper, 2011]. Thus, a 10-20 fold increase in cytosolic Ca^{2+} concentration $[Ca^{2+}]$c can be achieved more rapidly than for other types of ions and solutes that are maintained in a millimolar range of concentration [Sanders et al., 1999]. Moreover, the flexibility of Ca^{2+} in exhibiting different coordination numbers (it can coordinate from 6 to 8 non-charged oxygen atoms) and complex geometries allowed the evolution in proteins of specific Ca^{2+} binding sites [Kaufman Katz et al, 1996]. This characteristic, along evolution, favoured transduction mechanisms based on Ca^{2+} signalling [Sanders et al., 1999]. The tendency of Ca^{2+} to associate with the cytosolic proteins has also the effect of reducing the real diffusion coefficient of Ca^{2+} in the cytosol. $[Ca^{2+}]$c, indeed, is maintained around 200 nM but the real content of Ca^{2+} in the cytosol is higher depending on the buffering operated by a wide number of proteins that bind Ca^{2+} with a high affinity. It must be taken into consideration the presence of intracellular organelles that accumulate Ca^{2+} contributing to Ca^{2+} sequestration. The endoplasmic reticulum (ER), mitochondria and chloroplasts are all capable to sequester Ca^{2+}, but the vacuole, by virtue of its size and capacity for Ca^{2+} accumulation, is the most important sink for this ion in plant cells. Another important factor in $[Ca^{2+}]_c$ homeostasis is the extrusion of Ca^{2+} outside the cell, since both buffering mediated by Ca^{2+}-binding and its sequestration in intracellular compartments are mechanisms with a finite capacity [Sanders et al., 1999].

1.1 Cytosolic Ca^{2+}

A considerable electrochemical potential for Ca^{2+} ($\Delta\mu_{Ca2+}$) exists across all membranes in the cell: at the plasma membrane (PM), for example, the ratio (outside/inside) is typically of the order of 10^{-4} and the presence of a cytosolic negative electrical potential difference around -150 mV yields a $\Delta\mu_{Ca2+}$ of approximately -50 kj/mole [Sanders et al., 1999; Spalding and Harper, 2011]. Although the potential difference across the membranes of organelles, such as the vacuole and ER, is likely to be less negative than that across the PM, large driving forces nevertheless prevail and require energized removal of Ca^{2+} from the cytosol. Thanks to the negative $\Delta\mu_{Ca2+}$ a substantial increase of the cytoplasmic Ca^{2+} concentration can be achieved very rapidly and without any energy cost through Ca^{2+}-channels localised at the PM or at the membranes surrounding the intracellular stores. To return in the resting condition the ion must be actively transported outside the cytosol by Ca^{2+} pumps that use the hydrolysis of ATP (Ca^{2+}-ATPases) and Ca^{2+}/H^{+} antiporters that use the proton motive force [Sanders et al., 1999; White and Broadely, 2003; Spalding and Harper, 2011].

As mentioned above, Ca^{2+} is involved in the signalling of a vast number of stimuli. A fundamental question is how the increasing of $[Ca^{2+}]_c$ can specifically codify for each of the many different physiological outcomes in which Ca^{2+} signalling is involved. In 1995 MacAinsh and colleagues correlated the dynamic of cytosolic Ca^{2+} oscillations in guard cells with the strength of the external Ca^{2+} stimulus that turned into a steady-state stomatal aperture [MacAinsh et al., 1995]. More recently Kosuta and co-workers (2008) recorded in *Medicago truncatula* Ca^{2+} oscillations that were different, in period and amplitude, if they were triggered by Nod factors or mycorrhizal fungi. These evidences indicate that the specificity of a Ca^{2+} signal is correlated to characteristic oscillations in $[Ca^{2+}]_c$. Thus, the stimulus induced by specific signals is propagated into the cytosol as waves of Ca^{2+} that can differ for duration, amplitude, frequency and spatial distribution [Webb et al., 1996]. The shape and frequency of the Ca^{2+} waves determine the Ca^{2+}-signature of a specific stimulus. As a cytosolic Ca^{2+} transient is generated when there is a temporary exceeding of Ca^{2+} influx respect Ca^{2+} efflux, a fine regulation of both these processes has to be involved in the shaping of Ca^{2+} waves to produce a specific Ca^{2+}-signature [MacAinsh et al., 2009].

A specific expression in different plant tissues and stages of plant development of all types of Ca^{2+}-channels, Ca^{2+}/H^{+} antiporters and Ca^{2+} pumps is partially involved in determining a specificity of Ca^{2+}-signalling [Kudla et al., 2010]. Anyway no dramatic phenotypes, such as lethal knock out, have been reported, for example, for Ca^{2+}-ATPases of higher plants, even if they were reported for animals. Probably the redundancy of these transporters in plants circumvents the display of a strong phenotype resulting from the knock out of a single gene [Spalding and Harper, 2011]. The other way that the plant cell uses to ensure a signal-specific physiological outcome, is the regulation of the activity of all the transporters involved in the generation of cytosolic Ca^{2+} oscillations [Kudla et al., 2010].

The influx of Ca^{2+} inside the cytosol

Electrophysiological studies revealed the presence at the PM of depolarization-activated Ca^{2+} permeable channels (DACCs), involved in the short transient influx of Ca^{2+} in response to several stimuli, like chilling and microbe interaction [Thion et al., 1998]. Studies conducted by Gelli et al. (1997) and Gelli and Blumwald (1997), on suspension cultured tomato cells, report the presence of hyperpolarization-activated Ca^{2+} permeable channels (HACC) on the PM. HACCs result activated by blue light and ABA, a plant hormone that determines in guards cells an increase of $[Ca^{2+}]_c$ that triggers stomatal closure [Sanders et al., 1999]. Even though a lot of electrophysiological data indicate the presence of voltage-gated channels on the PM of plant cells, the protein involved in voltage-mediated Ca^{2+}-influx has not been identified jet [Kudla et al., 2010].

Besides voltage-gated Ca^{2+}-channels there are two classes of non-selective ligand-gated cation channels that are important for cellular homeostasis of cations and can mediate fluxes of Ca^{2+} ions: cyclic nucleotide-gated channels (CNGCs), activated by binding of cAMP and cGMP, and glutamate receptors (GLRs), activated by several amino acids, like Glu and Gly. CNGCs have been shown to be involved in the response to pathogens, salt stress adaptation and tip growth of pollen. It is assumed that GLRs are involved in plant Ca^{2+} nutrition and in the response of the plant to cold stress. Moreover it has been shown, both in rice and *Arabidopsis*, that GLRs are involved in different plant developmental aspects, such as photomorphogenesis and root elongation [Kudla et al., 2010; Spalding and Harper, 2011].

The presence of channels releasing Ca^{2+} has been reported also at the endomembranes. It has been shown that both voltage-gated channels and ligand-gated channels, activated by $InsP_3$ (Inositol TrisPhosphate) and cADPR (cyclic Adenosin Di-Phosphate Ribose), are located on the tonoplast. The voltage-gated channels were identified as slow vacuolar (SV) type Ca^{2+}-channels. SV channels are activated by membrane depolarization and regulated by Ca^{2+}: an increase of $[Ca^{2+}]_c$ activates the channels while an increasing in the vacuolar Ca^{2+} concentration inactivates the channels. Studies on knock out and gain of function mutants of the *Arabidopsis* TPC1 isoform demonstrate that the SV channels are involved in the pathogens-resistance signalling pathway [McAinsh and Pittman, 2009; Kudla et al., 2010; Spalding and Harper, 2011]. Voltage-dependent Ca^{2+}-channels have been identified also at the ER, activated by NAADP (Nicotinic Acid Adenine Dinucleotide Phosphate), cADPR e $InsP_3$ [Sanders et al., 2002; McAinsh and Pittman, 2009].

The efflux of Ca^{2+} outside the cytosol

The transport systems that energize efflux from the cytosol provide critical *housekeeping* functions: the restoring of $[Ca^{2+}]_c$ to resting levels, thereby terminating Ca^{2+} signals; the sequestering of Ca^{2+} into compartments such as the ER and vacuole to be used as sources for regulated Ca^{2+} release and to support specific biochemical functions of the organelles [Sanders et al., 1999; Pittman et al., 2011].

It has been shown that the efflux of Ca^{2+} is mediated by Ca^{2+}-ATPases, that use as main driving force the energy coming from the hydrolysis of ATP, and by H^+/Ca^{2+} antiporters that utilize the proton motive force [Sanders et al., 2002; Spalding and Harper, 2011; Geisler and Venema (Eds.), 2011]. Since Ca^{2+}-ATPases have a high affinity for Ca^{2+} (K_m = 1-10 μM) but a low capacity, while H^+/Ca^{2+} antiporters have a lower affinity for Ca^{2+} (K_m = 10-15 μM) but a higher capacity, it has been proposed that antiporters have a role in reducing Ca^{2+} concentration back to a few micromolar after its influx, while Ca^{2+}-ATPases are responsible to maintain the homeostasis of $[Ca^{2+}]_c$ in the resting conditions [Hirschi et al., 2000].

Plant Ca^{2+} ATPases have been localised both at the PM and at the membrane of the intracellular stores [Bonza and De Michelis, 2011]. The H^+/Ca^{2+} antiporters, also named CAX (CAtion/H+ eXchangers), are almost exclusively localised on the tonoplast. Ca^{2+}/H^+ antiport activity in plants was measured biochemically, first in the tonoplast [Schumaker and Sze, 1986], and later cloned as CAXs. Ca^{2+}/H^+ antiport activity in plants was measured also in the PM [Kasai and Muto, 1990] and chloroplast thylakoid membrane [Ettinger et al., 1999], however, since the genes encoding for non-tonoplast Ca^{2+}/H^+ antiporters have not been identified yet, it is possible that Ca^{2+}/H^+ antiport activity in PM and thylakoid membranes is conferred by cation antiporters that are distinct from CAXs [Shigaki and Hirschi, 2006]. The sequestration of Ca^{2+} into plant vacuoles mediated by CAXs is likely to be the most predominant pathway for vacuolar Ca^{2+} loading [Geisler and Venema (Eds.), 2011].

2. Plant Ca^{2+}-ATPases

Ca^{2+}-ATPases belong to the super-family of the P-type ATPases, a class of proteins that uses the hydrolysis of ATP to pump ions across membranes. During their catalytic cycle P-type ATPases switch between two conformational states with different affinity for the transported ion, called E1 and E2. In the E1 state the ion binding sites have a high affinity for the ion and are accessible from the cytoplasmic side, while in the E2 state the ion binding sites have a low affinity and are accessible from the lumen (in the case of the P-type ATPases of the endomembrane) or the extracellular side (in the case of the P-type ATPases of the PM) [Toyoshima and Inesi, 2004]. All the members of P-type ATPases are characterized by the formation of a phosphorylated intermediate during their catalytic cycle: the residue involved in the phosphorylation is an Asp localized in the consensus sequence DKTG. The conformational rearrangements induced by phosphorylation drive the translocation of the ion from one side of the membrane to the other [Axelsen and Palmgren, 1998; Palmgren and Nissen, 2011].

The general structure of P-type ATPases comprises a transmembrane portion consisting of 6-12 transmembrane domains (TM) and a cytosolic portion consisting of the C-terminal and the N-terminal regions, a small cytoplasmic loop (between TM2 and TM3) and a large cytoplasmic loop (between TM4 and TM5). These two loops, and the portion of the N-terminal region close to the first TM, define the catalytic head of the enzyme [Kuhlbrandt, 2004; Palmgren and Nissen, 2011].

The phylogenetic analysis of P-type ATPases defined five clades (indicated with numbers from 1 to 5) that differ for structural characteristics, transported substrate and organisms in which they are present. These five clades can be than sub-divided in two or more sub-groups (indicated by capital letters A, B, C, etc.). Ca^{2+} pumps belong to two sub-groups of the P-type ATPases: the sub-group 2A and 2B [Axelsen and Palmgren, 1998].

Plant type 2A Ca^{2+}-ATPases are named ECAs (ER-type Calcium ATPases), and share with their animal hortologue, the sarco/endoplasmic reticulum localised Ca^{2+}-ATPase (SERCA), a 50-56% identity; plant type 2B Ca^{2+}-ATPases are named ACAs (Autoinhibited Calcium ATPases) and share with their animal hortologue, the PM localised Ca^{2+}-ATPase (PMCA), around 50% identity [Geisler et al., 2000a; Sze et al., 2000].

It is known that the animal Ca^{2+}-ATPases catalyse the transport of Ca^{2+} in exchange with H^+: the stoichiometry of the exchange has not been precisely determined yet, but it is supposed that SERCA works with a stoichiometry of $2Ca^{2+}/2\text{-}3H^+$ while PMCA with a stoichiometry of $1Ca^{2+}/1H^+$. Then both families of Ca^{2+}-ATPases would be electrogenic pumps [Carafoli et al., 1991]. Since the Ca^{2+} binding site(s), two in type 2A Ca^{2+}-ATPases and only one in type 2B Ca^{2+}-ATPases, are conserved among the Ca^{2+}-ATPases [Kuhldbrandt et al., 2004] it is reasonable to assume that the mechanism of transport is the same between plants and animal. Anyway, in plant the mechanism of transport has been demonstrated only for PM ACAs: the transport of Ca^{2+} has been shown to occur in exchange with H^+ for both a PM Ca^{2+}-ATPase of *Raphanus sativus* seeds and a PM Ca^{2+}-ATPase of *A. thaliana*, ACA8. Thus, PM Ca^{2+}-ATPases of plants use to extrude Ca^{2+} from the cytosol both the energy of the ATP hydrolysis and the energy that comes from the proton gradient generated across the PM by the H^+-ATPase [Rasi-Caldogno et al., 1986; Luoni et al., 2000].

Besides the stoichiometry of transport, a characteristic that distinguish ECAs and ACAs is their sensitivity to specific inhibitors: ECAs, in contrast to ACAs, are inhibited by cyclopiazonic acid as reported for their hortologue SERCA [Brini and Carafoli, 2009]; on the other hand ACAs shows a group-specific high sensitivity to fluorescein derivatives such as erythrosin B or eosin Y [De Michelis et al., 1993]. Moreover, ACAs are the only P-type ATPases able to use ITP or GTP as nucleoside-triphosphate substrate in alternative to ATP: a very useful characteristic used for characterization of the PM isoforms in native membrane vesicles in which the ATPase activity of the H^+-ATPase is much more abundant [Williams et al., 1990; Carnelli et al., 1992; Hwang et al., 1997].

At the structural level the main difference that characterizes ACAs *versus* ECAs is the presence of an extended N-terminal region with a regulatory function, which in their hortologue PMCA is in the C-terminal portion of the enzyme [Di Leva et al., 2008; Bonza and De Michelis, 2011]. It has been shown for several ACA isoforms that the N-terminus of the enzyme contains an autoinhibitory domain as well as a partially overlapped CaM binding domain (CaM-BD): the interaction of the autoinhibitory domain with the catalytic core of the protein keeps the pump almost inactive at low Ca^{2+} concentrations; after a stimulus that induces an increase in cytosolic Ca^{2+} concentration the binding of Ca^{2+}-CaM to the CaM-BD disrupts the autoinhibitory interaction and activates the enzyme [Bonza and De Michelis, 2011].

In *Arabidopsis thaliana* four ECAs genes and ten ACAs genes have been identified (Baxter et al., 2003). Considering sequence alignments and intron number and/or positions, Baxter and colleagues suggested a division in clusters both for ECAs and ACAs genes: ECAs can be divided into two clusters and ACAs can be divided into four clusters. Some evidences indicate, with few exceptions, that cluster-division could correlate with subcellular localization. In *Arabidopsis thaliana* ECA1 belonging to ECAs cluster 1, has been localised in the ER, while ECA3, belonging to ECAs cluster 2 was localised associated with Golgi and post Golgi vesicles [Liang et al., 1997; Li et al., 2008; Mills et al., 2008]. In *Arabidopsis thaliana* ACAs cluster 1 comprehends ACA1 and ACA2, both localised at the ER [Hong et al., 1999; Dunkley et al., 2006] and ACA7, recently localised on the PM of pollen grains [Lucca and Léon, 2012]. Cluster 2 comprehends *A. thaliana* isoforms ACA4 and ACA11 and *Brassica oleracea* isoform BCA1, which are all localized at the tonoplast [Malmström et al., 1997, 2000; Geisler et al., 2000b; Lee et al., 2007]. On the other hand all the members of cluster 4, *Arabidopsis thaliana* isoforms ACA8, ACA9 and ACA10 have been shown to localise at the PM [Bonza et al., 2000; Schiøtt et al., 2004; George et al., 2008]. Little is known so far about the subcellular localisation of the members of cluster 3, which comprehends ACA12 and ACA13: based on the ability of ACA12 to rescue a pollen defect in an ACA9 knockout mutant, a PM localization has been proposed for this isoform [Boursiac and Harper, 2007].

Structure

All is known about the structure of Ca^{2+}-ATPases comes from the resolution of the structure of rabbit skeletal muscle SERCA1a in several different conformational states [Toyoshima and Inesi, 2004]. This analysis has been a turning point in the study of Ca^{2+}-ATPases, leading to a detailed definition of the catalytic site in the cytoplasmic head of the protein and of the ion binding site(s) in the transmembrane region [Kuhlbrandt, 2004; Toyoshima and Inesi, 2004].

Fig.1 shows the transmembrane portion consisting of 10 α-helixes, the cytosolic C-terminal and N-terminal cytosolic regions and the catalytic head of the enzyme, also cytosolic, in which three distinct domains are visible: the A domain (for Actuator), the N domain (for Nucleotide binding) and the P domain (for Phosphorylation).

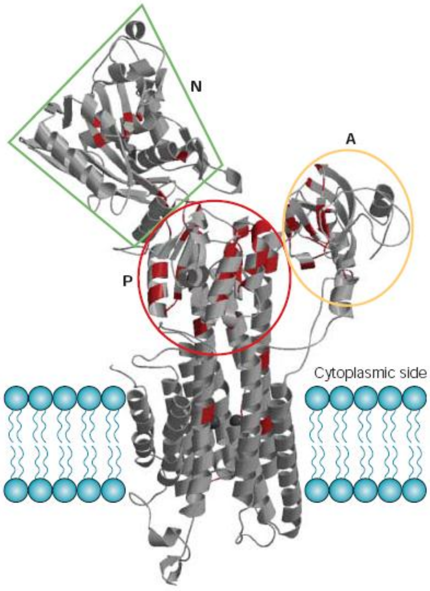

Fig.1 *Tridimensional representation of the structure of SERCA1a from rabbit skeletal muscle.*
From Kuhlbrandt, 2004.

The A domain is the smallest of the three cytoplasmic domains: it is formed by about 50 amino acids at the level of the N-terminal portion structured in two small α-helixes, and about 110 residues localised between TM2 and TM3 helixes, forming a distorted jelly roll motive. It acts as principal actor of the mechanism that regulates the binding and release of Ca^{2+}. The N domain, a long insertion between two portions of the large cytoplasmic loop forming the P domain, contains the binding site for the adenosynic nucleotide, whose γ-phosphate reacts with the Asp that is subjected to phosphorylation in the P domain. The three cytoplasmic domains are wide open in the conformational state $E1+2Ca^{2+}$, but they get close to form a compact head in the E2+TG state (TG, thapsigargin an inhibitor that block SERCA in the conformation in which Ca^{2+} is not bound). The A domain contains the consensus sequence TGES, highly conserved between all the members of P-type ATPases. This sequence generates a loop that in the E2 and E2P state gets close to the phosphorylation site of the enzyme covering the aspartyl-phosphate from the water.

The sites of ion binding in SERCA are defined by the polar and charged lateral chains of six conserved amino acids localised in the TM4, TM5, TM6 and TM8 able to coordinate two Ca^{2+} ions. In type 2B Ca^{2+}-ATPases, that translocate only one Ca^{2+} every catalytic cycle only three of these residues are conserved [Toyoshima and Inesi, 2004].

Physiological role

Different experimental evidences indicate an involvement of Ca^{2+}-ATPases in many important physiological processes: development, mineral nutrition, response to hormones and to stress.

Studies on knock out mutants demonstrate the involvement of *A. thaliana* ACA9 in growth of pollen tubes [Schiøtt et al., 2004]. Analysis of T-DNA insertional mutants have shown that *Arabidopsis thaliana* ECA1 and ECA3 genes have a role in Mn^{2+} nutrition and in tolerance to Mn^{2+} stress [Wu et al., 2002; Li et al., 2008]. Studies on knock out and over-expressing mutants suggested a role in gibberellin signalling in aleurone for *Oriza sativa* ECA1 [Chen *et al.,* 1997]. Moreover, some evidences indicated an involvement of ACAs in ABA signalling pathway. It was shown that in *Egeria densa* leaves ABA rapidly induces an increase in the activity of a PM localized ACA [Beffagna et al., 2000]. A role of PM localized ACAs in ABA signalling is suggested also by the ABA-induced stimulation of expression of ACA8 and ACA9 in *A. thaliana* seedlings, that correlate with an increase in the protein amount in the PM for the isoform ACA8 [Cerana et al., 2006]. It has been shown that in *Arabidopsis thaliana* over-expression of ACA4 and ACA2 improves salt tolerance in yeast, suggesting a role in salt tolerance also in plants [Geisler et al., 2000b; Anil et al., 2008]. Recently, studies on the knock out of an ACA isoform localized at small vacuoles of the moss *Physcomitrella patens* indicated an involvement of ACAs in the moss response to salt stress [Qudeimat et al., 2008]. PM localised ACAs have been found to be involved in the response to fungal elicitors oligogalacturonides (OGs). Indeed the Ca^{2+} efflux that follows the rapid spike of $[Ca^{2+}]c$ induced by OGs, is highly sensitive to inhibition by the fluorescein derivative eosin Y and correlates to an increase in formation of the active Ca-CaM-Ca^{2+}-ATPase complex; this is essential to turn the oxidative burst off [Romani et al., 2004]. In *A. thaliana* ACA12 and ACA13, that have very low or undetectable expression level in basal conditions, show a dramatic induction of their transcription upon exposure to pathogens [Boursiac and Harper, 2007].

3. ACA8

ACA8 is a PM localised CaM-activated Ca^{2+} pump of *A. thaliana* [Bonza et al., 2000]. Analysis of ACA8 expression patterns indicates that ACA8 specific transcript is present with a low level in almost all plant cells type. If compared with the expression level of ACA10, the other ubiquitous ACA of the PM, expression of ACA8 results favoured (from 2 to 6 fold) mainly in roots and mature pollen [EFp Browsers data: http://bar.utoronto.ca/efp/cgi-bin/efpWeb.cgi].

Only few evidences, to date, indicate the physiological role of ACA8 in Ca^{2+} signalling. The work of Schiøtt and Palmgren (2005) shows that ACA8 expression level is increased by cold stress, that was already known to determine large transient changes in cytosolic Ca^{2+} concentration: this up-regulation may lead to an increase of the capacity to extrude Ca^{2+} to the apoplast as that observed upon cold acclimation in winter rye leaves [Bonza and De Michelis, 2011]. ABA application to *A. thaliana* seedlings has been shown to stimulate ACA8 expression and determine an increase in ACA8 amount in the PM. However, the slow accumulation of At-ACA8 protein at the PM, after 8 hours, suggests that this event may be not involved in the short term response to ABA but rather in a long term response to the hormone under stress condition [Cerana et al., 2006].

ACA8 gene was the first gene isolated codifying a PM Ca^{2+}-ATPase of *A. thaliana* [Bonza et al., 2000]. ACA8 protein, purified by CaM affinity from cultured cells of *A. thaliana*, was subjected to extensive proteolysis with trypsin: three of the fragments obtained were sequenced and used to identify the genomic sequence in the *Arabidopsis* database. This procedure permitted to design primers used to clone by PCR ACA8 cDNA from which the amino acidic sequence of the protein has been deduced. ACA8 resulted in a 1.074 amino acids protein with 10 TM domains and an extended N-terminal domain with a high homology with the C-terminal regulative region of PMCA [Bonza et al., 2000].

As for other PM Ca^{2+}-ATPases belonging to cluster 4 (ACA9 and ACA10), that share with ACA8 a 70% of sequence identity, the ORF of ACA8 gene contains a high number of introns: 33 against 6 of ACAs of the endomembrane [Bonza et al., 2000; Baxter et al., 2003].

Regulation

ACA8, as all the ACAs, has an extended N-terminal region with regulative function that contains an autoinhibitory domain partially overlapped with a CaM-BD. ^{125}I-CaM overlay experiments with the first 122 amino acids of ACA8 fused to the GST, demonstrated that the CaM-BD is localised in the N-terminal region of the enzyme. In particular it has been observed that the sequence ^{41}Ile-Asn^{55} can form an amphiphilic α-helix, characteristic motive of CaM-BDs. The same overlay experiment performed by Bonza and colleagues with a peptide corresponding to ACA8 sequence ^{41}Ile-Asn^{55} localised the CaM-BD of ACA8 in the region ^{41}Ile-Asn^{55} [Bonza et al., 2000]. Further experiments performed by Bækgaard and colleagues (2006) identified the residues necessary for CaM binding. WT and mutants peptides corresponding to the ^{1}M-^{143} N-terminal sequence of ACA8, in which each of the residues between the ^{43}R-K^{68} sequence has been substituted by Ala, have been expressed in *E. coli* as His-tagged proteins. The binding of CaM has been analysed by CaM overlay of the purified peptides immobilized on nitrocellulose and by surface plasmon resonance (SPR) experiments. These experiments led to the identification of four amino acids (W47A, R48A, A56S and F60A) that when mutated determine a strong reduction of CaM affinity and nine amino acids (L44A, A51S, V53A, L54A, R58A, R61A, L64A, K67A and K68A) that when mutated determine a significant loss of CaM affinity. In particular the mutations W47A and F60A determine a dramatic reduction in CaM affinity, supporting the hypothesis that these residues, inside the CaM-BD of ACA8, act as anchor points for CaM. These data suggest that first four amino acids are involved directly in the CaM binding, while other nine amino acids could have an important function in determining the stability of the interaction with CaM [Bækgaard et al., 2006].

In order to investigate if the autoinhibitory domain of ACA8 was partially overlapped with the CaM-BD, Luoni and colleagues analysed the ability of a synthetic peptide, corresponding to the ^{41}I-T^{63} region (that comprise the CaM-BD), to inhibit the activity of the enzyme after tryptic cleavage (that deprives ACA8 of the N-terminal region) in comparison with the entire N-terminal of ACA8 (peptide 6His-^{1}M-I^{116}). These results demonstrate that both the peptides showed an inhibitory function, but ^{41}I-T^{63} was ten times less efficient in inhibition than the entire N-terminal. This indicates that the two domains are only partially overlapped, since the regions upstream and downstream the CaM-BD are necessary for a complete autoinhibition [Luoni et al., 2004].

Bækgaard and colleagues (2006) analysed the role of the N-terminal region in autoinhibition, focusing on the interplay between CaM binding and pump autoinhibition. For this purpose single point mutants of ACA8 in which each amino acid of the CaM-BD was mutated to Ala have been expressed in *S. cerevisiae* K616 strain, a yeast strain deprived of endogenous Ca^{2+}-ATPases [Cunningham and Finck, 1994] that can survive on low Ca^{2+} media only when heterologously expresses fully active Ca^{2+}-ATPases [Bonza and De Michelis, 2011]. Six mutants (W47A, R48A, L52A, N55A, R58A and F60A) were found able to complement K616 phenotype. Moreover, the biochemical characterization of the mutants showed that the mutation of these six amino acids deregulates the enzyme: in particular the basal activity resulted from 4 to 9 times higher than the basal activity of WT ACA8. These results indicate an involvement of these six residues in the mechanism of enzyme autoinhibition. A helical wheel projection of the amino acidic sequence corresponding to the CaM-BD of ACA8 highlighted that most of the residues involved in the autoinhibition stay on one side of the α-helix while the residues involved in the CaM binding are scattered along the helix.

Considering all these results a model has been proposed to explain how CaM binds and activates the pump. At basal Ca^{2+} concentration ACA8 is in the autoinhibited state thanks to the interaction of those residues that are located only on one side of the helix with the intramolecular counterpart in the catalytic head of the enzyme. In this condition the side of the helix that contains the residues with low affinity for CaM is exposed to the solvent. After an increasing in $[Ca^{2+}]_c$ CaM binds Ca^{2+} and undergoes some conformational changes that make it able to bind amino acidic residues W47 and F60, that are used as docking points. This first contact with CaM is then followed by the interaction with the other side of the helix, in competition with the intramolecular site of interaction. Once the binding has occurred at both sides of the helix the N-terminal domain is released from the intramolecular binding site and the pump is active [Bækgaard et al., 2006].

With the aim to identify the partner of intramolecular interaction of the N-terminal autoinhibitory domain of ACA8, the amino acidic sequence of ACA8 has been aligned with the sequence of ACA8 animal hortologue *h*PMCA4b, for which that region was already identified [Falchetto et al., 1991; 1992]. The result of the alignment blasts off a sequence of the plant protein, corresponding to its animal counterpart, in the region of the small cytoplasmic loop comprised between ^{268}E-W^{348}. Pull down experiment showed that the ACA8 ^{268}E-W^{348} peptide can interact with a 6His-^{1}M-I^{116} peptide reproducing the N-terminal region of ACA8 [Luoni et al., 2004]. The biochemical characterization of ACA8 mutants produced by Ala scanning of the conserved acidic residues in the region ^{268}E-W^{348} (Glu252, Asp273, Asp291, Asp303, Glu302 and Asp332) indicated that the mutation of any of these acidic residues generates a partially deregulated enzyme with a higher basal activity in absence of CaM [Fusca et al., 2009]. These results point out the importance of the presence of acidic residues in the small cytoplasmic loop for the mechanism of auto-inhibition. It has been proposed that electrostatic forces could be a component that participate in the autoinhibitory interaction established by the autoinhibitory domain and the small cytoplasmic loop: in fact, the negative charge due to the presence of acid residues in the small cytoplasmic loop can stabilize the interaction with the autoinhibitory domain that is, instead, positively charged [Bækgaard et al., 2006; Fusca et al., 2009].

ACA8 activity can be modulated also by interaction with acid phospholipids (APL): in particular PIP (phosphatidylinositol phosphate) and PIP_2 (phosphatidylinositol 4,5-bisphosphate) are stronger activators than PS (phosphatydil serin) and PA (phosphatidic acid). It has been shown that, in absence of CaM, APLs are able to activate ACA8 determining both an increase in V_{max} and a strong reduction of $K_{0.5}$ for Ca^{2+} far below the $K_{0.5}$ measured in presence of CaM. Moreover, the effect of APLs on the deletion mutant Δ74-ACA8 or on the proteolized enzyme (both missing the CaM-BD) or on the WT ACA8 in presence of CaM, doesn't change the V_{max} but further decreases the $K_{0.5}$ for Ca^{2+}. These results indicate a dual mechanism of ACA8 activation by APLs, involving their binding to different sites: APLs binding to a site in the protein N-terminus, overlapping the autoinhibitory and CaM-binding domain, stimulates ACA8 activity similar to CaM or to cleavage of the N-terminus, while binding to a second, and yet unidentified, site further stimulates ACA8 activity by lowering its $K_{0.5}$ for free Ca^{2+}. Analysis of the affinity for PI-4P of single mutants in the N-terminal regulatory region of ACA8 indicates that a binding site for the APL is localised in the portion that contains the CaM-BD and the autoinhibitory domain [Meneghelli et al., 2008].

4. Decoding Ca^{2+} signal

Any Ca^{2+}-mediated cellular process begins with the generation of a Ca^{2+} signature in the cytoplasm due to the synchronized activity of channels, pumps and Ca^{2+}/H^{+} antiporters. The information encoded by Ca^{2+} signals needs to be decoded and turned into a response by the cell. For this task, the cell employs an array of Ca^{2+} binding proteins (CBP), called Ca^{2+} sensors, that are able to sense the variation in the $[Ca^{2+}]c$ [Klimecka and Muzynska, 2007; De Falco et al., 2010]. A major group of Ca^{2+} sensor proteins possesses the EF-hand motif that consists in a 29 amino acids helix-loop-helix (HLH). The EF-hand modules bind Ca^{2+} ions in the loops of the HLH structure and undergo large conformational changes that result in the exposure of hydrophobic pockets, which in turn facilitates interactions of the protein with a variety of protein partners [De Falco et al., 2010]. The three largest categories of EF-hand proteins in plants are CaMs and CaM-like proteins (CMLs), CDPKs (Ca^{2+}-Dependent Protein Kinases) and CBLs (Calcineurin B-like Proteins). CaMs, CMLs and CBLs are all sensor relays, calcium sensors without any responder domains: they bind Ca^{2+} and undergo conformational changes that in turn regulate the activity of a variety of targets. Only CDPK are responders capable to directly transduce a signal via catalytic activity [Harper et al., 2004; Klimecka and Muzynska, 2007; De Falco et al., 2010].

CaM and CML

CaMs are conserved Ca^{2+} sensor proteins in eukaryotes that have been studied in great detail. The *Arabidopsis* genome contains seven different CaM genes: two sets (CaM1 and CaM4; CaM2, CaM3 and CaM5) encoding identical isoforms that are both approximately 89% identical with human CaM; in addition, two genes, CaM6 and CaM7, encode closely related (~ 99% identity with CaM2) but distinct CaM isoforms [De Falco et al., 2010].

Plant CaMs are about 16.7–16.8 kDa acidic proteins comprised of a flexible central helical region which joins two globular domains, both containing a pair of EF-hands that bind Ca^{2+} with positive co-operativity. The four EF-hand Ca^{2+}-binding domains are numbered I through IV, beginning from the N-terminus. Domain IV functions in concert with domain III, the most conserved region of the molecule among plant species, to form the high affinity site for Ca^{2+} binding and to initiate interaction between CaM and CaM-BD within the target proteins [Zielinski, 1998; De Falco et al., 2010]. CaM-BDs consist of a variable number (17-15) of basic amino acids that tend to structure in an amphiphilic α-helix. The high variability of CaM-BD in length and amino acidic composition (the only peculiarity is the presence of basic amino acids but not a real consensus sequence) enable CaM to interact with a vast number of targets [Zielinski, 1998]. This targets, that act as effector in the transduction of Ca^{2+}-based signals, belong to various and very different type of protein families, such as transporters, transcription factors and protein kinases.

Arabidopsis and rice genomes are predicted to encode respectively 50 and 26 CMLs, which show 16-75% sequence identity with CaM2 isoform of *Arabidopsis*. CMLs are supposed to have evolved from ancestral CaM and exhibit high structural divergence: most CMLs have four predicted EF-hands, although this number may range from 1 to 6. According to these, it is reasonable to suppose that the structural divergences among the members of this family enable differential response to Ca^{2+} signals [De Falco et al., 2010].

CDPKs

As already mentioned before, CDPKs are unique protein kinases owing to the presence of CaM-like domains (CLD) that are able to couple the Ca^{2+} sensor directly to its responder kinase. This group of kinases is unique to plants (and some protists) and have been implicated in the majority of Ca^{2+} responsive kinase activity [De Falco et al., 2010]. In plants, CDPKs are encoded by multigene families: 34 members of CDPKs have been identified in *Arabidopsis thaliana*, 31 in rice and 30 in poplar [Klimecka and Muzynska, 2007; De Falco et al., 2010]. CDPKs are monomeric proteins, with a molecular mass of 40 to 90 kDa, and consist of five domains (Fig.2): an N-terminal variable region, a catalytic region, a junction domain (JD) with autoinhibitory action, a CLD and a C-terminal domain of variable length [Harmon, 2003].

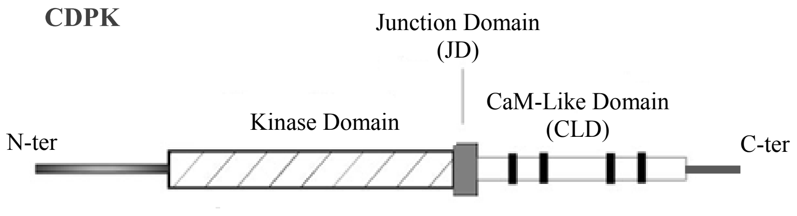

Fig 2. *Schematic structure of Ca^{2+}-dependent protein kinases. Modified from Harper et al., 2004.*

The most variable region, both in length and sequence identity, is the N-terminus; conversely the catalytic region is a highly conserved serine/threonine kinase domain. The junction domain is a pseudosubstrate-containing domain, capable of inhibiting kinase activity via interaction with the active site. The CLD consists of four EF-hands that comprise two binding sites, each responsible for the binding of one Ca^{2+} ion [De Falco et al., 2010].

The most important regulator of CDPKs activity is Ca^{2+}. Two models of CDPKs activation by Ca^{2+} ions exist. Model I states that, after Ca^{2+} binding, the CLD undergoes conformational changes that enable it to bind the JD, displacing the autoinhibitory interaction. In model II, the CLD would be loaded with one Ca^{2+} ion and already bound to the JD at basal Ca^{2+} concentrations. This implies that activation occurs through the binding of second Ca^{2+} ion. Consistent with this prediction, the second binding site displays a K_d for Ca^{2+} around 1 μM. Evidences show that CDPKs can be also activated by 14-3-3 proteins, phospholipids, auto-phosphorylation and/or phosphorylation events mediated by other protein kinases [Klimecka and Muzynska, 2007].

CDPKs are widely distributed among subcellular compartments including PM, ER, peroxisome membrane, mitochondria and the cytosol [De Falco et al., 2010]. Localisation studies of mutants in the N-terminal domain of *Oriza sativa* CDPK2 indicated that myristoylation and palmitoylation are required to a correct targeting of the CDPK to the membrane fraction: myristoylation being essential for membrane localization and palmitoylation for its full association [Martín and Busconi, 2000]. Subcellular localisation of nine *Arabidopsis thaliana* CDPKs, based on green fluorescent protein fusions, showed that the isoforms 7, 8, 9, 16, 21 and 28 (which harbour a predicted myristoylation site) are localised at the PM; two isoforms, CDPK3 and CDPK4 (which do not contain any acylation site) are localised in the cytosol and in the nucleus [Dammann et al., 2003] and one isoform, CDPK1 (which contain a myristoylation and a palmitoylation site), is localised in the peroxisomes. However a complete analysis to understand the molecular basis of various localisations of all CDPKs in the cell has not been accomplished yet.

Consistent with CDPKs localization studies, various membrane proteins have been identified as target substrates of these kinases. In *Arabidopsis* the PM localized slow (S-type) anion efflux channel SLAC1, which functions in the regulation of stomata closure in response to ABA, is regulated by the kinases CDPK21 and CDPK23. Upon co-expression of SLAC1 with CDPK21 and CDPK23, anion currents documented SLAC1 stimulation by both protein kinases. However, Ca^{2+}-sensitive activation of SLAC1 was assigned only to CDPK21 because CDPK23 appeared to be rather Ca^{2+}-insensitive in *in vitro* phosphorylation assays [Geiger et al., 2010; Franz et al., 2011]. The ER membrane localized Ca^{2+} pump ACA2 is negatively regulated *in vitro* by *Arabidopsis* CDPK1 through phosphorylation of the N-terminus [Hwang et al., 2000].

The function of CDPKs in regulating substrates appears not to be restricted to membrane proteins, because several CDPKs have been shown to function in the cytosol and the nucleus. *Arabidopsis* CDPK4, CDPK11 and CDPK32, for example, phosphorylate and positively regulate ABA responsive bZIP transcription factors (ABFs) [Choi et al., 2005; Zhu et al., 2007].

CBL/CIPKs signalling network

CBLs are plant Ca^{2+} sensor proteins most similar to animal calcineurin B and neuronal Ca^{2+} sensors, which have been initially identified in *Arabidopsis thaliana* [Chin et al., 2000]. CBLs share a rather conserved core region consisting of four EF-hands (that can be canonical or non-canonical) spaced by a conserved number of amino acids, and they show a difference in number and arrangement of canonical to non-canonical EF-hands. This isoform-specific difference suggests that CBL proteins may exhibit distinct affinities for Ca^{2+} that would influence interaction with the target.

According to their N-terminal domain CBLs can be divided in two groups: the first group consists of CBL1, CBL4, CBL5, CBL8 and CBL9 that have a short N-terminal domain with a myristoylation site; the second group is formed by CBL2, CBL3, CBL6, CBL7 and CBL10 with an extended N-terminal domain that does not contain lipid modification motifs. Besides this main difference CBL10 has a peculiar characteristic since it harbours a predicted transmembrane domain in the N-terminal region [Batistič and Kudla, 2009].

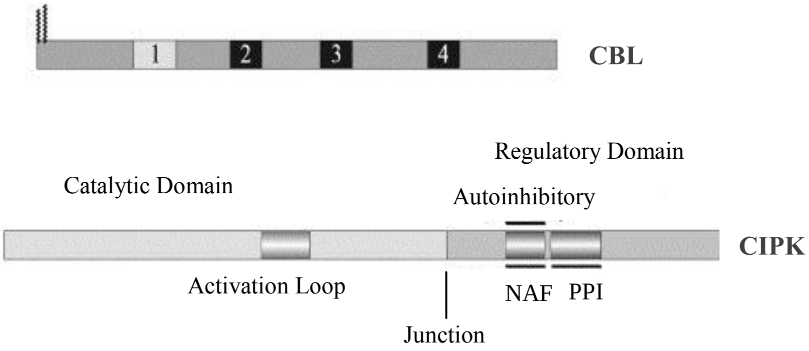

Fig 3. *General domain structure of CBLs and CIPKs.*
From Batistič and Kudla, 2009.

Localisation studies of *Arabidopsis* CBL proteins transiently expressed as GFP-fusion proteins in *Nicotiana benthamiana* leaves, revealed that, a part from some exceptions, these proteins are predominantly localised at the PM or vacuolar membrane. CBL10 is expressed predominantly in the tonoplast and the endosomal compartment [Batistič et al., 2010]. CBL2, CBL3 and CBL6 have been identified as exclusive membrane bound proteins that are targeted to the tonoplast, since these CBLs do not contain any TM domain or membrane docking sites, the molecular basis of their presence in the membrane is not clear yet. CBL7 has been found in the cytoplasm and in the nucleus, while

CBL1 and CBL9 are localised at the PM [D'Angelo et al., 2006; Cheong et al., 2007; Batistič et al., 2010]. In particular, it has been shown that CBL1 is subjected to palmitoylation on a Cys residue in position 3 (conserved also in CBL4, CBL5 and CBL9) and that myristoylation and palmitoylation together are important to drive the protein to the PM [Kolukisaoglu et al., 2004; Batistič et al., 2010]. Localisation of CBL4 and CBL5 and CBL8 the localisation results still unclear [Batistič et al., 2010].

Targets of the CBLs are the CIPKs (CBL Interacting Protein Kinases). CIPKs are serine/threonine kinases that belong to the group 3 of the SnRKs (Sucrose non-fermenting Related protein Kinases), a family of proteins closely related to SNF1 (Sucrose Non Fermenting 1) kinase in yeast and to the animal AMPK (AMP activated protein Kinase), that play a central role in the regulation of cell metabolism [Batistič and Kudla, 2009; Luan, 2009; Polge and Thomas, 2006]. CIPKs have an N-terminal kinase domain, which is separated by a junction domain from the less conserved C-terminal regulatory domain (Fig.3). Within the regulatory region, a conserved NAF domain functions as an autoinhibitory domain and mediates the binding of CBLs. Binding of CBLs to the NAF motif removes the autoinhibitory domain from the kinase domain, thereby conferring auto-phosphorylation and activation of the kinase. CIPKs can also associate with PP2Cs (Protein Phosphatases 2C) protein, like ABI1 and ABI2, *via* the C-terminal protein-phosphatase interaction domain (PPI), but currently nothing more is known about PP2Cs and CIPKs interaction.

CIPKs do not possess recognizable localisation signals and when expressed as GFP fusion proteins exhibit a cytoplasmic and nucleoplasmic localisation [Batistič et al., 2010]. Biomolecular Florescence Complementation (BiFC) analysis of CIPK-CBLs complexes reveal that CIPKs are targeted to different membranes by their interacting CBL proteins. For example BiFC experiments performed in *Nicotiana benthamiana* leaves indicate that CIPK1 is targeted to the PM by CBL1 and CBL9 [Cheong et al., 2007; Waadt et al., 2008] but localises at the tonoplast upon interaction with CBL2 [Batistič et al., 2008]. Similarly CIPK14-CBL2 complexes have been detected at the tonoplast while the same kinase is targeted to the PM by CBL8 [Batistič et al., 2010]. CIPK24 has been localised at the PM upon interaction with CBL1 and at the vacuolar membrane upon interaction with CBL10 [Kim et al. 2007]. An important aspect for the dynamics of Ca^{2+} signalling is that Multicolour BiFC analysis confirmed that some of the complexes mentioned above can occur simultaneously within the same cell [Waadt et al., 2008].

Genomic analyses revealed that *Arabidopsis* and rice genomes each encoding for 10 CBL proteins that form an interaction network with 26 (*Arabidopsis*) and 30 (rice) CIPKs respectively [Kolukisaoglu et al., 2004; Weinl and Kudla, 2009]. Forward genetic screens aiming to identify critical components of plant salt tolerance have provided insights into the physiological function of CBL-CIPK complexes. The CBL Ca^{2+} sensor SOS3 (At-CBL4) and the CIPK-type kinase SOS2

(At-CIPK24) are part of a Ca^{2+}-regulated signalling pathway that specifically mediates salt stress adaptation by regulating the PM Na^+/H^+ antiporter SOS1 [Liu and Zhu, 1998; Halfter et al., 2000; Qiu et al., 2002]. Recent studies revealed that mutation of CBL10 renders plants salt sensitive. Since CIPK24 has been localised at the tonoplast upon interaction with CBL10, a functional model has been suggested wherein alternative complex formation of CIPK24 with either CBL4 or CBL10 creates a dual functioning kinase [Kim et al., 2007]. CBL4-CIPK24 complexes mediate Na^+ extrusion via the regulation of the H^+/Na^+ antiporter SOS1 at the PM, while formation of CBL10/CIPK24 likely results in Na^+ sequestration into the vacuole by regulating unknown targets [Kim et al., 2007; Kudla et al., 2010].

Reverse genetics analyses have greatly advanced the understanding of CBLs and CIPKs and have uncovered crucial functions of these proteins for plant mineral nutrition and for responses to abiotic stresses and hormones, such as ABA. Moreover, these types of analysis showed that the CBL-CIPK system has a role in regulating K^+ homeostasis. Indeed, the activity of the shaker-like PM potassium channel AKT1 is regulated by CIPK23 upon its interaction with CBL1 and CBL9 [Xu et al., 2006; Li et al., 2006]. Besides the regulation of K^+ uptake in roots, the Ca^{2+}-decoding CBL1/CBL9-CIPK23 module appears to be involved in stomata regulation under dehydrating conditions [Cheong et al., 2007].

Furthermore, the PM H^+-ATPase AHA2 has been identified as an additional target of CBL-CIPK signalling complexes. Phosphorylation of a Ser residue within the C-terminal domain of AHA2 by CIPK11 prevents binding of 14-3-3 proteins to this domain and leads to down regulation of AHA2 proton transport activity [Fuglsang et al., 2007].

5. Aim of the project

As reported above, phosphorylation is a key mechanism in the transduction of Ca^{2+} signalling and represents a central and critical system for decoding of Ca^{2+} signals in response to a wide range of stimuli. In the past years it has been reported that this type of post-traductional modification has a role in the modulation of CaM-regulated Ca^{2+}-ATPases activity. For example, it is well known that PMCA autoinhibition is modulated by phosphorylation of its C-terminal regulative region by different protein kinases that phosphorylate different amino acids in different isoforms. In particular, PKA (protein kinase A) phosphorylates PMCA isoform 1 within the consensus sequence KRNSS, that is localised downstream the CaM-BD. The phosphorylation increases both V_{max} and the affinity of the pump for Ca^{2+}. PKC (protein kinase C), instead, phosphorylates different isoforms of PMCA on a Thr residue within the CaM-BD determining the activation of the pump with a mechanism similar but not overlapped to the mechanism of CaM-activation [Penniston and Enyedi, 1998; Di Leva et al., 2008]. In plants, it has been shown that *in vitro* phosphorylation by CDPK1 decreases ACA2 basal activity and CaM stimulation, without abolish CaM binding. The target of ACA2 phosphorylation is Ser45, localised near the CaM-BD. Thus, in this case phosphorylation stabilizes the autoinhibited form of the enzyme [Hwang et al., 2000]. Moreover, by *in vitro* phosphorylation experiments, Malmström and colleagues (2000) showed that two Ser residues in the N-terminus of BCA1 (an isoform of CaM-regulated Ca^{2+}-ATPase of the tonoplast of *Brassica oleracea*) are target of *in vitro* PKC phosphorylation: one of the Ser residues involved in the phosphorylation is localised in the CaM-BD of the pump; however in this case the effect of phosphorylation on pump activity was not determined [Malmström et al., 2000].

Large-scale phospho-proteomic studies identified several phosphopeptides corresponding to portions of the regulative N-terminus of ACA8. Ser that have been found phosphorylated are: S19, S22, S27, and S29, localised upstream the CaM-BD, Ser57 within the CaM-BD, and S99 downstream the CaM-BD [Nühse et al., 2003, 2004, 2007; Benschop et al., 2007; Niittylä et al., 2007; Sugiyama et al., 2008; Whiteman et al., 2008; Jones et al., 2009; Reiland et al., 2009; Chen et al., 2010; Nakagami et al., 2010]. A different level of phosphorylation in response to different type of treatments has been reported for four of these Ser residues: stimulation with hormones such as ABA and gibberellins up-regulates the phosphorylation of S27 and S29 [Chen et al., 2010]; elicitors such as flagellin up-regulate the phosphorylation of S27 and S99 [Nühse et al., 2003, 2004, 2007; Benschop et al., 2007]; the administration of sucrose to cultured cells, instead, down-regulates the phosphorylation of S22 [Niittylä et al., 2007].

In order to understand the effect of ACA8 phosphorylation on these Ser residues, we decided to produce ACA8 single point mutants in which, one by one, each of these six Ser residues have been mutated to Ala (making the residue non-phosphorylable) or to Asp (mimicking residue phosphorylation). ACA8 WT and mutants were expressed in *S. cerevisiae* K616, a yeast strain routinely used in our laboratory for the heterologous expression of WT and mutant Ca^{2+}-ATPases [Bonza et al., 2004; Bækgaard et al., 2006; Meneghelli et al., 2008; Fusca et al., 2009; Bonza and Luoni, 2010], for a biochemical characterization of their activity.

At the same time we attempted to find the kinase/s involved in ACA8 phosphorylation. Since we knew that S19 is in a consensus motif for CDPKs, while S27 is in a consensus motif for SnRKs [Nühse et al., 2004], we decided to focus our attention on these two classes of protein kinases. The ability to phosphorylate the N-terminal regulatory region of ACA8 of two isoforms of CDPKs (kindly provided by Professor J. Harper, University of Nevada, USA) has been tested by *in vitro* phosphorylation experiments. Moreover, in collaboration with Professor J. Kudla (University of Münster, Germany) we screened by yeast two-hybrid the CIPK family (the sub-group 3 of the SnRKs) using the N-terminal region of ACA8 as bait. *In planta* BiFC experiments and *in vitro* phosphorylation experiments were used to confirm the interactions we found.

Main Results

Main Results

1. Analysis of the effect of phosphorylation on ACA8 activity

In order to study the effects of phosphorylation on ACA8 activity we replaced by site directed mutagenesis each of the six ACA8 N-terminal Ser residues (S19, S22, S27, S29, S57 and S99) found to be phosphorylated *in vivo* [Nühse et al., 2003, 2004, 2007; Benschop et al., 2007; Niittylä et al., 2007; Sugiyama et al., 2008; Whiteman et al., 2008; Jones et al., 2009; Reiland et al., 2009; Chen et al., 2010; Nakagami et al., 2010] with an Ala (S/A) to prevent phosphorylation or with an Asp (S/D) to mimic phosphorylation.

ACA8 WT and mutants were expressed in *S. cerevisiae* K616. Western blot and immunodecoration of the ACA8 WT and mutant microsomal fractions showed that all the proteins were substantially intact. The assay of their Ca^{2+}-ITPase activity in presence of saturating concentrations of CaM indicated that all the mutants were functional.

Effect of S/D mutations on ACA8 autoinhibition

In order to test the degree of autoinhibition of ACA8 mutants, we measured the Ca^{2+}-ITPase activity of ACA8 WT and mutants in presence or absence of saturating concentration of CaM. Results are reported in Figure 4. Under the applied experimental conditions, CaM stimulated the activity of WT ACA8 by ~300%. The response to CaM was drastically reduced in two of the mutants, S19D and S57D, which were stimulated by ~100%; S/A mutation of the same residues only marginally affected CaM stimulation. Mutations of S22 and S27 generated proteins somewhat less stimulated by CaM (150–180%, $P < 0.05$) than the WT, but in these cases the effect was independent of the substitution made. S/D mutation of residues S29 and S99 did not affect ACA8 response to CaM; unespectedly, the S29A mutant was less stimulated by CaM than the WT and the S29D mutant. This result could suggest that ACA8 was phosphorylated at Ser29 *in vivo* by some yeast kinase. However, mass spectrometric analysis of WT ACA8 purified from yeast microsomes by CaM affinity chromatography [Fusca et al., 2009; Bonza and Luoni, 2010] showed that the protein had not been phosphorylated *in vivo* under the applied yeast growth conditions. Since the activities in the presence of CaM of the S19D, S22D, S27D, and S57D mutants were similar to that of WT ACA8, the decrease in CaM stimulation reflects to an increase of their basal activity.

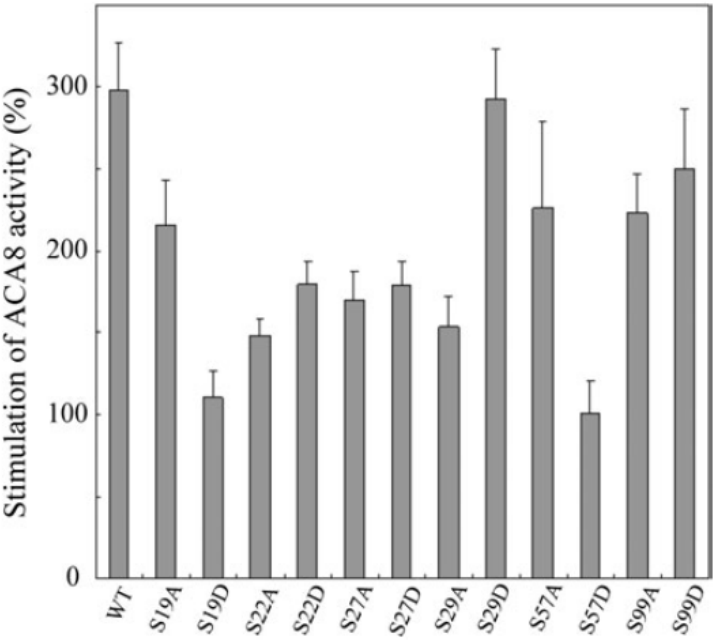

Fig 4. *Stimulation of WT and mutant ACA8 by CaM.* ACA8 activity was measured in the presence or absence of 1 μM CaM. Results are shown as percentage stimulation over the activity measured in the absence of added CaM. Values reported are the mean of 3–10 experiments ± standard error of the mean.

Thus, the results reported above indicate that the introduction of a negative charge on these Ser residues hampers the autoinhibitory action of the N-terminal domain, generating partially deregulated mutants. Moreover, the low response to CaM of ACA8 mutants S22A, S27A, and S29A point the relevance of these serine residues *per se* in determining the amplitude of the response of ACA8 to CaM.

Effect of S/D mutations on ACA8 affinity for CaM

We assayed the Ca^{2+}-ITPase activity of all the mutants in the presence of increasing concentrations of CaM, to analyse the effect of the S/D mutations on ACA8 affinity for CaM. Only in the case of the S/D mutant in S57, the only Ser located inside the CaM-BD, the CaM activation curve was shifted to higher CaM concentrations respect to that of WT ACA8. This result indicates that mimicking phosphorylation of S57 determines a decrease of ACA8 apparent affinity for CaM.

To better analyse the affinity of S/D mutants for CaM and to determine also the effect of the S/D mutations on the kinetics of interaction between ACA8 and CaM, peptides corresponding to the first 116 amino acids of WT or different mutants of ACA8 were used for CaM binding measurements by surface plasmon resonance [Bækgaard et al., 2006; Luoni et al., 2006]. The results, reported in table

1, shows that the most part of the mutants presented variations of the rate of complex association (k_a) and all of them presented substantial variations of the rate of complex dissociation (k_d).

	k_a ($\times 10^5$ $M^{-1}s^{-1}$)	k_d ($\times 10^{-3}$ s^{-1})	K_D (nM)
WT	1.27±0.02	2.44±0.01	19.3±0.3
S19D	2.24±0.06	3.25±0.02	14.5±0.4
S22D	0.58±0.02	1.39±0.01	23.9±0.6
S27D	1.96±0.03	5.20±0.03	26.5±0.4
S29D	1.71±0.02	3.82±0.02	22.3±0.2
S57D	1.54±0.01	25.5±0.22	165±1.8
S99D	1.21±0.04	1.37±0.01	11.3±0.4

Tab 1. *Kinetics of binding of bovine testes CaM to the N-terminus of WT and ACA8 mutants measured by surface plasmon resonance*. Each value with the corresponding standard error of the mean is the average of constants derived from the analysis of at least five binding curves.

In case of the S57 the S/D mutation had no major effect on the rate of complex association, but it drastically increases the rate of complex dissociation, resulting in a dissociation constant (K_D) about 10-folds higher than the K_D of the WT. On the other hand, in the case of S99 the S/D mutation stabilized the complex, since it decreased the rate of complex dissociation, resulting in a K_D that is about half that of the WT. All the other analysed mutations affect the kinetics of interaction with CaM, but the balance between changes in k_a and k_d results only in minor changes of the K_D values.

2. *In vitro* phosphorylation of the ACA8 N-terminus by CDPKs

Since S19 is in a consensus motif for CDPKs [Nühse et al., 2004], we tested the ability of two isoforms of *Arabidopsis thaliana* CDPKs to phosphorylate ACA8 N-terminus *in vitro*: CDPK1, the best characterized isoform of CDPK, known to phosphorylate ACA2 an ER localized isoform of *A. thaliana* [Hwang et al., 2000], and CDPK16, a PM isoform of CDPK [Dammann et al., 2003]. *In vitro* phosphorylation assay, performed using ACA8 WT ^{1}M-I^{116} peptide as substrate, showed that ACA8 N-terminus is phosphorylated by both kinases, but at higher extent by CDPK16.

To map the phosphorylation site of CDPK16 we performed *in vitro* phosphorylation assays using the His-tagged N-termini of ACA8 S/D mutants. Results in figure 5 (top panel) show that while mutants S29D, S57D, and S99D were phosphorylated similarly to WT ACA8, the phosphorylation level was drastically reduced in mutant S22D and was lower than the WT also in mutants S19D and S27D. These results indicate an involvement of S19, S22 and S27 in ACA8 phosphorylation; anyway, since the introduction of the negative charge of the Asp residue may affect phosphorylation of the neighbouring serine residues, phosphorylation assays were performed also on the respective S/A mutant peptides.

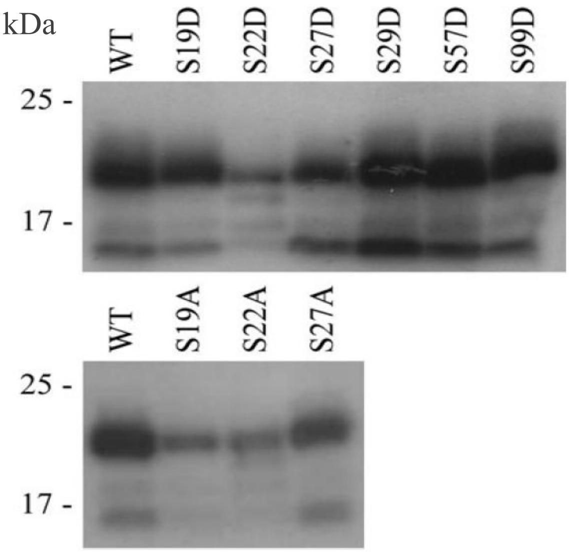

Fig 5. *Phosphorylation of WT and mutant ACA8 N-termini by CPK16.* WT or mutant ACA8 N-termini were phosphorylated with a Ca^{2+}-independent mutant of *A. thaliana* CPK16. Samples were solubilized and aliquots corresponding to 3 µg (top panel) or 2 µg (bottom panel) of 6His-^{1}M-I^{116} were subjected to SDS–PAGE, blotting, and autoradiography.
Results are from one experiment representative of three.

The bottom panel of Figure 5 shows that phosphorylation of ACA8 by CPK16 was strongly reduced by mutations S19A and S22A, while mutant S27A was phosphorylated similarly to the WT. These results show that S19 and S22 in ACA8 N-terminus are targets of CDPK16 *in vitro* phosphorylation.

3. ACA8 is a target of CBL-Interacting Protein Kinases

It is known that Ser 27 is in a consensus motif for SnRKs [Nühse et al., 2004], a class of kinases that have their animal orthologue in AMPK, an enzyme that plays a central role in the regulation of cell metabolism. It has been shown that plant SnRKs and animal AMPKs phosphorylate the same synthetic substrates, such as ALARA and syntide-2 peptides, with a high affinity [Hashimoto et al., 2012]. Moreover, AMPK has been successfully used to phosphorylate plant substrates [Harthill et al., 2006; Lu et al., 2007]. With the aim of understanding if this class of protein could phosphorylate ACA8, we performed a preliminary screening of the SnRK family, testing the ability of a commercial AMPK to phosphorylate the N-terminus of ACA8. Results showed that the kinase was able to phosphorylate the 6His-tagged peptide corresponding to the sequence ^{1}M-I^{116} of ACA8.

Identification of CIPK interacting with ACA8 by yeast two hybrid and BiFC experiments

The plant SnRKs family consists of three different subgroups, but only one is directly involved in Ca^{2+} signalling: the SnRK3, which groups the CBL Interacting Protein Kinases (CIPKs). Looking for a SnRK able to phosphorylate ACA8 we performed a two hybrid screening using ACA8 N-terminus as bait and all the members of the *Arabidopsis* CIPK family as prays. As a result of the two hybrid screening we found two CIPKs, CIPK9 and CIPK14, able to interact with ACA8 N-terminus.

BiFC experiments in *Nicotiana benthamiana* leaf cells, using ACA8 FL protein fused to the C-terminal part of the YFP (YC::ACA8) and the kinases fused to the N-terminal part of the YFP (YN::CIPK9 and YN::CIPK14), confirmed the interaction identified by yeast two-hybrid. Indeed, as reported in Figure 6, both in the case of ACA8-CIPK9 and ACA8-CIPK14 a fluorescence signal is present indicating the formation of the complexes *in vivo*. Moreover, the signals distribution along the periphery of the cells clearly indicates that the interactions occur at the PM.

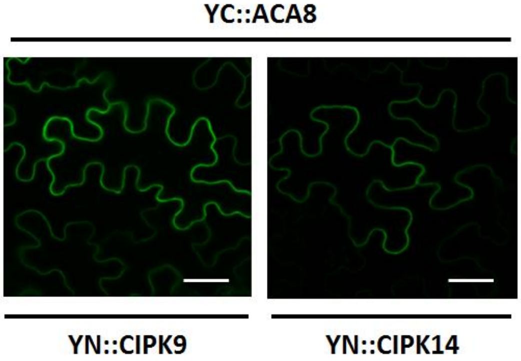

Fig 6. *CIPK9 and CIPK14 interact with ACA8 FL in BiFC*. The BiFC analysis were performed using YC::ACA8 and YN::CIPK9 or YN::CIPK14 in transiently transformed *Nicotiana benthamiana* leaves. Results, collected after 4 days from infiltration, are from one representative of at least three independent experiments. Scale bars: 40 µm

Phosphorylation of the ACA8 N-terminus by CIPK9 and CIPK14

Based on the yeast two-hybrid screening and BiFC results we checked whether recombinant strepII-tagged CIPK9 and CIPK14 [Hashimoto et al., 2012] were able to phosphorylate the ACA8 WT ^{1}M-I^{116} peptide. Figure 7 shows that both kinases are subjected to auto-phosphorylation as expected (lane 1 and 4). Moreover results reported in lane 2 and 5 demonstrate that both CIPKs are able to phosphorylate ACA8 N-terminus.

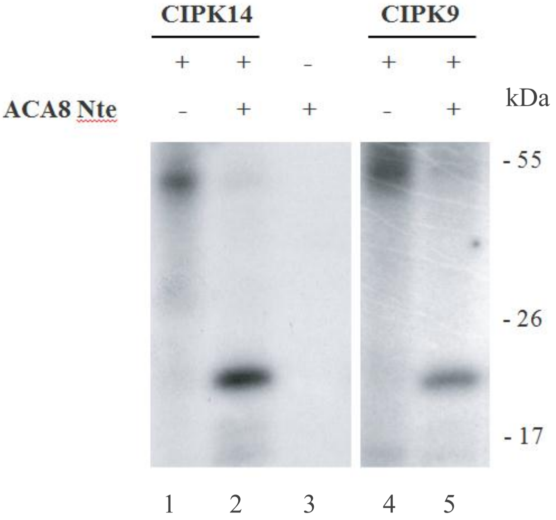

Fig 7. *CIPK9 and CIPK14 phosphorylate ACA8 N-terminus in vitro*. Results of *in vitro* phosphorylation assays using purified strepII-tagged CIPK9 (lane 4 and 5) or strepII-tagged CIPK14 (lane 1 and 2) without (lane 1 and 4) or in presence of 6His-^{1}M-I^{116} (ACA8Nte). Samples were solubilized and aliquots corresponding to 700 ng of 6His-^{1}M-I^{116} were subjected to SDS-PAGE, blotting and autoradiography. Results are from one experiment representative of three.

Discussion

Discussion

Arabidopsis thaliana ACA8 is the best biochemically characterized isoform of PM Ca^{2+}-ATPase in plants [Bonza et al., 2000; Bonza and De Michelis, 2011]. However, not much was known so far about the connection between regulation of ACA8 activity and its physiological role. With this work we provide the first evidences that phosphorylation regulates ACA8 activity and we identify two classes of protein kinases related to different stimulus-induced Ca^{2+}-signalling pathways involved in ACA8 phosphorylation.

The biochemical characterization of S/D mutants of each of the six Ser residues in ACA8 N-terminus that have been found phosphorylated in phosphoproteomic studies [Nühse et al., 2003, 2004, 2007; Benschop et al., 2007; Niittylä et al., 2007; Sugiyama et al., 2008; Whiteman et al., 2008; Jones et al., 2009; Reiland et al., 2009; Chen et al., 2010; Nakagami et al., 2010] indicates that phosphorylation affects pump activity in different ways: in some cases hampering the autoinhibitory action of the N-terminus (S19, S22, S27 and S57), in few cases changing affinity for CaM (S57 and S99) and in all cases modifying the kinetic of interaction with CaM.

Mutation to Asp of S19, S22, S27 and S57, generates partially deregulated proteins, with a basal activity (in absence of CaM) higher than that of the WT. It has been demonstrated that ACA8 N-terminal autoinhibitory domain, enriched in positively charged amino acids [Bækgaard et al., 2006], interacts with a region in the small cytoplasmic loop characterized by the presence of negatively charged amino acids [Luoni et al, 2004]. Indeed, alanine scanning mutagenesis experiments showed that the selective mutation of these negatively charged amino acids in the small cytoplasmic loop partially deregulate ACA8 activity, indicating a role of electrostatic forces in determining the autoinhibitory interaction between the small cytoplasmic loop and the N-terminal autoinhibitory domain [Fusca et al., 2009]. Thus, a phosphorylation event, which introduces one or more negative charges into ACA8 N-terminus, implies a repulsive component that could lead to a partial displacement of autoinhibitory interaction of ACA8 N-terminus with its intramolecular counterpart.

Results showed that also S/A mutation of S22, S27 and S29 partially deregulates the pump, indicating the importance of the amino acidic identity of these residues *per se* in the mechanism of autoinhibition. The characteristic feature of the serine residue is the presence of an OH group, capable to form a dipole according to the difference of electronegativity between the two atoms: with a negative density on the oxygen atom and a positive density on the hydrogen atom. Therefore, our results indicate the possibility that Ser residues in the N-terminal domain of ACA8 could participate to the autoinhibitory interaction by forming hydrogen bonds with acidic residues in the small cytoplasmic loop.

All the analysed mutations affect the kinetics of ACA8 interaction with CaM to some extent: we observed a kd 10-fold higher for the mutant S57D and 2-fold changes in one or both of the kinetic constants of the interaction in mutants S19D, S22D, S27D, and S99D. Despite the different kinetics, the affinity for CaM of most mutants is fairly similar to that of WT, around 20 nM, with two exceptions: mutant S99D which has a K_D value of 11 nM and mutant S57D which has a K_D value of 165 nM.

The strongest effects on K_D of mutant S57D can be easily explained by the localization of S57 within the sequence defining CaM-BD [Bonza et al., 2000; Bækgaard et al., 2006]. On the other hand the effect of S/D mutation of S99, localised far downstream the CaM-BD, seemed to be more obscure. Only very recently Tidow and colleagues (2012) defined with high-resolution the crystal structure of ACA8 regulatory-domain in complex with CaM. Their data confirmed the presence of a CaM-BD around the region comprising the two hydrophobic anchor points W47 and F60 and interestingly, indicated the presence of a second CaM-BD arranged in the region comprising the two hydrophobic anchor points I79 and F92. This new CaM-BD, that has been called CaM-BD2 while the best characterized has been called CaM-BD1, displays a higher K_D than CaM-BD1: 0.5 µM respect to 20 nM. On the light of these new findings that localised S99 very close to CaM-BD2, the effect of S99D mutant on ACA8 affinity for CaM can be better understood.

Based on these results, a major effect of phosphorylation of serine residues in the ACA8 N-terminus would be to modify the rate of pump activation/deactivation. After an increase of cytoplasmic Ca^{2+} concentration which increases the concentration of the active Ca^{2+}–CaM complex, the rate of pump activation would be halved upon phosphorylation of S22 and nearly doubled upon phosphorylation of S19 or S27. On the contrary, when the return of the cytosolic free Ca^{2+} concentration toward basal levels drastically lowers the concentration of Ca^{2+}–CaM, the rate of pump deactivation would be halved in the case of phosphorylation of S99 and would increase from 2- to 10-fold following phosphorylation of S27 or of S57 (see *Main Results*, Table 1).

Phosphorylation of some of these serine residues affects both the kinetics of CaM activation and deactivation and the autoinhibitory action of the ACA8 N-terminus. The two effects may exert a similar or contrasting effect on Ca^{2+} extrusion, depending on the phosphorylated residue and on the values of the relevant cytoplasmic parameters. Altogether, the subtle effects of phosphorylation of one or more of these Ser on ACA8 activity may have important consequences on the shaping of Ca^{2+} waves and then on the determination of a specific Ca^{2+}-signature. These results point out the importance of the identification of regulators involved in the control of ACA8 phosphorylation-state in response to different signals. With this work we show that at least two classes of protein kinases, CDPKs and CIPKs, are involved in ACA8 phospho-regulation.

Concerning CDPKs, we demonstrate that both CDPK1 and CDPK16 can phosphorylate ACA8 N-terminus *in vitro*. In addition, we identified the phosphorylation site of CDPK16, the more efficient isoform of the two tested which is PM-localised [Dammann et al., 2003]. CDPK16 phosphorylates ACA8 N-terminus at S19, which is part of a CDPKs consensus motif, and at S22. To understand the effect of CDPKs phosphorylation on ACA8 activity a biochemical characterization of the S19D/S22D ACA8 double mutant is in progress.

We showed that ACA8 interacts *in vivo* at the PM with two isoform of CIPKs: CIPK9 and CIPK14. Furthermore, we demonstrate that the N-terminal regulative region of ACA8 is phosphorylated *in vitro* by CIPK9 and CIPK14. These preliminary results indicate that ACA8 is a target of the CBL-CIPK signalling network, which has a crucial function in many biological processes such as salt tolerance, potassium transport, nitrate sensing, and stomatal regulation [Kudla et al., 2010]. In the light of the results obtained on ACA8 S/D mutants, these findings indicate a possible mechanism of ACA8 regulation that determines a rapid modulation of the pump activity in response to specific stimuli triggered by specific CBL-CIPK complexes. Nevertheless, further work is needed to unravel the physiological role of CIPK-CBL mediated ACA8 phosphorylation and its correlation with Ca^{2+} signalling pathways.

No phenotype has been reported so far for ACA8 knock out mutant. On the other hand, experiments on CIPK9 knock out mutants in *Arabidopsis* show that this isoform of CIPK is a critical regulator of low potassium response [Pandey et al., 2007], while CIPK14 knock out mutants show a higher sensitivity to ABA and salt stress, displayed as low germination rate and less root elongation [Qin et al., 2008]. To investigate the physiological outcome of ACA8 interaction with these two isoform of CIPKs it would be very important to test if ACA8 knock out mutant displays a phenotype in the same conditions in which CIPK9 and CIPK14 knock out phenotypes are evident.

Another crucial aspect to analyse the physiological role of CIPK-ACA8 interaction would be to determine if *in vivo* the reconstitution of CBL-CIPK-ACA8 phosphorylation complex produces an effect on cellular Ca^{2+} homeostasis. In order to answer to this question we are setting the conditions to perform a complementation test of the *S. cerevisiae* mutant K616 [Cunningam and Finck, 1994]. This yeast strain is deprived of endogenous Ca^{2+}-ATPases; for this reason it is able to survive only in presence of high external Ca^{2+} concentrations or if a constitutively active Ca^{2+} pump is heterologously expressed [Bonza and De Michelis, 2011]. The expression in K616 of an autoinhibited isoform of plant Ca^{2+}-ATPase, such as ACA8, is not able to complement the yeast phenotype; on the other hand the expression of deleted mutants of ACA8, like Δ74ACA8 that is constitutively active, complements K616 phenotype [Bonza et al., 2004; Bækgaard et al. 2006; Fusca et al., 2009; Bonza and Luoni, 2010; Tidow et al., 2012]. Thus, if the phosphorylation of

ACA8 by CBL-CIPK complex activates the enzyme, the co-expression of these three proteins in K616 may complement its phenotype on selective medium.

In the last 15 years FRET-based genetically encoded Ca^{2+}-sensors called Yellow Chameleons (YCs) have been developed as tools to monitor the spatio-temporal dynamics of Ca^{2+} transients [Miyawaki et al., 1997; Krebs et al., 2012]. The YC sensors are constituted by two fluorescent proteins, the CFP (cyan fluorescent protein) and the YFP, linked by CaM and M13 (the CaM-binding peptide of mammalian myosin light chain kinase). Upon binding of Ca^{2+}, the CaM domain binds to the M13 peptide causing a conformational change in the hinge region that results in a change in proximity/orientation between the CFP and YFP. This alteration in the relationship between these two fluorescent proteins causes the fluorescence resonance energy transfer (FRET) between them to increase. By monitoring the rise in FRET, a change in Ca^{2+} can therefore be inferred, with the increase in ratiometric signal being quantitatively linked to the magnitude of the Ca^{2+} increase [Choi et al., 2012]. In plants, YCs have been successfully used to study guard cell-specific Ca^{2+} dynamics [Allen et al., 1999, 2000, 2001], to monitor cytoplasmic Ca^{2+} changes during the interaction of the pollen tube with synergid cells [Iwano et al., 2012] or in response to ATP and Al^{3+} treatments in roots [Tanaka et al., 2010; Rincón-Zachary et al., 2010] or to monitor the intra-mitochondrial Ca^{2+} dynamics [Loro et al., 2010]. We will use this tool to study the effect of ACA8 and/or CIPKs transient over- expression in *Nicotiana benthamiana* leaf cells on the cytosolic Ca^{2+} dynamics: this technique will allow us to analyse *in vivo* the effect of the interaction of CIPKs with the pump on the shape of Ca^{2+}-oscillation.

Since we know that phosphorylation influences ACA8 activity in a different way according to the Ser residue(s) involved in the phosphorylation events, mapping CIPKs phosphorylation site will be crucial to understand the effect of CIPKs phosphorylation. The effect of single point mutations on phosphorylation indicates that CIPK9 and CIPK14 phosphorylate ACA8 at more than three sites; unfortunately these experiments were not conclusive to determine CIPKs phosphorylation site. To circumvent this problem we are setting-up of the conditions for an extensive *in vitro* phosphorylation of ACA8 N-terminus which allows identification of phosphorylation sites by mass spectroscopy analysis. An intriguing question that could be answered mapping CIPK9 and CIPK14 phosphorylation sites, knowing CDPK16 phosphorylation site, is if different classes of protein kinases (or even different isoforms belonging to the same class) phosphorylate different Ser residues in the N-terminal region of ACA8. Since we know that different classes of kinases are involved in different types of stimuli, these findings could indicate that phosphorylation is a way the plant cell uses to modulate ACA8 activity in order to obtain stimulus-specific Ca^{2+}-signatures.

It has been demonstrated for CIPK1, CIPK23 and CIPK24 that CBLs have a role not only in targeting the kinase on the appropriate subcellular compartment [Batistič et al., 2010] but also in stimulating the kinase activity [Hashimoto et al., 2012]. According to these data it would be very interesting to determine if the activity of CIPK9 and CIPK14 on ACA8 N-terminus can be stimulated by CBL1, a PM CBL which we showed to be able to interact with both kinases in BiFC experiments. With this aim we would perform *in vitro* phosphorylation experiments using of ACA8 N-terminus CIPK9 and CIPK14 in presence of CBL1.

References

References

Allen GA, Kwak JM, Chu SP, Llopis J, Tsien RY, Harper JF and Schroeder JI (1999). Cameleon calcium indicator reports cytoplasmic calcium dynamics in Arabidopsis guard cells. Plant Journal. **19**:735–747.

Allen GJ, Chu SP and Schumacher K (2000). Alteration of stimulus specific guard cell calcium oscillations and stomatal closing in *Arabidopsis* det3 mutant. Science. **289**:2338–2342.

Allen GJ, Chu SP, Harrington CL, Schumacher K, Hoffmann T, Tang YY, Grill E and Schroeder JI (2001). A defined range of guard cell calcium oscillation parameters encodes stomatal movements. Nature. **411**:1053–1057.

Anil VS, Rjkumar P, Kumar P, Mathew MK (2008) A plant Ca^{2+} pump, ACA2, relieves salt hypersensitivity in yeast. Modulation of cytosolic calcium signature and activation of adaptive Na^+ homeostasis. Journal of Biological Chemistry. **283**: 3497-3506.

Axelsen, K and Palmgren, MG (1998). Evolution of substrate specificities in the P-type ATPases superfamily. Journal of Molecular Evolution **46**:84-101.

Bækgaard L, Luoni L, De Michelis MI and Palmgren MG (2006). The plant plasma membrane Ca2+ pump ACA8 contains overlapping as well as physically separated autoinhibitory and calmodulin-binding domains. Journal of Biological Chemistry. **281**:1058-1065.

Batistič O, Waadt R, Steinhorst L, Held K, and Kudla J (2010). CBL-mediated targeting of CIPKs facilitates the decoding of calcium signals emanating from distinct cellular stores. Plant Journal; **61**: 211–222.

Batistič O and Kudla (2009). Plant calcineurin B-like proteins and their interacting protein kinases. Biochim. and Biophys. Acta. **1793**: 985-992.

Batistič O, Sorek N, Schültke S, Yalovsky S, Kudla J (2008). Dual fatty acyl modification determines the localization and plasma membrane targeting of CBL/CIPK Ca^{2+} signalling complexes in *Arabidopsis*. Plant Cell; **20(5)**:1346-62.

Baxter I, Tchieu J, Sussman MR, Boutry M, Palmgren MG, Gribskov M, Harper JF and Axelsen KB (2003) Genomic comparison of P-type ATPase ion pumps in *Arabidopsis* and rice. Plant Physiology. **132**: 618-628.

Beffagna N, Romani G and Sforza MC (2000) H^+ fluxes at plasmalemma level: in vivo evidences for a significant contribution of the Ca^{2+}-ATPase and for the involvement of its activity in the abscisic acid-induced changes in *Egeria densa* leaves. Plant Biology. **2**: 168- 175.

Benschop JJ, Mohammed S, O'Flaherty M, Heck AJR, Slijper M, Menke FLH (2007). Quantitative phosphoproteomics of early elicitor signalling in *Arabidopsis*. Molecular and Cellular Proteomics; **6**: 1198–1214.

Bonza MC and De Michelis MI (2011). The plant Ca^{2+}-ATPase repertoire: biochemical features and physiological functions. Plant Biology; **13**: 421–430.

Bonza MC and Luoni L (2010). Plant and animal type 2B Ca^{2+}-ATPases: evidence for a common auto-inhibitory mechanism. FEBS Lett. **584(23)**:4783-8.

Bonza MC, Luoni L, De Michelis MI (2004). Functional expression in yeast of an N-deleted form of At-ACA8, a plasma membrane Ca^{2+}-ATPase of *Arabidopsis thaliana*, and characterization of a Hyperactive mutant. Planta **218**: 814-823.

Bonza MC, Morandini P, Luoni L, Geisler M, Palmgren MG, De Michelis MI (2000). *At*-ACA8 encodes a plasma membrane-localized calcium-ATPase of *Arabidopsis* with a calmodulin-binding domain at the N terminus. Plant Physiol; **123**: 1495-1505.

Boursiac Y and Harper JF (2007). The origin and function of calmodulin regulated Ca^{2+} pumps in plants. Journal of Bioenergetic and Biomembranes **39**, 409-414.

Brini M and Carafoli E (2009). Calcium pumps in health and disease. Physiological Review. **89**:1341-1378.

Carafoli E (1991). Calcium pump of the plasma membrane. Physiol. Rev. **71**: 129-153.

Carnelli A**, De Michelis MI and Rasi-Caldogno F** (1992). Plasma membrane Ca^{2+}-ATPase of radish seedlings. I. Biochemical characteristics using ITP as a substrate. Plant Physiol **98**: 1196-1201.

Cerana M, Bonza MC, Harris R, Sanders D, De Michelis MI (2006). Abscisic acid stimulates the expression of two isoforms of plasma membrane Ca^{2+}-ATPase in *Arabidopsis thaliana* seedlings. Plant Biology; **8**: 572-578.

Chen XF, Chang MC, Wang BY, Wu R (1997) Cloning of a Ca^{2+}-ATPase gene and the role of cytosolic Ca^{2+} in the gibberellin-dependent signaling pathway in aleurone cells. Plant Journal. **11**: 363-371.

Chen Y, Hoehenwarter W, Weckwerth W (2010). Comparative analysis of phytohormone-responsive phosphoproteins in *Arabidopsis thaliana* using TiO2-phosphopeptide enrichment and mass accuracy precursor alignment. Plant Journal; **63**: 1–17.

Cheong YH, Pandey GK, Grant JJ, Batistič O, Li L, Kim BG, Lee SC, Kudla J and Luans S (2007). Two calcineurin B-like calcium sensors, interacting with protein kinase CIPK23, regulate leaf transpiration and root potassium uptake in *Arabidopsis*. Plant Journal. **52**:223–239.

Chin D, and Means AR (2000). Calmodulin a prototypical calcium sensor. Trends Cell Biol. **10**:322-328.

Choi HI, Park HJ, Park JH, Kim S, Im MY, Seo HH, Kim YW, Hwang I and Kim SY (2005). *Arabidopsis* calcium-dependent protein kinase AtCPK32 interacts with ABF4, a transcriptional regulator of abscisic acid-responsive gene expression, and modulates its activity. Plant Physiol. **139(4)**:1750-61.

Choi WG, Swanson SJ and Gilroy S (2012). High-resolution imaging of Ca^{2+} , redox status, ROS and pH using GFP biosensors. Plant Journal. **70(1)**:118-28.

Cunningham KW, and Fink GR (1994). Calcineurin-dependent growth control in *Saccharomyces cerevisiae* mutant lacking PMC1, a homolog of plasma membrane Ca^{2+}-ATPases. Journal of Cell Biology; **124**: 351-363.

D'Angelo C, Weinl S, Batistič O, Pandey GK, Cheong YH, Schültke S, Albrecht V, Ehlert B, Schulz B, Harter K, Luan S, Bock R, and Kudla J (2006). Alternative complex formation of the Ca^{2+}-regulated protein kinase CIPK1 controls abscisic acid-dependent and –independent stress responses in *Arabidopsis*. Plant Journal; **48**: 857–872.

Dammann C, Ichida A, Hong B, Romanowsky SM, Hrabak EM, Harmon AC, Pickard BG and Harper JF (2003). Subcellular targeting of nine calcium-dependent protein kinase isoforms from *Arabidopsis*. Plant Physiology. **132**: 1840–1848.

De Falco TA, Bender KW and Snedden WA (2010). Breaking the code: Ca^{2+} sensors in plant signalling. Biochem. Journal. **425**:27-40.

De Michelis MI, Carnelli A and Rasi-Caldogno, F (1993). The Ca^{2+} pump of the plasma membrane of *Arabidopsis thaliana*: characteristics and sensitivity to fluorescein derivatives. Botanical Acta. **106**: 20-25.

Di Leva F, Domi T, Fedrizzi L, Lim D and Carafoli E (2008). The plasma membrane Ca^{2+}-ATPase of animal cells: structure, function and regulation. Arch. Biochem. Biophys. **476**: 65-74.

Dunkley TPJ, Hester S, Shadforth IP, Runions J, Weimar T, Hanton SL, Griffin JL, Bessant C, Brandizzi F, Hawes C, Watson RB, Dupree P and Lilley KS (2006) Mapping the *Arabidopsis* organelle proteome. Proceedings of the National Academy of Science USA. **103**: 6518-6523.

Ettinger WF, Clear AM, Fanning KJ and Peck ML (1999). Identification of a $Ca^{2+/}H^{+}$ antiport in the plant chloroplast thylakoid membrane. Plant Physiol. **119(4)** :1379-86.

Falchetto, R., Vorherr, T., Brunner, J., Carafoli, E. (1991). The plasma membrane Ca^{2+} pump contains a site that interacts with its calmodulin-binding domain. Journal of Biological Chemistry. **266**: 2930-2936.

Falchetto, R., Vorherr, T., Carafoli, E. (1992). The calmodulin-binding site of the plasma menbrane Ca^{2+} pump interacts with the transduction domain of the enzyme. Protein Science **1**: 1613-1621.

Franz S, Ehlert B, Liese A, Kurth J, Cazalé AC, Romeis T (2011). Calcium-dependent protein kinase CPK21 functions in abiotic stress response in *Arabidopsis thaliana*. Mol. Plant. **4**:83-96.

Fuglsang AT, Guo Y, Cuin TA, Qiu Q, Song C, Kristiansen KA, Bych K, Schulz A, Shabala S, Schumaker KS, Palmgren MG, and Zhu JK (2007). *Arabidopsis* protein kinase PKS5 inhibits the plasma membrane H^{+}-ATPase by preventing interaction with 14-3-3 protein. Plant Cell. **19**: 1617–1634.

Fusca T, Bonza MC, Luoni L, Meneghelli S, Marrano C and De Michelis MI (2009) Single point mutations in the small cytoplasmic loop of ACA8, a plasma membrane Ca^{2+}-ATPase of *Arabidopsis thaliana*, generate partially deregulated pumps. Journal of Biological Chemistry. **284**: 30881-30888.

Geiger D, Becker D, Voslo D, Gambale F, Palme K, Rehers M, Anschuetz U, Dreyer I, Kudla J and Hedrich R (2009). Heteromeric AtKC1/AKT1 channels in *Arabidopsis* roots facilitate growth under K^+-limiting conditions. Journal Biol. Chem. **284**: 21288–21295.

Geisler, **M., Frangne, N., Malmström, S., Gomès, E., Smith, J.A.C., Martinoia, E. and Palmgren, M.G.** (2000a). The ACA4 gene of Arabidopsis encodes a vacuolar calcium pump that is involved in calcium signalling upon salt stress. Plant Physiol **124**: 1814-1827.

Geisler, **M., Axelsen, K., Harper, J.F. and Palmgren, M.G.** (2000b). Molecular aspects of higher plant P-type Ca^{2+}-ATPases. Biochim. Biophis. Acta **1465**: 52-78.

Gelli A and Blumwald E (1997). Hyperpolarization-activated Ca^{2+} permeable channels in the plasma membrane of tomato cells. J. Membr. Biol. **155**:35–45.

Gelli A, Higgins VJ and Blumwald E (1997). Activation of plant plasma membrane Ca^{2+} permeable channels by race-specific fungal elicitors. Plant Physiol. **113**: 269–279.

George, L., Romanowsky, S.M., Harper, J.F., Sharrok, R.A. (2008). The ACA10 Ca^{2+}-ATPase regulates adult vegetative development and inflorescence architecture in Arabidopsis. Plant Physiol **146**: 716-728.

Halfter U, Ishitani M and Zhu JK (2000). The *Arabidopsis* SOS2 protein kinase physically interacts with and is activated by the calcium-binding protein SOS3. Proc. Natl. Acad. Sci. USA **97**: 3735–3740.

Harmon AC (2003). Calcium-regulated protein kinases of plants. Gravit Space Biol Bull. **16(2)**:83-90.

Harper JF, Breton G and Harmon A (2004). Decoding Ca^{2+} signals
through plant protein kinases. Annu. Rev. Plant Biol. **55**: 263–288.

Harthill JE, Meek SE, Morrice N, Peggie MW, Borch J, Wong BH, Mackintosh C (2006). Phosphorylation and 14-3-3 binding of *Arabidopsis* trehalose-phosphate synthase 5 in response to 2-deoxyglucose. Plant Journal; **47(2)**:211-23.

Hashimoto K, Eckert C, Anshütz U, Scholz M, Held K, Waadt R, Reyer A, Hippler M, Becker D, Kudla J (2012). Phosphorylation of calcineurin B-like (CBL) calcium sensor proteins by their CBL-interacting protein kinases (CIPKs) is required for full activity of CBL-CIPK complexes toward their target proteins. The Journal of Biological Chemistry; **287**: 7956-7968.

Hashimoto K and Kudla J (2011). Calcium decoding mechanism in plants. Biochimie; **93**: 2054-2059.

Hirschi KD, Korenkov VD, Wilganowski NL, and Wagner GJ (2000). Expression of *Arabidopsis* CAX2 in tobacco. Altered metal accumulation and increased manganese tolerance. Plant Physiol. **124**: 125–133.

Hong B, Ichida A, Wang Y, Gens JS, Pickard BG and Harper JF (1999). Identification of a calmodulin-regulated Ca^{2+}-ATPase in the endoplasmic reticulum. Plant Physiology. **119**:1165-1175.

Hwang I, Ratterman DM and Sze H (1997) Distinction between endoplasmic reticulum-type and plasma membrane-type Ca^{2+} pumps. Partial purification of a 120-kilodalton Ca^{2+-}ATPase from endomembranes. Plant Physiology. **113**: 535-548.

Hwang I, Sze H and Harper JF (2000). A calcium-dependent protein kinase can inhibit a calmodulin-stimulated Ca^{2+} pump (ACA2) located in the endoplasmic reticulum of *Arabidopsis*. Proc. Natl. Acad. Sci. USA **97**: 6224–6229.

Iwano M, Ngo QA, Entani T, Shiba H, Nagai T, Miyawaki A, Isogai A, Grossniklaus U, Takayama S (2012). Cytoplasmic Ca^{2+} changes dynamically during the interaction of the pollen tube with synergid cells. Development. **139(22)**:4202-9.

Jones AME, MacLean D, Studholme DJ, Sanz A, Andreasson E, Rathjen JP, Peck SC (2009). Phosphoproteomic analysis of nucleienriched fractions from *Arabidopsis thaliana*. Journal of Proteomics; **72**: 439–451.

Kasai M and Muto S (1990). Ca^{2+} pump and Ca^{2+}/H^+ antiporter in plasma membrane vesicles isolated by aqueous two-phase partitioning from corn leaves. J. Membr. Biol. **114**: 133–142.

Kaufman Katz A, **Glusker JP, Beebe SA and Bock CW** (1996). Calcium Ion Coordination: A Comparison with That of Beryllium, Magnesium, and Zinc. Journal Am. Chem. Soc. **118 (24**):5752–5763.

Kim BG, Waadt R, Cheong YH, Pandey GK, Dominguez-Solis JR, Schultke S, Lee SC, Kudla J and Luan S (2007). The calcium sensor CBL10 mediates salt tolerance by regulating ion homeostasis in *Arabidopsis*. Plant Journal. **52**: 473–484.

Klimecka M and Muzyńska G (2007). Structure and function of plant calcium-dependent protein kinases. Acta Biochimica Polonica. **54(2)**: 219-233.

Kolukisaoglu U, Weinl S, Blazevic D, Batistič O and Kudla J (2004). Calcium sensors and their interacting protein kinases: genomics of the *Arabidopsis* and rice CBL-CIPK signaling networks. Plant Physiol. **134**: 43–58.

Kosuta S, Hazledine S, Sun J, Miwa H, Morris RJ, Downie JA and Oldroyd GE (2008). Differential and chaotic calcium signatures in the symbiosis signaling pathway of legumes. Proc. Natl. Acad. Sci. USA. **105**: 9823–9828.

Krebs M, Held K, Binder A, Hashimoto K, Herder GD, Parniske M, Kudla J and Schumacher K (2012). FRET-based genetically encoded sensors allow high-resolution live cell imaging of Ca^{2+} dynamics. The Plant Journal. **69**:181–192.

Kudla J, Batistič O, Hashimoto K (2010). Calcium signals: the lead currency of plant information processing. Plant Cell; **22**: 541-63.

Kuhlbrandt W (2004). Biology, Structure and Mechanism of P-type ATPases. Mol. Cell. Biol. **5**: 282:295.

Lee SM, Kim HS, Han HJ, Moon BC, Kim CY, Harper JF and Chung WS (2007). Identification of a calmodulin-regulated autoinhibited Ca^{2+}-ATPase (ACA11) that is located to vacuole membranes in *Arabidopsis*. FEBS Lett. **581**: 3943-3949.

Li L, Kim BG, Cheong YH, Pandey GK and Luan S (2006). A Ca^{2+} signaling pathway regulates a K^+ channel for low-K response in *Arabidopsis*. Proc. Natl. Acad. Sci. USA. **103**: 12625–12630.

Li X, Chanroj S, Wu Z, Romanowsky SM, Harper JF and Sze H (2008). A distinct endosomal Ca^{2+}/Mn^{2+} pump affects root growth through the secretory process. Plant Physiol. **147**: 1675–1689.

Liang F, Cunningham KW, Harper JF and Sze H (1997). ECA1 complements yeast mutants defective in Ca^{2+} pumps and encodes an endoplasmic reticulum-type Ca^{2+}-ATPase in *Arabidopsis thaliana*. Proc. Natl. Acad. Sci. USA. **94**: 8579–8584.

Liu, J., and Zhu, J.K. (1998). A calcium sensor homolog required for plant salt tolerance. Science. **280**: 1943–1945.

Loro G, Drago I, Pozzan T, Schiavo FL, Zottini M and Costa A (2012). Targeting of Cameleons to various subcellular compartments reveals a strict cytoplasmic/mitochondrial Ca^{2+} handling relationship in plant cells. Plant Journal. **71(1)**:1-13.

Lu CA, Lin CC, Lee KW, Chen JL, Huang LF, Ho SL, Liu HJ, Hsing YI and Su-May Yu (2007). The SnRK1A protein kinase plays a key role in sugar signaling during germination and seedling growth of rice. The Plant Cell; **19**: 2484–2499

Luan S (2009). The CBL-CIPK network in plant calcium signaling. Trends Plant Sci. **14**: 37–42.

Lucca N and Léon G (2012). *Arabidopsis* ACA7, encoding a putative auto-regulated Ca^{2+}-ATPase, is required for normal pollen development. Plant Cell. Rep. **31**:651-659.

Luoni, L., Bonza, M.C., De Michelis, M. I. (2000). H^+/Ca^{2+} exchange driven by the plasma membrane Ca^{2+}-ATPase of *Arabidopsis thaliana* reconstituted in proteoliposomes after calmodulin-affinity purification. FEBS Lett. **24174**: 225-230.

Luoni L, Bonza MC and De Michelis MI (2006). Calmodulin/Ca^{2+}-ATPase interaction at the *Arabidopsis thaliana* plasma membrane is dependent on calmodulin isoform showing isoform-specific Ca^{2+} dependencies. Physiologia Plantarum. **126**: 175-186.

Luoni L, Meneghelli S, Bonza MC, and De Michelis MI (2004). Auto-inhibition of *Arabidopsis thaliana* plasma membrane Ca^{2+}-ATPase involves an interaction of the N-terminus with the small cytoplasmic loop. FEBS Letters; **574**: 20-24.

Malmström S, Askerlund P and Palmgren MG (1997). A calmodulin stimulated Ca^{2+}-ATPase from plant vacuolar membranes with a putative regulatory domain at its N-terminus. FEBS Letters. **400**: 324-328.

Malmström S., Akerlund, H.E. and Askerlund, P. (2000). Regulatory role of the N terminus of the vacuolar calcium-ATPase in cauliflower. Plant Physiol. **122**: 517-526.

Martìn ML and Busconi L (2000). Membrane localisation of a rice calcium-dependent protein kinase (CDPK) is mediated by myristoylation and palmytoylation. Plant Journal. **24**:429-435.

McAinsh MR, Webb A, Taylor JE and Hetherington AM (1995). Stimulus-induced oscillations in guard cell cytosolic free calcium. Plant Cell. **7**: 1207–1219.

McAinsh MR and Pittman JK (2009). Shaping the calcium signature. New Phytology; **181 (2)**: 275-294.

Meneghelli S, Fusca T, Luoni L, De Michelis MI (2008). Dual mechanism of activation of plant plasma membrane Ca^{2+}-ATPase by acidic phospholipids: evidence for a phospholipid binding site which overlaps the calmodulin-binding site. Molecular Membrane Biology; **25**:539-46.

Miyawaki A, Llopis J, Heim R, McCaffery JM, Adams JA, Ikura M and Tsien RY (1997). Fluorescent indicators for Ca^{2+} based on green fluorescent proteins and calmodulin. Nature. **388**:882–887.

Mills RF, Doherty ML, Lopez-Marques RL, Weimar T, Dupree P, Palmgren MG, Pittman JK and Williams LE(2008). ECA3, a Golgi-localized P2A-type ATPase, plays a crucial role in manganese nutrition in *Arabidopsis*. Plant Physiol. **146**: 116–128.

Nakagami H, Sugiyama N, Mochida K, Daudi A, Yoshida Y, Toyoda T, Tomita M, Ishihama Y and Shirasu K (2010). Large-scale comparative phosphoproteomics identifies conserved phosphorylation sites in plants. Plant Physiology; **153**: 1161–1174.

Niittylä T, Fuglsang AT, Palmgren MG, Frommer WB and Schulze WX (2007). Temporal analysis of sucrose-induced phosphorylation changes in plasma membrane proteins of *Arabidopsis*. Molecular Cell Proteomics; **6 (10)**: 1711-1726.

Nühse TS, Bottrill A, Jones AME and Peck SC (2007). Quantitative phosphoproteomics analysis of plasma membrane proteins reveals regulatory mechanisms of plant innate immune responses. Plant Journal; **51**: 931–940.

Nühse TS, Stensballe A, Jensen ON, Peck SC (2004). Phosphoproteomics of the *Arabidopsis* plasma membrane and a new phosphorylation site database. Plant Cell; **16**: 2394–2405.

Nühse TS, Stensballe A, Jensen ON and Peck SC (2003). Large-scale analysis of in vivo phosphorylated membrane proteins by immobilized metal ion affinity chromatography and mass spectrometry. Molecular and Cellular Proteomics; **2**: 1234–1243.

Palmgren MG and Nissen P (2011). P-type ATPases. Annual Rev. Biophys. **40**: 243-266.

Pandey GK, Cheong YH, Kim B, Grant JJ, Li L and Luan S (2007). CIPK9: a calcium sensor-interacting protein kinase required for low-potassium tolerance in *Arabidopsis*. Cell Research; **17**:411-421.

Penniston, J.T., Enyedi, A. (1998). Modulation of the plasma membrane Ca^{2+} pump. J. Membr. Biol. **165**: 101-109.

Pittman JK, Bonza MC and De Michelis MI (2010) Ca^{2+} pumps and Ca^{2+} antiporters in plant development. In: **M. Geisler & K. Venema (Eds).** *Transporters and pumps in plant signalling*. Springer-Verlag, Berlin, Heidelberg, D.

Polge C and Thomas M (2006). SNF1/AMPK/SnRK1 kinases, global regulators at the heart of energy control? Trends in Plant Science; **12(1)**: 20-28.

Qin Y, Li X, Guo M, Deng K, Lin J, Tang D, Guo X and Liu X (2008). Regulation of salt and ABA responses by CIPK14, a calcium sensor interacting protein kinase in Arabidopsis. Sci China C Life Sci. **51(5)**:391-401.

Qiu QS, Guo Y, Dietrich MA, Schumaker KS and Zhu JK (2002). Regulation of SOS1, a plasma membrane Na^+/H^+ exchanger in *Arabidopsis thaliana*, by SOS2 and SOS3. Proc. Natl. Acad. Sci. USA. **99**: 8436–8441.

Qudeimat E, Faltusz AM, Wheeler G, Lang D, Brownlee C, Reski R and Frank W (2008). A PIIB-type Ca^{2+}-ATPase is essential for stress adaptation in *Physcomitrella patens*. Proc. Natl. Acad. Sci. USA. **105**: 19555–19560.

Reiland S, Messerli G, Baerenfaller K, Gerrits B, Endler A, Grossman J, Gruissem W and Baginsky S (2009). Large scale *Arabidopsis* phosphoproteomic profiling reveals novel choloroplast kinase substrates and phosphorylation networks. Plant Physiology; **150**: 889–903.

Rincón-Zachary M, Teaster ND, Sparks JA, Valster AH, Motes CM and Blancaflor EB (2010). Fluorescence resonance energy transfer-sensitized emission of yellow cameleon 3.60 reveals root zone-specific calcium signatures in *Arabidopsis* in response to aluminum and other trivalent cations. Plant Physiol. **152(3)**:1442-58.

Romani G, Bonza MC, Filippini I, Cerana M, Beffagna N and De Michelis M.I. (2004). Involvement of the plasma membrane Ca^{2+}-ATPase in the short term response of *Arabidopsis thaliana* cultured cells to oligogalacturonides. Plant Biology; **6**:192-200.

Sanders D, Brownlee C and Harper JF (1999). Communicating with calcium. Plant Cell; **11**: 691-706.

Sanders D, Pelloux J, Brownlee C and Harper JF (2002). Calcium at the crossroads of signaling. Plant Cell; supplement: 401-417.

Schiǿtt M, Romanowsky SM, Bǽkgaard L, Jakobsen MK, Palmgren MG and Harper JF (2004) A plant plasma membrane Ca^{2+} pump is required for normal pollen tube growth and fertilization. PNAS. **101(25)**: 9502-9507.

Schiǿtt M and Palmgren MG (2005). Two plant Ca^{2+} pump expressed in stomatal guard cells show opposite expression patterns during cold stress. Physiologia Plantarum; **124**: 278-283.

Shigaki T, Rees I, Nakhleh L and Hirschi KD (2006). Identification of three distinct phylogenetic groups of CAX cation/proton antiporters. Journal Mol. Evol. **63**: 815–825.

Schumaker KS and Sze H (1986). Calcium transport into the vacuole of oat roots. Characterization of H^+/Ca^{2+} exchange activity. Jurnal Biol. Chem. **261**:12172–12178.

Spalding EP and Harper JF (2011) The ins and outs of cellular Ca^{2+} transport. Current Opininion in Plant Biology; **14**:715-20.

Sugiyama N, Nakagami H, Mochida K, Daudi A, Tomita M, Shirasu K and Ishihama Y(2008). Large-scale phosphorylation mapping reveals the extent of tyrosine phosphorylation in *Arabidopsis*. Molecular Systems Biology; **4**: article 193.

Sze, H., Liang, F., Hwang, I., Curran, A.C. and Harper J.F. (2000). Diversity and regulation of plant Ca^{2+} pumps: insights from expression in yeast. Ann. Rev. Plant Physiol. Plant Mol. Biol. **51**: 433-462.

Tanaka K, Swanson SJ, Gilroy S and Stacey G (2010). Extracellular nucleotides elicit cytosolic free calcium oscillations in *Arabidopsis*. Plant Physiol. **154(2)**:705-19.

Thion L, Mazars C, Nacry P, Bouchez D, Moreau M, Ranjev R and Thuleau P (1998). Plasma membrane depolarization activated calcium channels, stimulated by microtubule-depolymerizing drugs in wild-type Arabidopsis thaliana protoplasts, display constitutively large activities and a longer half-life in ton 2 mutant cells affected in the organization of cortical microtubules. Plant Journal. **13**: 603–610.

Toyoshima, C., and Inesi, G. (2004a). Structural basis of ion pumping by Ca^{2+}-ATPase of the sarcoplasmic reticulum. Annu. Rev. Biochem. **73**: 269-92.

Waadt R, Schmidt LK, Lohse M, Hashimoto K, Bock R and Kudla J (2008). Multicolor bimolecular fluorescence complementation reveals simultaneous formation of alternative CBL-CIPK complexes *in planta*. Plant Journal; **56**: 505–516.

Webb AAR, McAinsh MR, Taylor JE and Hetherington AM (1996). Calcium ions as intracellular second messengers in higher plants. Adv. Bot. Res. **22**: 45–96.

Weinl S and Kudla J (2009). The CBL-CIPK Ca^{2+}-decoding signalling network: Function and perspectives. New Phytol. **184**: 517–528.

White PJ and Broadley MR (2003). Calcium in plants. Annals of Botany **92**: 487-511.

Whiteman S, Serazetdinova L, Jones AME, Sanders D, Rathjen J, Peck SC, Maathuis FJM (2008). Identification of novel proteins and phosphorylation sites in a tonoplast enriched membrane fraction of *Arabidopsis thaliana*. Proteomics; **8**: 3536–3547.

Williams LE, Schueler SB and Briskin DP (1990). Further characterization of the red beet plasma membrane Ca^{2+}-ATPase using GTP as an alternative substrate. Plant Physiology. **92**: 747-1754.

Wu Z, Liang F, Hong B, Young JC, Sussman MR, Harper JF and Sze H. (2002). An Endoplasmic Reticulum-Bound Ca^{2+}/Mn^{2+} Pump, ECA1, Supports Plant Growth and Confers Tolerance to Mn^{2+} Stress. Plant Physiology. **130**: 128-137.

Xu J, Li HD, Chen LQ, Wang Y, Liu LL, He L and Wu WH (2006). A protein kinase, interacting with two calcineurin B-like proteins, regulates K^+ transporter AKT1 in *Arabidopsis*. Cell. **125**: 1347–1360.

Zhu SY, Yu XC, Wang XJ, Zhao R, Li Y, Fan RC, Shang Y, Du SY, Wang WF, Wu FQ, Xu YH, Zhang XY and Zhang DP (2007). Two calcium-dependent protein kinases, CPK4 and CPK11, regulate abscisic acid signal transduction in *Arabidopsis*. Plant Cell. **19**: 3019–3036.

Zielinski RE (1998). Calmodulin and calmodulin-binding proteins in plants. Annu. Rev. Plant Physiol. Plant Mol. Biol. **49**: 697-725.

PART II

Published paper

Phosphorylation of serine residues in the N-terminus modulates the activity of ACA8, a plasma membrane Ca^{2+}-ATPase of *Arabidopsis thaliana*.

Giacometti* S, Marrano* CA, Bonza MC, Luoni L, Limonta M and De Michelis MI.

Journal of Experimental Botany; (2012) **63**: 1215–1224.

Journal of Experimental Botany, Vol. 63, No. 3, pp. 1215–1224, 2012
doi:10.1093/jxb/err346 Advance Access publication 16 November, 2011
This paper is available online free of all access charges (see http://jxb.oxfordjournals.org/open_access.html for further details)

Journal of
Experimental
Botany
www.jxb.oxfordjournals.org

RESEARCH PAPER

Phosphorylation of serine residues in the N-terminus modulates the activity of ACA8, a plasma membrane Ca^{2+}-ATPase of *Arabidopsis thaliana*

Sonia Giacometti*, Claudia Adriana Marrano*, Maria Cristina Bonza, Laura Luoni, Margherita Limonta and Maria Ida De Michelis†

Dipartimento di Biologia 'L. Gorini', Università degli Studi di Milano, Istituto di Biofisica del CNR, Sezione di Milano, via G. Celoria 26, 20133 Milano, Italy

* These authors contributed equally to this work.
† To whom correspondence should be addressed. E-mail: mariaida.demichelis@unimi.it

Received 20 September 2011; Revised 20 September 2011; Accepted 4 October 2011

Abstract

ACA8 is a plasma membrane-localized isoform of calmodulin (CaM)-regulated Ca^{2+}-ATPase of *Arabidopsis thaliana*. Several phosphopeptides corresponding to portions of the regulatory N-terminus of ACA8 have been identified in phospho-proteomic studies. To mimic phosphorylation of the ACA8 N-terminus, each of the serines found to be phosphorylated in those studies (Ser19, Ser22, Ser27, Ser29, Ser57, and Ser99) has been mutated to aspartate. Mutants have been expressed in *Saccharomyces cerevisiae* and characterized: mutants S19D and S57D—and to a lesser extent also mutants S22D and S27D—are deregulated, as shown by their low activation by CaM and by tryptic cleavage of the N-terminus. The His-tagged N-termini of wild-type and mutant ACA8 (6His-^{1}M-I^{116}) were expressed in *Escherichia coli*, affinity-purified, and used to analyse the kinetics of CaM binding by surface plasmon resonance. All the analysed mutations affect the kinetics of interaction with CaM to some extent: in most cases, the altered kinetics result in marginal changes in affinity, with the exception of mutants S57D (K_D ~10-fold higher than wild-type ACA8) and S99D (K_D about half that of wild-type ACA8). The ACA8 N-terminus is phosphorylated *in vitro* by two isoforms of *A. thaliana* calcium-dependent protein kinase (CPK1 and CPK16); phosphorylation of mutant 6His-^{1}M-I^{116} peptides shows that CPK16 is able to phosphorylate the ACA8 N-terminus at Ser19 and at Ser22. The possible physiological implications of the subtle modulation of ACA8 activity by phosphorylation of its N-terminus are discussed.

Key words: *Arabidopsis thaliana*, Ca^{2+}-ATPase, calcium-dependent protein kinase, calmodulin, plasma membrane, phosphorylation.

Introduction

Cytosolic calcium is a key element in the transduction of a variety of endogenous and environmental signals in plant cells. An increasing amount of evidence indicates that signal specificity is encoded by the amplitude, frequency, and time extension of cytosolic Ca^{2+} waves, which in turn depend on the activity of Ca^{2+} channels—which when open flood the cytosol with Ca^{2+} from the apoplast and/or intracellular stores—and of active Ca^{2+} transporters—which extrude Ca^{2+} to the apoplast or sequester it in intracellular stores. Fine-tuning of the Ca^{2+} transport systems in response to different signals is thus a crucial feature of Ca^{2+}-mediated signal transduction (Sanders *et al.*, 2002; Boursiac and Harper, 2007; McAinsh and Pittman, 2009; Das and Pandey, 2010; Dodd *et al.*, 2010; Bonza and De Michelis, 2011; Pittman *et al.*, 2011).

In plant cells, Ca^{2+} extrusion from the cytoplasm is accomplished either through tonoplast-localized Ca^{2+}–H^+ antiporters powered by a proton-motive force, or through

---

Abbreviations: BSA, bovine serum albumin; Brij 58, polyoxyethylene 20 cethyl ether; BTP, BIS TRIS propane {1-3-bis[tris(hydroxymethyl)methylamino]propane}; CaM, calmodulin; IPTG, isopropyl-β-D-thiogalactopyranoside; NTA, nitrilotriacetic acid; PM, plasma membrane; PMSF, phenylmethylsulphonyl fluoride; WT, wild type.

© 2011 The Author(s).

This is an Open Access article distributed under the terms of the Creative Commons Attribution Non-Commercial License (http://creativecommons.org/licenses/by-nc/3.0), which permits unrestricted non-commercial use, distribution, and reproduction in any medium, provided the original work is properly cited.

Ca^{2+} pumps powered by ATP hydrolysis, localized both at the plasma membrane (PM) and at intracellular membranes. PM Ca^{2+} pumps are likely to play a crucial role in re-establishing the low basal Ca^{2+} concentration especially after its increase due to opening of PM Ca^{2+} channels. Indeed, the available evidence, albeit fragmentary, demonstrates their involvement in fundamental processes such as development, hormonal regulation, and response to biotic and abiotic stresses; however, their physiological role and the mechanisms underlying their regulation in response to specific signals have not been ascertained yet (Boursiac and Harper, 2007; Bonza and De Michelis, 2011; Pittman *et al.*, 2011).

PM Ca^{2+} pumps are calmodulin (CaM)-regulated Ca^{2+}-ATPases, belonging to the P-type ATPase superfamily: three isoforms of CaM-regulated Ca^{2+}-ATPase, all belonging to the same cluster, have been identified as PM-localized pumps in *Arabidopsis thaliana*: among these, the best characterized at the biochemical level is ACA8, a widely expressed isoform found in all plant organs (Bonza and De Michelis, 2011; Pittman *et al.*, 2011).

ACA8, like other plant isoforms of CaM-regulated Ca^{2+}-ATPases, has an extended cytosolic N-terminal domain containing an autoinhibitory domain partially overlapping the CaM-binding site: CaM binding suppresses the autoinhibitory action of the N-terminal domain and determines both the increase of V_{max} and the decrease of the $K_{0.5}$ for free Ca^{2+} (Bonza and De Michelis, 2011; Pittman *et al.*, 2011).

ACA8 is also regulated by acidic phospholipids such as phosphatidylserine or phosphatidylinositol-4P, which activate the pump via two distinct mechanisms, involving their binding to different sites: acidic phospholipids binding to a site in the protein N-terminus, overlapping the autoinhibitory and CaM-binding domain, stimulates ACA8 activity similar to CaM or to cleavage of the N-terminus, while their binding to a second, as yet unidentified, site further stimulates ACA8 activity by lowering its $K_{0.5}$ for free Ca^{2+} (Meneghelli *et al.*, 2008).

CaM-regulated Ca^{2+}-ATPases can also be modulated by phosphorylation. In the pumps of animal cells, which have the regulatory domain localized at the extended C-terminus, the C-terminal portion is the target of phosphorylation by different protein kinases that phosphorylate different amino acids in different isoforms: each phosphorylation event has a peculiar effect on the pump activity (Enyedi *et al.*, 1996, 1997; Penniston and Enyedi, 1998; Verma *et al.*, 1999). In plants, it has been shown that *in vitro* phosphorylation of a serine residue just downstream the CaM-binding site of ACA2—an *A. thaliana* isoform of the endoplasmic reticulum—by a calcium-dependent protein kinase (CDPK) severely inhibits CaM-stimulated enzyme activity, without disrupting CaM binding (Hwang *et al.*, 2000). Also the N-terminus of BCA1—an isoform of CaM-regulated Ca^{2+}-ATPase of the tonoplast of *Brassica oleracea*—can be phosphorylated *in vitro* by protein kinase C at two serine residues, one within the CaM-binding domain, but the effect of phosphorylation on pump activity was not determined (Malmström *et al.*, 2000).

Data from large-scale phospho-proteomic studies have identified several phosphopeptides corresponding to portions of the N-terminus of ACA8. In particular (Table 1), four serine residues that are phosphorylated (S19, S22, S27, and S29) are localized ~20 amino acids upstream of the CaM-binding and autoinhibitory domain, one (S57) is within the CaM-binding site, and one (S99) is 30 amino acids downstream (Nühse *et al.*, 2003, 2004, 2007; Benschop *et al.*, 2007; Niittylä *et al.*, 2007; Sugiyama *et al.*, 2008; Whiteman *et al.*, 2008; Jones *et al.*, 2009; Reiland *et al.*, 2009; Chen *et al.*, 2010; Nakagami *et al.*, 2010). For some of these residues, evidence has also been provided that phosphorylation is up-regulated by hormones such as abscisic acid and gibberellins (S27 and S29; Chen *et al.*, 2010) or by elicitors such as flagellin (S27 and S99; Nühse *et al.*, 2003, 2004, 2007; Benschop *et al.*, 2007), or down-regulated in response to sucrose administration to cultured cells (S22; Niittylä *et al.*, 2007). Since these serine residues are not conserved in most isoforms of *A. thaliana* ACA, phosphorylation of any of them could represent an isoform-specific mechanism of regulation of pump activity.

Here it is shown that substitution of any of the above-mentioned serine residues with aspartate, which mimics the effect of phosphorylation, affects the regulatory properties of ACA8, generating partially deregulated pumps (mutants S19D, S57D, and, to a lesser extent, mutants S22D and S27D), modifying the kinetics of interaction with CaM (all tested mutations), and/or changing the affinity for CaM (S57D and S99D mutants). It is also shown that the ACA8 N-terminus is phosphorylated *in vitro* by CDPK (Harper *et al.*, 2004; Das and Pandey, 2010) at Ser19 and Ser22.

Table 1. Serine residues in the ACA8 N-terminus that have been found to be phosphorylated in vivo

Phosphorylated residue	Plant material	Effectors	Reference
Ser19	Cultured cells		Nühse *et al.* (2003, 2004)
Ser22	Cultured cells	Sucrose (–)	Nühse *et al.* (2003, 2004); Niittyla *et al.* (2007); Sugiyama *et al.* (2008); Nakagami *et al.* (2010)
Ser27	Cultured cells, seedlings, shoots, leaves	Abscisic acid (+), flagellin 22 (+)	Nühse *et al.* (2003, 2004, 2007); Benschop *et al.* (2007); Sugiyama *et al.* (2008); Whiteman *et al.* (2008); Jones *et al.* (2009); Reiland *et al.* (2009); Chen *et al.* (2010); Nakagami *et al.* (2010)
Ser29	Cultured cells	Abscisic acid (+), gibberellins (+)	Nühse *et al.* (2003, 2004); Sugiyama *et al.* (2008); Chen *et al.* (2010); Nakagami *et al.* (2010)
Ser57	Cultured cells		Sugiyama *et al.* (2008); Nakagami *et al.* (2010)
Ser99	Cultured cells	Flagellin 22 (+)	Benschop *et al.* (2007)

Materials and methods

Plasmid constructs

Site-directed mutagenesis of ACA8 was conducted using the Quickchange site-directed mutagenesis kit (Stratagene, Santa Clara, CA, USA, catalogue no. 200518) according to the manufacturer's protocol using wild-type (WT) ACA8 full-length cDNA inserted in the pYES2 vector (Invitrogen, Carlsbad, CA, USA, catalogue no. V825-20v) as a template; primers are listed in Supplementary Table S1 available at *JXB* online. Introduction of the correct mutations and absence of errors were confirmed by sequencing.

Standard PCRs performed with GoTaq® polymerase (Promega, Madison, WI, USA, catalogue no. M3175) were used to amplify the first 116 amino acids (^{1}M-I^{116}) at the N-terminus of ACA8 mutants, using mutated ACA8 full-length cDNA as templates and the following specific oligonucleotides: (S) 5′ CTTGGTCATATGACGAGTCTCTTGAAGTC; and (AS) 5′ GCTCGGGATCCTCAAATTCCAAAATCACCAGCC. The S primer contains an *Nde*I restriction site and the AS primer contains a *Bam*HI restriction site (underlined). To produce recombinant WT and mutated N-terminal domains that could later be purified by NTA affinity chromatography, the coding sequences for the N-termini of WT and mutants of ACA8, obtained using the restriction enzymes reported above, were inserted into *Escherichia coli* expression vector pET15b (Merck KGaA, Darmstadt, Germany, catalogue no. 69661), in this way fusing a 6His tag to the N-terminus of the peptide. Introduction of the correct mutations and absence of errors were confirmed by sequencing.

Ps 658 G-CPK1ci and Ps 652 G-CPK16-F399A plasmids encoding, respectively, calcium-independent mutants of isoforms CPK1 and CPK16 of *A. thaliana* CDPK, sandwiched between N-terminal glutathione *S*-transferase (GST) and a C-terminal 6His tag, were kindly provided by Professor J. F. Harper (University of Nevada, Reno, NV, USA).

Yeast transformation and growth media

The DNA coding for WT and mutant ACA8 proteins is inserted in the pYES2 vector (Invitrogen), under the control of a galactose-inducible promoter. Those plasmids were used for transformation of *Saccharomyces cerevisiae* strain K616 (MATα *pmr1::HIS3 pmc1::TRP1 cnb1::LEU2, ade2, ura3*; Cunningham and Fink, 1994) using a lithium acetate/polyethylene glycol method (Bækgaards *et al.*, 2006). Transformants were selected for uracil prototrophy on synthetic complete medium lacking uracil (SC-URA) as described (Bonza *et al.*, 2004). Plant pumps were expressed in yeast grown in SC-URA medium containing 2% (w/v) galactose, 1% (w/v) raffinose, 50 mM succinic acid/TRIS (pH 5.5), 0.7% (w/v) yeast nitrogen base, and 10 mM CaCl$_2$, for 24 h at 30 °C.

Isolation of yeast microsomes

Yeast cells were homogenized and microsomes were harvested as previously reported (Bonza *et al.*, 2004). Protein concentration was determined using the Bio-Rad assay (Bio-Rad, Hercules, CA, USA, catalogue no. 500-001).

Electrophoresis and immunoblotting analysis

SDS–PAGE, western blotting, and immunodecoration with polyclonal antibody against the ACA8 small cytoplasmic loop region were performed as described (Luoni *et al.*, 2004); the antibody does not recognize any protein band in microsomes extracted from K616 yeast transformed with the empty vector (data not shown). Signal quantification was performed using the Fluor-Chem™SP Imaging System and AlphaEaseFC software by Alpha Innotech (MMedical, Cornaredo, MI, Italy).

Trypsin treatment

The microsomal fraction (1 mg protein ml^{-1}) was incubated for 10 min at 25 °C in 0.1 mM EDTA, 0.5 mM ITP, 80 mM BTP (BIS TRIS propane)-HEPES pH 7.0, in the presence or absence of 150 μg ml^{-1} trypsin. The reaction was stopped by addition of a 100-fold excess of soybean trypsin inhibitor. Proteins were precipitated by centrifugation at 20 000 *g* for 1 h at 4 °C. Pellets were resuspended in 25 mM MOPS-KOH pH 7.0, 10% (w/w) glycerol, 5 μg ml^{-1} leupeptin, 10 mM benzamidine, 1 μg ml^{-1} chymostatin, 1 μg ml^{-1} pepstatin. Quantitative and reproducible recovery of proteins was tested using the Bio-Rad assay and western blot signal quantification.

Assays of ACA8 activity

ACA8 activity in yeast microsomes (~2–4 μg of protein per sample) was measured as eosin-sensitive MgITP hydrolysis, taking advantage of the high sensitivity of plant PM Ca^{2+}-ATPase to this inhibitor (De Michelis *et al.*, 1993; Bonza *et al.*, 2004; Fusca *et al.*, 2009). The assay medium contained 80 mM BTP-HEPES pH 7.0, 5 mM (NH$_4$)$_2$SO$_4$, 50 mM KNO$_3$, 1 μM A$_{23187}$, 0.1 mg ml^{-1} Brij58, 1 μg ml^{-1} oligomycin, 2 mM phosphoenolpyruvate, 10 U ml^{-1} pyruvate kinase, and MgSO$_4$ and ITP at a final concentration of 3 mM and 1 mM respectively. The free Ca^{2+} concentration was buffered at 10 μM with 1 mM EGTA. Unless otherwise specified, bovine testes CaM (Sigma, St. Louis, MO, USA, catalogue no. P1431) was supplied at 1 μM. Eosin-sensitive ITPase activity was evaluated as the difference between activity measured in the absence of inhibitor and that measured in the presence of 0.2 μM eosin Y in the assay medium. Samples were incubated at 25 °C for 60 min, during which the reaction proceeds linearly. All the assays were performed at least three times, with three replicates.

Expression and purification of the WT and mutated His-tagged ACA8 N-terminus

Vectors coding for WT and mutated His-tagged ACA8 N-terminus (6His-^{1}M-I^{116}) were used to transform *E. coli* strain BL21(DE3)-pLysE (Merck KGaA, Darmstadt, Germany, catalogue no. 69389-3) by standard procedures. Purification of fusion proteins was performed as described (Luoni *et al.*, 2004).

Surface plasmon resonance

Surface plasmon resonance spectroscopy analysis was performed with a BIAcoreX optical biosensor instrument (Biacore AB, Uppsala, Sweden) as described (Bækgaard *et al.*, 2006; Luoni *et al.*, 2006), but using a free Ca^{2+} concentration of 3.5 μM in the eluent buffer. The His-tagged ACA8 N-termini were injected into the measure flow cell of an NTA sensor chip (Biacore, AB, catalogue no. BR-1004-07) until a resonance response of 300–850 units was obtained. After changing the immobilization buffer with eluent buffer, bovine testes CaM, 50–350 nM in eluent buffer, was injected over the two flow cells. After the dissociation phase, the NTA chip was completely regenerated by injection of regeneration buffer. Results are presented as a reference cell-subtracting sensorgram, a plot of resonance signal changes as a function of time. The data were analysed using BIA evaluation 3.0 software (Biacore AB), and kinetics analyses of primary sensorgrams were carried out by global fitting using a 1:1 Langmuir binding model.

Expression and purification of CPK1 and CPK16

Vectors coding for CPK1 and CPK16 were used to transform *E. coli* strain DH5α by standard procedures. *E. coli* harbouring recombinant plasmids were grown in Luria–Bertani complete medium (GENESPIN, Milan, Italy, catalogue no. STS-LB1000) under ampicillin selection. Overnight cultures grown at 37 °C were diluted 10-fold and grown for 2 h at 28 °C (~0.6 OD$_{600}$) before 0.5 mM isopropyl-β-D-thiogalactopyranoside (IPTG) addition, and growth was continued for 2 h more. All the following steps were carried out at 4 °C. A 400 ml aliquot of culture was centrifuged for 15 min at 3000 *g* and the pellet was suspended in 20 ml of lysis buffer containing 20 mM TRIS-HCl pH 7.8, 500 mM NaCl, and 1 mM phenylmethylsulphonyl fluoride (PMSF). Cells were lysed by the addition of 1 mg ml^{-1} lysozyme, incubation on ice for 15 min, and addition of 0.4% Triton X-100 followed by sonication. Cellular debris and unlysed cells were removed by centrifugation at 12 000 *g* for 10 min. The supernatant was incubated for 30 min with ~1 ml of nickel-NTA–agarose (Qiagen GmbH, Germany, catalogue no. 1018244) on a rocking platform. Resin was pelleted by centrifugation at 3000 *g* for 10 min, washed extensively with 20 mM TRIS-HCl pH 7.8 plus 500 mM NaCl, and eluted with 300 mM imidazole in 20 mM TRIS-HCl pH 6.0 plus 500 mM NaCl. The eluate was diluted 5-fold with GST binding buffer containing 50 mM TRIS-HCl pH 7.4, 150 mM NaCl, 10 mM EDTA, 1 mM dithiothreitol (DTT), and 0.4 % Triton X-100, and incubated for 30 min with 2 ml of glutathione–Sepharose 4B (GE Healthcare Bio-Science AB, Sweden, catalogue no. 20182003-2). Resin was pelleted by centrifugation at 3000 *g* for 10 min and washed extensively with binding buffer, followed by one wash with 50 mM TRIS-HCl pH 7.5. Protein was eluted with 10 mM glutathione in 50 mM TRIS-HCl pH 8.0 and concentrated by centrifugation in 30 000 Da cut-off VIVASPIN6 concentrators (SartoriusStedim Biotech GmbH, Germany, catalogue no. VS0621). Purified enzyme was stored at –80 °C in 50% glycerol, 20 mM TRIS-HCl pH 7.5, 100 mM NaCl, 1 mM DTT. Typically, a purification starting from 400 ml of culture yielded ~0.5–1.5 mg of pure protein, capable of phosphorylating the synthetic substrate Syntide 2 (data not shown).

Kinase assay

The kinase assay was performed in 20 mM TRIS-HCl pH 7.5, 6 mM $MgCl_2$, 0.5 mg ml^{-1} bovine serum albumin (BSA), 1 mg ml^{-1} phosphatidylcholine suspended in buffer by sonication, and 2.8 mM ATP labelled with 0.95 kBq nmol^{-1} [γ-^{32}P]ATP (Perkin-Helmer ITALIA S.p.A., catalogue no. NEG502A250UC), using 2.5 μg of purified enzyme in a 25 μl reaction. Assays were initiated by the addition of 20 μM substrate and transferred from ice to 22 °C controlled temperature for 3 h. Reactions were terminated by solubilization in Laemmli buffer (Laemmli, 1970). For autoradiography, aliquots corresponding to 2–3 μg of purified substrate protein were loaded on to 18% polyacrylamide gel and subjected to SDS–PAGE and blotting as described in Luoni *et al.* (2004). Blots were exposed to Kodak Biomax MS film at 80 °C for 2–4 d. For quantification of phosphate incorporation, 5 μl of each solubilized sample were spotted on a 0.2 μm nitrocellulose filter paper square (GE Healthcare Bio-Science AB, catalogue no. RPN3032D). Filters were immersed in 75 mM phosphoric acid, washed three times (7 min) with the same solution, allowed to dry, and dissolved in 10 ml of Filter Count (Packard, Meriden, CT, USA, catalogue no. 6013149). Radioactivity was measured by liquid scintillation counting (Tri-carb LSC 1500, Packard). Radioactivity associated with samples incubated in the absence of substrate protein was subtracted from the reported data.

Results

Each of the serine residues of ACA8 which have been found to be phosphorylated *in vivo* (Nühse *et al.*, 2003, 2004, 2007; Benschop *et al.*, 2007; Niittylä *et al.*, 2007; Sugiyama *et al.*, 2008; Whiteman *et al.*, 2008; Jones *et al.*, 2009; Reiland *et al.*, 2009; Chen *et al.*, 2010; Nakagami *et al.*, 2010) has been mutated to aspartate whose negative charge mimics phosphorylation, or to alanine to make it non-phosphorylatable. Mutant proteins have been expressed in *S. cerevisiae* strain K616, which is devoid of endogenous Ca^{2+}-ATPases (Cunningham and Fink, 1994), and characterized in the isolated microsomal fraction.

Western blot of the microsomal proteins with an antiserum against a sequence in the small cytoplasmic loop of ACA8 (Luoni *et al.*, 2004) shows that all the proteins were substantially intact (Fig. 1, top panel) and functional (Fig. 1, line a). The expression level of the mutants was evaluated by quantification of signal intensity in western blot of microsomes isolated from at least two yeast inductions (Fig. 1, line b). Expression of most mutants was similar to that of WT ACA8: only the expression level of mutants S57D and S99D was significantly different (60% and 140%, respectively, P <0.05) from that of WT ACA8. Molecular activities (Fig. 1, line c) were computed from the ratio between activity in the presence of CaM (Fig. 1, line a) and signal intensity in western blot (Fig. 1, line b). Molecular activities of the mutants were not significantly different from that of WT ACA8 (values ranged between 50±10% and 163±31% of the WT), indicating that the introduced mutations had no major effect on ACA8 activity.

Effect of S/D mutations on ACA8 autoinhibition

To test the degree of autoinhibition of ACA8 mutants, the effects of CaM on pump activity were evaluated. Figure 2 shows that under the applied experimental conditions, CaM stimulated the activity of WT ACA8 by ~300%. The response to CaM was drastically reduced ($P < 0.01$) in two of the mutants, S19D and S57D, which were stimulated by ~100%; S/A mutation of the same residues only marginally affected CaM stimulation. Mutations of Ser22 and Ser27 generated proteins somewhat less stimulated by CaM (150–180%, $P < 0.05$) than the WT, but in these cases the effect was independent of the substitution made. S/D mutation of residues Ser29 and S99 did not affect ACA8 response to CaM; strangely, the S29A mutant was less stimulated by CaM than the WT and the S29D mutant. This result could suggest that ACA8 was phosphorylated at Ser29 *in vivo* by some yeast kinase. However, mass spectrometric analysis of WT ACA8 purified from yeast microsomes by CaM affinity chromatography (Fusca *et al.*, 2009; Bonza and Luoni, 2010) showed that the protein had not been phosphorylated *in vivo* under the applied yeast growth conditions, with the possible exception of Ser19, which was not identified in any tryptic peptide (data not shown). Thus, the low response to CaM of ACA8 mutants S22A, S27A, and S29A points to the relevance of these serine residues *per se* in determining the amplitude of the response of ACA8 to CaM.

Altogether, the results reported above suggest that the introduction of a negative charge at Ser19 or at Ser57 of ACA8—and, to a lesser extent, also at Ser22 or at Ser27—hampers the autoinhibitory action of the N-terminal domain, generating partially deregulated mutants. Alternative explanations of the low degree of CaM activation in these mutants would be a dramatic loss of affinity for CaM or the inability to shift to the active conformation upon

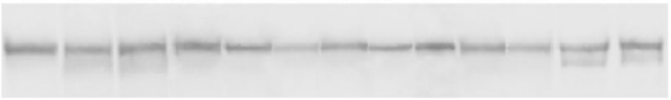

	WT	S19A	S19D	S22A	S22D	S27A	S27D	S29A	S29D	S57A	S57D	S99A	S99D
ACA8 activity[a]	122±11	105 ± 13	220 ± 33	86 ± 6	135 ± 14	109 ± 13	98 ± 11	73 ± 9	94 ± 9	55 ± 7	88 ± 9	76 ± 15	132 ± 26
ACA8 protein[b]	1.0±0.1	0.9 ± 0.1	1.1 ± 0.1	1.0 ± 0.1	1.1 ± 0.1	0.7 ± 0.1	0.9 ± 0.1	1.0 ± 0.2	1.2 ± 0.2	0.9 ± 0.1	0.6 ± 0.1	0.8 ± 0.1	1.4 ± 0.2
ACA8 molecular activity[c]	100± 14	95 ± 15	163 ± 31	70 ± 7	100 ± 12	127 ± 26	89 ± 11	60 ± 14	64 ± 11	50±10	120 ± 24	78 ± 18	77 ± 20

Fig. 1. Expression of single point S/D or S/A ACA8 mutants in yeast strain K616. Top: after SDS–PAGE and blotting, yeast microsomal proteins (4 µg per lane) were immunodecorated with an antiserum against the ACA8 small cytoplasmic loop; the blot shown in the figure is one representative of three or more. Bottom: [a]ACA8 activity (nmol Pi min^{-1} mg^{-1} protein) was measured in the presence of 1 µM CaM. Results are the mean of 3–10 experiments performed on at least two different microsomal membrane preparations, ±SEM. [b]Quantification of ACA8 protein was performed by densitometric scanning analysis of western blots immunodecorated with an antiserum against the ACA8 small cytoplasmic loop, setting the WT value at 1 arbitrary unit; values reported are the mean of at least three quantification analyses performed on at least two different microsomal membrane preparations, ±SEM; variability of WT expression was evaluated by loading six independent microsomal preparations on the same gel. [c]Molecular activities, evaluated as the ratio between ACA8 activity in the presence of CaM and the ACA8 protein level, are expressed as a percentage of that of WT ACA8 ±SEM.

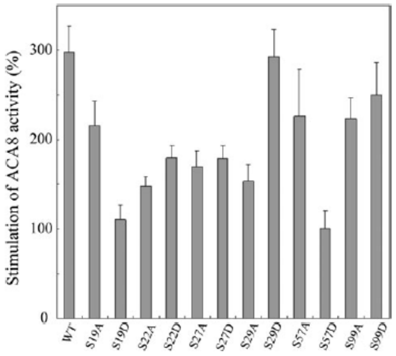

Fig. 2. Stimulation of WT and mutant ACA8 by CaM. ACA8 activity was measured in the presence or absence of 1 µM CaM. Results are shown as percentage stimulation over the activity measured in the absence of added CaM. Values reported are the mean of 3–10 experiments ±SEM.

CaM binding. The finding that the molecular activities in the presence of CaM of the S19D, S22D, S27D, and S57D mutants are similar to that of WT ACA8 (see Fig. 1) makes the latter explanation unlikely. However, if this was the case, these mutants should be as responsive as the WT to tryptic cleavage of the N-terminus (Rasi-Caldogno *et al.*, 1993; Luoni *et al.*, 2004; Fusca *et al.*, 2009; Bonza and De Michelis, 2011). Figure 3 shows that, in agreement with previously reported results (Luoni *et al.*, 2004; Fusca *et al.*, 2009), tryptic cleavage of the N-terminus stimulated the activity of WT ACA8 similarly to CaM and that the two effects were not additive. The same was true for all of the tested mutants, which were equally less stimulated than the WT by CaM and by tryptic cleavage of the N-terminus. *Saccharomyces cerevisiae* strain K616 is unable to grow in Ca^{2+}-deprived media (Cunningham *et al.*, 1994; Bonza *et al.*, 2004; Bækgaards *et al.*, 2006; Fusca *et al.*, 2009). None of the produced mutants was able to complement the phenotype of the K616 yeast strain (data not shown). This result confirms previous observations (Bonza *et al.*, 2004; Bækgaards *et al.*, 2006; Fusca *et al.*, 2009) that only largely deregulated ACA8 mutants allow growth of K616 in the presence of very low Ca^{2+} concentrations.

Effect of S/D mutations on ACA8 affinity for CaM

Preliminary experiments were performed by measuring the effect of increasing concentrations of CaM on the activity of WT and mutant ACA8. Figure 4 shows the results of such an experiment conducted on the S57D ACA8 mutant. The S57D activation curve was shifted to higher CaM concentrations than that of WT ACA8, indicating a lower apparent affinity for CaM of the mutant protein. The activation curves of all the other mutants were roughly similar to that of WT ACA8 (data not shown).

It has previously been shown that mutations which weaken the autoinhibitory interaction of the N-terminus with the catalytic head of the pump can diminish steric hindrance to CaM binding, distorting evaluation of the effect of mutation on ACA8 affinity for CaM as measured by concentration dependence of activation (Fusca *et al.*, 2009). Thus, to determine the effect of the S/D mutations on ACA8 affinity for CaM, the first 116 amino acids of WT or mutant ACA8 fused to a 6His-tag were expressed in *E. coli*, purified, and used for CaM binding measurements by surface plasmon resonance (Bækgaard *et al.*, 2006; Luoni *et al.*, 2006), a technique which allows one to measure not only the affinity of the partners but also the kinetics of interaction.

Figure 5 shows the results of a representative experiment performed on the N-terminus of WT and S57D ACA8: the S57D mutation had no major effect on the rate of complex formation, but drastically increased the rate of complex dissociation, resulting in an increase of the dissociation constant (K_D) from 19 nM to 165 nM (Table 2). All of the other analysed mutations had less dramatic effects on the interaction of the ACA8 N-terminus with CaM (Table 2). The association rate constant (k_a) values of the mutants ranged between half (S22D) and about twice (S19D) that of the N-terminus of WT ACA8. Values of the dissociation rate constant (k_d) of the mutants ranged between about half (S22D and S99D) and about twice (S27D) that of the N-terminus of WT ACA8. For most mutants, the changes of the kinetic parameters brought about only minor changes of the k_d values (e.g. in mutant S22D, the decrease in k_a was largely compensated by the decrease in k_d): only in mutant S99D did the decreased rate of dissociation determine a decrease of the K_D value to about half that of the WT.

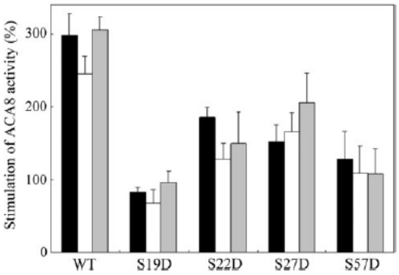

Fig. 3. Effect of controlled proteolysis on the activity of WT and mutant ACA8. The microsomal fraction purified from yeast expressing WT or mutant ACA8 was treated with (white and grey bars) or without (black bars) trypsin as detailed in the Materials and methods; ACA8 activity was measured in the presence (black and grey bars) or absence (white bars) of 1 µM CaM. Results are shown as percentage stimulation over the activity measured in control membranes in the absence of added CaM. Values reported are the mean of 3–5 experiments ±SEM.

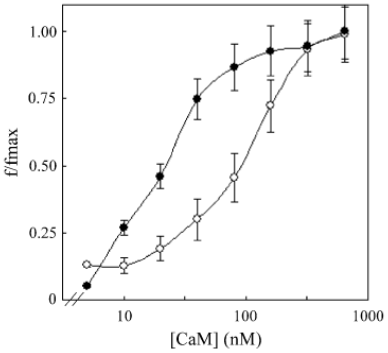

Fig. 4. Stimulation of WT and S57D ACA8 as a function of CaM concentration. Eosin-sensitive ITPase activity of microsomal fractions (2–4 µg of total proteins) from yeast expressing WT (filled circles) and S57D (open circles) ACA8 mutant was measured in the presence of increasing concentrations of exogenous CaM. Activation of WT and S57D ACA8 (f/fmax) is expressed as the ratio between stimulation by CaM at the indicated CaM concentration (f) and maximal stimulation (fmax). Fmax values were 417±23% for WT ACA8 and 93±1% for the S57D mutant. Values reported are the mean of three experiments ±SEM.

Phosphorylation of the ACA8 N-terminus by CDPK

Evidence has been presented that CPK1, an *A. thaliana* isoform of CDPK, phosphorylates a serine residue in the N-terminus of ACA2, an isoform of *A. thaliana* CaM-regulated Ca^{2+}-ATPase localized at the endoplasmic reticulum (Hwang *et al.*, 2000). It was checked whether CPK1 was also able to phosphorylate the N-terminus of ACA8; since CPK1 is localized at peroxisomes, CPK16, a PM-localized *A. thaliana* isoform, was also tested (Dammann *et al.*, 2003). Ca^{2+}-independent mutants (Harper *et al.*, 1994; Vitart *et al.*, 2000) of CPK1 and CPK16 were expressed in *E. coli* sandwiched between N-terminal GST and a C-terminal 6His-tag and purified by two-step affinity chromatography (Harper *et al.*, 1994). Figure 6 shows that both kinases were able to phosphorylate the His-tagged ACA8 N-terminus: upon phosphorylation with CPK16 under the applied conditions, phosphate incorporation was 0.60±0.08 nmol $nmol^{-1}$ of ACA8 N-terminus. To determine which residue(s) of the ACA8 N-terminus are

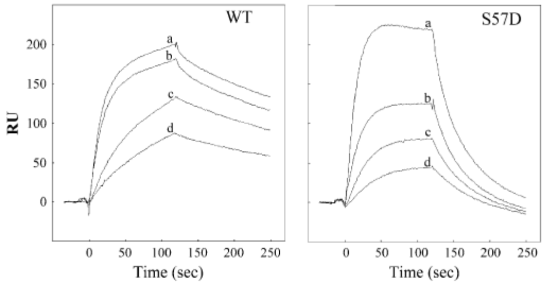

Fig. 5. Kinetics of CaM binding to the N-terminus of WT and S57D ACA8. Phases of the interaction between CaM and peptides 6His-^{1}M-I^{116} derived from WT and S57D ACA8 were registered by surface plasmon resonance spectroscopy, using different concentrations of bovine testes CaM (a=350 nM; b=200 nM; c=100 nM; d=50 nM) as the flowing analyte. The reported signal (RU) is the difference in resonance units between the signal recorded in the measuring cell, with immobilized peptide, and the signal recorded in the peptide-free reference cell.

Table 2. Kinetics of binding of bovine testes CaM to the N-terminus of WT and mutant ACA8 measured by surface plasmon resonance Each value with the corresponding SEM is the average of constants derived from the analysis of at least five binding curves.

	k_a ($\times 10^5$ $M^{-1}s^{-1}$)	k_d ($\times 10^{-3}$ s^{-1})	K_D (nM)
WT	1.27±0.02	2.44±0.01	19.3±0.3
S19D	2.24±0.06	3.25±0.02	14.5±0.4
S22D	0.58±0.02	1.39±0.01	23.9±0.6
S27D	1.96±0.03	5.20±0.03	26.5±0.4
S29D	1.71±0.02	3.82±0.02	22.3±0.2
S57D	1.54±0.01	25.5±0.22	165±1.8
S99D	1.21±0.04	1.37±0.01	11.3±0.4

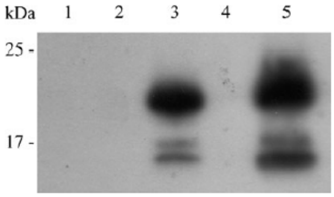

Fig. 6. Phosphorylation of the ACA8 N-terminus by different isoforms of CDPK. The N-terminus of WT ACA8 (6His-^{1}M-I^{116}) was phosphorylated with Ca^{2+}-independent mutants of *A. thaliana* CPK1 or CPK16 as described in the Materials and methods. Samples were solubilized and aliquots corresponding to 3 µg of 6His-^{1}M-I^{116} were subjected to SDS–PAGE, blotting, and autoradiography (lane 1, 6His-^{1}M-I^{116}; lane 2, CPK1; lane 3, 6His-^{1}M-I^{116} plus CPK1; lane 4, CPK16; lane 5, 6His-^{1}M-I^{116} plus CPK16). Results are from one experiment representative of four.

phosphorylated by CPK16, phosphorylation assays were performed on the His-tagged N-termini of ACA8 S/D mutants (Fig. 7, top panel). While mutants S29D, S57D, and S99D were phosphorylated similarly to WT ACA8, the phosphorylation level was drastically reduced in mutant S22D and lower than that of the WT also in mutants S19D and S27D. The fact that none of the mutations abolished ACA8 phosphorylation by CPK16 indicates that the enzyme is able to phosphorylate the ACA8 N-terminus at more than one residue. Since the introduction of the negative charge of the aspartate residue may affect phosphorylation of the neighbouring serine residues, phosphorylation assays were performed on the His-tagged N-termini of ACA8 S/A mutants. The bottom panel of Fig. 7 shows that phosphorylation of ACA8 by CPK16 was strongly reduced by mutations S19A and S22A, while mutant S27A was phosphorylated similarly to the WT.

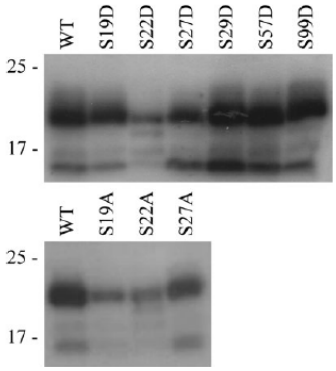

Fig. 7. Phosphorylation of WT and mutant ACA8 N-termini by CPK16. WT or mutant ACA8 N-termini were phosphorylated with a Ca^{2+}-independent mutant of *A. thaliana* CPK16 as described in the Materials and methods. Samples were solubilized and aliquots corresponding to 3 µg (top panel) or 2 µg (bottom panel) of 6His-^{1}M-I^{116} were subjected to SDS–PAGE, blotting, and autoradiography. Results are from one experiment representative of three.

Discussion

The finding that ACA8, a widely expressed isoform of PM Ca^{2+}-ATPase, is phosphorylated *in vivo* at serine residues localized within or close to the autoinhibitory and CaM-binding domain, and that phosphorylation of at least some of these residues is responsive to nutritional, hormonal, and pathogenic signals (Nühse *et al.*, 2003, 2004, 2007; Benschop *et al.*, 2007; Niittylä *et al.*, 2007; Sugiyama *et al.*, 2008; Whiteman *et al.*, 2008; Jones *et al.*, 2009; Reiland *et al.*, 2009; Chen *et al.*, 2010; Nakagami *et al.*, 2010) opens up a new avenue for fine-tuning of its activity. To investigate the possible effect of phosphorylation on ACA8 activity, each of these residues was mutated to aspartate, which introduces a negative charge mimicking the effect of phosphorylation. The results obtained by biochemical analysis of these mutants indicate that phosphorylation of serine residues can affect ACA8 activity both by hampering the autoinhibitory action of the N-terminus and by changing the kinetics of activation by CaM and de-activation by CaM release, and, thus, at least in some instances, ACA8 affinity for CaM.

Mutation to aspartate of several phosphorylatable serine residues in the N-terminus of ACA8 generates partially deregulated proteins, with higher basal activity, less responsive to activation by CaM, and less stimulated by tryptic cleavage of the N-terminus. The effect is strongest in mutants S19D and S57D, but significant ($P < 0.05$) also in mutants S22D and S27D; only ACA8 mutants S29D and S99D are autoinhibited similarly to the WT protein. The ACA8 N-terminal autoinhibitory domain, which is enriched in basic residues (Bækgaard *et al.*, 2006), interacts with a sequence in the small cytoplasmic loop rich in acidic residues (Luoni *et al.*, 2004). Alanine scanning mutagenesis of these acidic residues generates partially deregulated ACA8 mutants, indicating that the electrostatic interaction between the positively charged N-terminal autoinhibitory domain and the negatively charged domain in the small cytoplasmic loop plays a role in ACA8 autoinhibition (Fusca *et al.*, 2009). Thus, the negative charge introduced by the S/D mutations—or by serine phosphorylation—in the N-terminus would hamper its autoinhibitory interaction with the small cytosolic loop. However, in the case of Ser22 and Ser27, the phenotype of the S/A ACA8 mutants is similar to that of the S/D mutants, suggesting that the -OH group of serine is also important *per se* in the autoinhibitory mechanism.

All the analysed mutations affect the kinetics of interaction with CaM to some extent. The strongest phenotype is that of mutant S57D, which has a k_d value ~10-fold higher than that of WT ACA8, but 2-fold changes in one or both of the kinetic constants of the interaction are also evident in mutants S19D, S22D, S27D, and S99D. Despite the different kinetics, the affinity for CaM of most mutants is fairly similar to that of WT ACA8 (K_D values ranging between 15 nM and 26 nM for the mutants, versus 19 nM for the WT), with two exceptions: mutant S99D which has a K_D value of 11 nM and mutant S57D which has a K_D value of 165 nM, nearly 10-fold higher than that of WT ACA8, largely due to its higher k_d value. The strongest phenotype of mutant S57D can be easily explained by the localization of this serine residue within the sequence defining the ACA8 CaM-binding site (Bonza *et al.*, 2000; Bækgaard *et al.*, 2006); interestingly, mutation of ACA8 Ser57 to alanine determines a decrease in the k_d, resulting in a K_D value about half that of the WT (Bækgaard *et al.*, 2006). Thus residue Ser57 in ACA8 CaM-binding domain plays a crucial role in determining the stability of its interaction with CaM.

Based on these results, a major effect of phosphorylation of serine residues in the ACA8 N-terminus would be to modify the rate of pump activation following an increase of cytoplasmic Ca^{2+} concentration which increases the concentration of the active Ca^{2+}–CaM complex or of its de-activation when the return of the cytosolic free Ca^{2+} concentration toward basal levels drastically lowers the concentration of Ca^{2+}–CaM. The rate of activation would be halved upon phosphorylation of Ser22 and nearly doubled upon phosphorylation of Ser19 or Ser27; the rate of de-activation would by halved in the case of phosphorylation of Ser99 and would increase from 2- to 10-fold following phosphorylation of Ser27 or of Ser57 (see Table 2).

Phosphorylation of some of these serine residues affects both the kinetics of CaM activation and de-activation and the autoinhibitory action of the ACA8 N-terminus. The two effects may exert a similar or contrasting effect on Ca^{2+} extrusion, depending on the phosphorylated residue and on the values of the relevant cytoplasmic parameters. For example, phosphorylation of Ser19 would favour ACA8 activation following an increase of cytosolic Ca^{2+}, both by inhibiting the autoinhibitory action of the N-terminus and by accelerating binding of the Ca^{2+}–CaM complex; activation would probably last longer, despite the slightly increased rate of CaM release, unless de-phosphorylation intervenes. Similarly, in the case of Ser57, the destabilizing effect of phosphorylation on ACA8 interaction with CaM might be largely counteracted by the inhibition of the autoinhibitory action of the N-terminus. Upon phosphorylation of Ser22, the rate and extent of ACA8 activation following an increase of cytosolic Ca^{2+} would be the result of its opposite effects on the autoinhibitory action of the N-terminus and on the rate of CaM binding; conversely, the moderate decrease of autoinhibition and the decrease of the CaM dissociation rate would both contribute to keep the pump active longer.

Altogether, the subtle effects of phosphorylation of one or more serine residues in the N-terminus on ACA8 activity may have important consequences on the spatio-temporal characteristics of cytoplasmic Ca^{2+} waves, and thus participate in deciphering the Ca^{2+} signal. This makes identification of protein kinase(s) and phosphatase(s) controlling the phosphorylation state of ACA8 in response to different signals an important goal for future research. Here it has been shown that two isoforms of *A. thaliana* CDPK—CPK1 and CPK16—are able to phosphorylate the ACA8 N-terminus *in vitro*. The effect of single point mutations on phosphorylation indicates that CPK16, the more efficient of the two isoforms tested, phosphorylates the ACA8 N-terminus at two different serine residues: Ser19—which is part of a consensus motif recognized by CDPKs (Cheng *et al.*, 2002)—and Ser22. Further work is needed to determine which isoform(s) of CDPK phosphorylate ACA8 *in vivo* and under which conditions phosphorylation occurs.

Supplementary data

Supplementary data are available at *JXB* online.

Table S1. Pairs of primers used for site-directed mutagenesis of ACA8.

Acknowledgements

This work was supported in part by the Italian Ministry for Instruction, University and Research in the PRIN 2007 framework. The authors are grateful to Professor J. F. Harper, University of Nevada, Reno, NV, USA for kindly providing plasmids encoding different isoforms of *A. thaliana* CDPK and for helpful suggestions regarding their expression, purification, and assay.

References

Bækgaards L, Luoni L, De Michelis MI, Palmgren MG. 2006. The plant plasma membrane Ca^{2+} pump ACA8 contains overlapping as well as physically separated autoinhibitory and calmodulin-binding domains. *Journal of Biological Chemistry* **281,** 1058–1065.

Benschop JJ, Mohammed S, O'Flaherty M, Heck AJR, Slijper M, Menke FLH. 2007. Quantitative phosphoproteomics of early elicitor signaling in *Arabidopsis*. *Molecular and Cellular Proteomics* **6,** 1198–1214.

Bonza MC, De Michelis MI. 2011. The plant Ca^{2+}-ATPases repertoire: biochemical features and physiological functions. *Plant Biology* **13,** 421–430.

Bonza MC, Luoni L. 2010. Plant and animal type 2B Ca^{2+}-ATPases: evidence for a common auto-inhibitory mechanism. *FEBS Letters* **584,** 4783–4788.

Bonza MC, Luoni L, De Michelis MI. 2004. Functional expression in yeast of an N-deleted form of At-ACA8, a plasma membrane Ca^{2+}-ATPase of *Arabidopsis thaliana*, and characterization of a hyperactive mutant. *Planta* **218,** 814–823.

Bonza MC, Morandini P, Luoni L, Geisler M, Palmgren MG, De Michelis MI. 2000. At-ACA8 encodes a plasma membrane-localized calcium-ATPase of Arabidopsis with a calmodulin-binding domain at the N terminus. *Plant Physiology* **123,** 1495–1505.

Boursiac Y, Harper JF. 2007. The origin and function of calmodulin regulated Ca^{2+} pumps in plants. *Journal of Bioenergetic and Biomembranes* **39,** 409–414.

Chen Y, Hoehenwarter W, Weckwerth W. 2010. Comparative analysis of phytohormone-responsive phosphoproteins in *Arabidopsis thaliana* using TiO2-phosphopeptide enrichment and mass accuracy precursor alignment. *The Plant Journal* **63,** 1–17.

Cheng S-H, Willmann MR, Chen H-C, Sheen J. 2002. Calcium signaling through protein kinases. The Arabidopsis calcium-dependent protein kinase gene family. *Plant Physiology* **129,** 469–485.

Cunningham KW, Fink GR. 1994. Calcineurin-dependent growth control in *Saccharomyces cerevisiae* mutants lacking PMC1, a homolog of plasma membrane Ca^{2+}-ATPases. *Journal of Cell Biology* **124,** 351–363.

Dammann C, Ichida A, Hong B, Romanowsky SM, Hrabak EM, Harmon AC, Pickard BG, Harper JF. 2003. Subcellular targeting of nine calcium-dependent protein kinase isoforms from Arabidopsis. *Plant Physiology* **132,** 1840–1848.

Das R, Pandey GK. 2010. Expressional analysis and role of calcium regulated kinases in abiotic stress signalling. *Current Genomics* **11,** 2–13.

De Michelis MI, Carnelli A, Rasi-Caldogno F. 1993. The Ca^{2+} pump of the plasma membrane of *Arabidopsis thaliana*—characteristics and sensitivity to fluorescein derivatives. *Botanica Acta* **106,** 20–25.

Dodd AN, Kudla J, Sanders D. 2010. The language of calcium signaling. *Annual Review of Plant Biology* **61,** 593–620.

Enyedi A, Elwess NL, Filoteo AG, Verma AK, Paszty K, Penniston JT. 1997. Protein kinase C phosphorylates the 'a' forms of plasma membrane Ca^{2+} pump isoform 2 and 3 and prevents binding of calmodulin. *Journal of Biological Chemistry* **272,** 27525–27528.

Enyedi A, Verma AK, Filoteo AG, Penniston JT. 1996. Protein kinase C activates the plasma membrane Ca^{2+} pump isoform 4b by phosphorylation of an inhibitory region downstream of the calmodulin-binding domain. *Journal of Biological Chemistry* **50,** 32461–32467.

Fusca T, Bonza MC, Luoni L, Meneghelli S, Marrano CA, De Michelis MI. 2009. Single point mutations in the small cytoplasmic loop of ACA8, a plasma membrane Ca^{2+}-ATPase of *Arabidopsis thaliana*, generate partially deregulated pumps. *Journal of Biological Chemistry* **284,** 30881–30888.

Harper JF, Breton G, Harmon A. 2004. Decoding Ca^{2+} signals through plant protein kinases. *Annual Review of Plant Biology* **55,** 263–288.

Harper JF, Huang J-F, Lloyd SJ. 1994. Genetic identification of an autoinhibitor in CDPK, a protein kinase with a calmodulin-like domain. *Biochemistry* **33,** 7267–7277.

Hwang I, Sze H, Harper JF. 2000. A calcium-dependent protein kinase can inhibit a calmodulin-stimulated Ca^{2+} pump (ACA2) located in the endoplasmic reticulum of *Arabidopsis*. *Proceedings of the National Academy of Sciences, USA* **97,** 6224–6229.

Jones AME, MacLean D, Studholme DJ, Sanz A, Andreasson E, Rathjen JP, Peck SC. 2009. Phosphoproteomic analysis of nuclei-enriched fractions from *Arabidopsis thaliana*. *Journal of Proteomics* **72,** 439–451.

Laemmli UK. 1970. Cleavage of structural proteins during the assembly of the head of bacteriophage T4. *Nature* **227,** 680–685.

Luoni L, Bonza MC, De Michelis MI. 2006. Calmodulin/Ca^{2+}-ATPase interaction at the *Arabidopsis thaliana* plasma membrane is dependent on calmodulin isoform showing isoform-specific Ca^{2+} dependencies. *Physiologia Plantarum* **126,** 175–186.

Luoni L, Meneghelli S, Bonza MC, De Michelis MI. 2004. Auto-inhibition of *Arabidopsis thaliana* plasma membrane Ca^{2+}-ATPase involves an interaction of the N-terminus with the small cytoplasmic loop. *FEBS Letters* **574,** 20–24.

Malmström S, Åkerlund HE, Askerlund P. 2000. Regulatory role of the N terminus of the vacuolar calcium-ATPase in cauliflower. *Plant Physiology* **122,** 517–526.

McAinsh MR, Pittman JK. 2009. Shaping the calcium signature. *New Phytologist* **181,** 275–294.

Meneghelli S, Fusca T, Luoni L, De Michelis MI. 2008. Dual mechanism of activation of plant plasma membrane Ca^{2+}-ATPase by acidic phospholipids: evidence for a phospholipid binding site which overlaps the calmodulin-binding site. *Molecular Membrane Biology* **25,** 539–546.

Nakagami H, Sugiyama N, Mochida K, Daudi A, Yoshida Y, Toyoda T, Tomita M, Ishihama Y, Shirasu K. 2010. Large-scale comparative phosphoproteomics identifies conserved phosphorylation sites in plants. *Plant Physiology* **153,** 1161–1174.

Niittylä T, Fuglsang AT, Palmgren MG, Frommer WB, Schulze WX. 2007. Temporal analysis of sucrose-induced phosphorylation changes in plasma membrane proteins of Arabidopsis. *Molecular and Cellular Proteomics* **6,** 1711–1726.

Nühse TS, Bottrill A, Jones AME, Peck SC. 2007. Quantitative phosphoproteomics analysis of plasma membrane proteins reveals regulatory mechanisms of plant innate immune responses. *The Plant Journal* **51,** 931–940.

Nühse TS, Stensballe A, Jensen ON, Peck SC. 2004. Phosphoproteomics of the Arabidopsis plasma membrane and a new phosphorylation site database. *The Plant Cell* **16,** 2394–2405.

Nühse TS, Stensballe A, Jensen ON, Peck SC. 2003. Large-scale analysis of *in vivo* phosphorylated membrane proteins by immobilized metal ion affinity chromatography and mass spectrometry. *Molecular and Cellular Proteomics* **2,** 1234–1243.

Penniston JT, Enyedi A. 1998. Modulation of the plasma membrane Ca^{2+} pump. *Journal of Membrane Biology* **165,** 101–109.

Pittman JK, Bonza MC, De Michelis MI. 2011. Ca^{2+} pumps and Ca^{2+} antiporters in plant development. In: Geisler M, Venema K, eds. *Transporters and pumps in plant signalling*. Berlin: Springer-Verlag, 133–161.

Rasi-Caldogno F, Carnelli A, De Michelis MI. 1993. Controlled proteolysis activates the plasma membrane Ca^{2+} pump of higher plants. *Plant Physiology* **103,** 385–390.

Reiland S, Messerli G, Baerenfaller K, Gerrits B, Endler A, Grossman J, Gruissem W, Baginsky S. 2009. Large scale Arabidopsis phosphoproteomic profiling reveals novel choloroplast kinase substrates and phosphorylation networks. *Plant Physiology* **150,** 889–903.

Sanders D, Pelloux J, Brownlee C, Harper JF. 2002. Calcium at the crossroads of signaling. *The Plant Cell* **14,** S401–S417.

Sugiyama N, Nakagami H, Mochida K, Daudi A, Tomita M, Shirasu K, Ishihama Y. 2008. Large-scale phosphorylation mapping reveals the extent of tyrosine phosphorylation in Arabidopsis. *Molecular Systems Biology* **4**, article 193.

Verma AK, Paszty K, Filoteo AG, Penniston JT, Enyedi A. 1999. Protein kinase C phosphorylates plasma membrane Ca^{2+} pump isoform 4a at its calmodulin binding domain. *Journal of Biological Chemistry* **1,** 527–531.

Vitart V, Christodoulou J, Huang J-F, Chazin WJ, Harper JF. 2000. Intramolecular activation of a Ca^{2+}-dependent protein kinase is disrupted by insertions in the tether that connects the calmodulin-like domain to the kinase. *Biochemistry* **39,** 4004–4011.

Whiteman S, Serazetdinova L, Jones AME, Sanders D, Rathjen J, Peck SC, Maathuis FJM. 2008. Identification of novel proteins and phosphorylation sites in a tonoplast enriched membrane fraction of Arabidopsis thaliana. *Proteomics* **8,** 3536–3547.

Work in progress

The *Arabidopsis thaliana* Ca^{2+} pump ACA8 is a target of CBL Interacting Protein Kinases

Marrano CA, Giacometti S, Bonza MC and De Michelis MI

In collaboration with Professor Jörg Kudla group Institut für Biologie und Biotechnologie der Pflanzen, Universität Münster, Münster, Germany

Abstract

ACA8 is a plasma membrane-localized Ca^{2+}-ATPase of *Arabidopsis thaliana* that extrudes Ca^{2+} from the cytoplasm to the apoplast after a stimulus-induced increase of cytosolic Ca^{2+} concentration. A recent study indicates that phosphorylation of one to six Ser residues, localised in the N-terminal regulative region of the pump, could lead to a finely tuned modulation of ACA8 activity. However, the kinase(s) involved in the *in vivo* phosphorylation of these Ser residues remain unidentified so far. In this work we identify by two-hybrid screening two isoforms of CBL-interacting protein kinases (CIPKs) as putative interactors of ACA8 N-terminus region: CIPK9 and CIPK14. We show by BiFC experiments that the interaction with ACA8 full length occurs *in planta* at the plasma membrane. Moreover we demonstrate that both kinases can phosphorylate ACA8 N-terminus region *in vitro*.

Introduction

Ca^{2+} signalling is crucial in many plant regulative mechanisms and different aspects of plant development, such as stomatal closure and opening, tip growth in pollen tubes, response to cold and salt stress [Sanders et al., 1999; 2002; Spalding and Harper, 2011]. Very important for the role of Ca^{2+} as a second messenger is its toxicity for the cell metabolism that imposes to keep a very low free concentration of the ion in the cytosol (100-200 nM). Thanks to this feature a robust increase in Ca^{2+} concentration can rapidly be achieved through the opening of Ca^{2+}-channels. The following activation of vacuolar Ca^{2+}/H^{+}-antiporters and plasma membrane (PM) or intracellular membranes-localized Ca^{2+}-pumps, that extrude Ca^{2+} outside the cytosol, determines the end of the Ca^{2+} transient. The shape of Ca^{2+} transients that codify for different responses triggered by different stimuli is called Ca^{2+} signature and depends on the fine regulation of these passive and active Ca^{2+} transporters [McAinsh et al., 2009; Spalding and Harper, 2011; Kudla et al., 2010].

In *A. thaliana* Ca^{2+} pumping outside the cytosol involves two classes of Ca^{2+}-ATPases: ER-type Ca^{2+}-ATPases (ECAs) and autoinhibited Ca^{2+}-ATPases (ACAs). The main difference between these two groups of pumps is that, unlike ECAs, ACAs have an extended N-terminus region that contains a domain with autoinhibitory action, which keeps the pump almost inactive at low Ca^{2+} concentrations [Bonza and De Michelis, 2011]. The N-terminus region of ACAs also contains a CaM-binding domain (CaM-BD) partially overlapped to the autoinhibitory domain: when Ca^{2+}-CaM binds CaM-BD the autoinhibitory interaction is disrupted and the enzyme activated [Bonza and De Michelis, 2011].

One of the best characterized isoform of plant ACAs is *Arabidopsis thaliana* ACA8, a CaM-activated Ca^{2+}-pump localized at the PM known to be involved in cold stress, ABA and oligogalacturonides signalling pathway [Bonza et al., 2000; Romani et al., 2004; Schiøtt et al., 2005; Cerana et al., 2006]. Beside CaM the interaction with acidic phospholipids (APLs) is another mechanism that regulates ACA8 activity. APLs action is accomplished *via* a dual mechanism: it has been shown that APLs can bind ACA8 N-terminus in a region partially overlapped to the CaM-BD stimulating the pump in the same way of CaM; however their action on pump activity is only partially additive to the action of CaM, indicating the presence of a second binding site [Meneghelli et al., 2008].

ACA8 is also target of phospho-regulation. Phosphoproteomic studies performed on *Arabidopsis* cultured cells in the presence of different stimuli, like bacterial and fungal elicitors or phytohormones as ABA, revealed the presence of several phospho-peptides corresponding to ACA8 N-terminus region. The six Ser residues that have been found phosphorylated are: S19, S22, S27, S29 localized upstream the CaM-BD, S57 located inside the CaM-BD and S99 located downstream the CaM-BD [Nhüse et al., 2003, 2004, 2007; Benshop et al., 2007; Niittylä et al., 2007; Sugiyama et al., 2008; Whiteman et al., 2008; Jones et al., 2009; Reiland et al., 2009; Chen et al., 2010; Nakagami et al., 2010]. Mutagenesis experiments in which each of these Ser residues has been changed into Asp, to mimic phosphorylation, indicate that phosphorylation could act on the pump activity deregulating the pump (S19, S57, S22, S27), or changing the affinity for CaM (S57 and S99) and in all the cases modifying the kinetic of CaM interaction [Giacometti et al., 2012]. All these results suggest that phosphorylation is a mechanism that can specifically – depending on the Ser residue/s involved – finely tune the pump activity.

Phosphorylation assays with calcium dependent protein kinases (CDPKs) indicate that the N-terminus can be phosphorylated *in vitro* by this class of protein kinases on Ser19 and S22 [Giacometti et al., 2012]. Otherwise the family(es) of protein kinases involved in the *in vivo* phosphorylation of the ACA8 are unknown so far.

Nühse and colleagues localize S27 in a consensus motif for SnRKs (Sucrose non-fermenting Related Kinases), a family of plant protein kinases that encompasses three different sub-groups; only one of them, the sub-group 3, is known to be involved in Ca^{2+} signalling. SnRK3 are also called CIPKs (CLB Interacting Protein Kinases) for their ability to interact with the Ca^{2+} sensors Calcineurin-B like Proteins (CBLs). In *Arabidopsis* the 26 members of CIPKs are cytosolic fully autoinhibited kinases that differently interact with 10 CBLs: after an appropriate stimulus-induced increase in cytosolic free Ca^{2+} concentration, CBLs bind Ca^{2+} and undergo a conformational change that makes them able to bind, target on the appropriate membrane and activate CIPKs [Spalding and Harper, 2010; Kudla et al., 2010; Hashimoto and Kudla, 2011].

Here we show that the ACA8 N-terminus (^{1}M-I^{116}) interacts in yeast two-hybrid screening with two isoforms of CIPKs, CIPK9 and CIPK14. This interaction has been confirmed by biomolecular fluorescence complementation (BiFC) experiments *in planta* using ACA8 full-length (FL) protein. *In vitro* phosphorylation assays show that both kinases are able to phosphorylate ACA8 N-terminus.

Materials and methods

Plasmid constructs

For the yeast two hybrid assay the coding sequence (CDS) of the first 116 aa (^{1}M-I^{116}) of ACA8 inserted in the *E. coli* expression vector pET15b [Giacometti et al., 2012] was sub-cloned into the activation domain (AD) vector pGADT7 (Clontech, catalogue no. #630442, kindly provided by professor Colombo, Milan, Italy), taking advantage of the restriction sites *NdeI* and *BamHI* already present respectively at the 5’ and 3’ of the CDS of ACA8.

A PCR performed with Phusion® High-Fidelity DNA Polymerase (New England Biolabs, Ipswich, MA, USA, product no. M0530S) according to the manufacturer’s protocol was used to amplify the complete sequence of ACA8; wild type (WT) ACA8 full-length (FL) CDS inserted has been used as template and amplified with the following specific oligonucleotides: (S) 5’ TCCGCTGGAGATGACGAGTCTCTTGAAGTCATCG and (AS) 5’ CATATCCCGGGGAGTGAACCTTCTCCAGACGA. The S primer contains a *XhoI* restriction site, the AS primer contains a *XmaI* restriction site (both underlined) and eliminate the stop codon at the 3’ of ACA8 FL CDS. Following *XhoI/XmaI* digestion, ACA8 FL CDS, obtained using the restriction enzymes reported above, was inserted into the plant expression vector pGPTVII [Waadt et al., 2008] under the control of the cauliflower mosaic virus (CaMV) 35S promoter at the 5’ of the CDS of GFP (pGFP::ACA8) . Absence of errors was confirmed by sequencing. This vector, that provides the strong expression of ACA8::GFP chimeric protein, was used for ACA8 subcellular localization studies in *Nicotiana benthamiana* leaves cells. The ACA8 FL CDS was also inserted into pSPYCE(M)_155 vector [Waadt et al., 2008] under the control of CaMV 35S promoter upstream the CDS for the last 155 amino acids of the YFP C-terminus (YC). This pSPYCE(M)::ACA8 vector, coding for the ACA8::YC chimeric construct, was used for BiFC studies.

Yeast-two-hybrid assays

The CDS of all 26 isoforms of CIPKs already cloned into the DNA-binding domain (BD) vector pGBT9.BS were kindly provided by professor Kudla (Münster, Germany). The soluble ACA8 N-terminus (^{1}M-I^{116}) was cloned into the activation domain (AD) vector pGADT7 as previously described (see *Materials and Methods, Plasmid constructs* section). Construct combinations (see *Results* section) were transformed into the yeast strain PJ69-4A using a lithium acetate /polyethylene glycol method [Waadt et al., 2008] and selected on SD agar medium lacking Trp and Leu (SD-W-L) composed as followed: 900 mg/L HSM drop-out –His –Leu –Trp –Ura (FOREMEDIUM LTD, Hunstanton, England, ref. number DHSM155), 200 mg/L uracil (Fluka Chemie GmbH, Germany, prod. number 94220), 200 mg/L His (Sigma-Aldrich, Stenheim, Germany, prod. number H8000), 2% glucose (FOREMEDIUM LTD, Hunstanton, England, prod. number GLU03), 6,9 g/L yeast nitrogen base (FOREMEDIUM LTD, Hunstanton, England, prod. number CYN0405) in ddH_2O. To verify the interaction of the two proteins, all the positive transformants were grown on SD-W-L liquid medium at 30 °C for 16 hrs and 10-fold serial dilutions (10^{-1} to 10^{-4}) of the transformants were prepared starting from an A_{600}=1. A 5 µl drop for each dilution was spotted on agar plates of SD medium lacking Trp, Leu and His (SD-W-L-H) and supplemented with 2.5 mM 3-amino-1,2,4-triazole (3AT; Sigma-Aldrich, Stenheim, Germany, prod. number A8056). Plates were incubated at 30 °C for 3 to 5 days.

ACA8 localization and BiFC studies

Vectors pGFP::ACA8, pSPYNE(R)::CIPK9, pSPYNE(R)::CIPK14, pSPYCE(M)::CBL1 [Batistič et al., 2008; 2010] and pSPYCE(M)::ACA8 vectors were used to transform *Agrobacterium tumefaciens* strains (GV3101/pMP90). *A. tumefaciens* transformants expressing fluorescent proteins, or part of them, were infiltrated into *N. benthamiana* leaves according to Waadt and Kudla, 2008. Confocal microscopy analysis was performed using an inverted microscope, Leica DMIRE2, equipped with a Leica TCS SP2 laser scanning device (Leica) as previously described in details in Batistič et al., 2008 and Batistič et al., 2010.

Expression and purification of the 6His-tagged ACA8 N-terminus.

The vector coding for the 6His-tagged ACA8 N-terminus (6His-^{1}M-I^{116}), produced as described in Luoni et al., 2004, was used to transform *E. coli* strain BL21(DE3)-pLysE (Merck KGaA, Darmstadt, Germany, catalogue no. 69389-3) by standard procedures. Purification of the fusion protein was performed as described [Luoni et al., 2004].

Wheat germ-based cell-free CIPKs synthesis and protein purification

StrepII-tagged CIPK9 and CIPK14 proteins were synthetized using a RTS 500 wheat germ CECF kit (5 PRIME) following the manufacturer's instructions. For affinity purification, each *in vitro* translation reaction (1 ml) was mixed with 0.8 ml of Strep-Tactin Macroprep (IBA) and incubated for 30 min at 4 °C. StrepII-tagged proteins were eluted by gravity flow in elution buffer (100 mM Tris pH 8.0, 150 mM NaCl, and 2.5 mM desthiobiotin) and collected in 0.4 ml fractions. Abundance of purified proteins was confirmed by Western blot analysis using Strep-Tactin horseradish peroxidase (HRP) conjugate (1:5000, IBA). In addition, SDS-PAGE followed by Comassie staining (R-250) was performed to estimate the concentration of each purified protein. Stained bands of the purified proteins were compared with known amounts of BSA standard. The concentration of StrepII-CIPK9 and StrepII-CIPK14 purified fraction was determined respectively as 20 ng/μl and 30 ng/μl.

In Vitro Phosphorylation Assays

The AMPK kinase assay was performed using 4 μg/ml AMPK (SignalChem, Richmond, Canada, catalogue no. P47-1 0H) in a 1:4 dilution of 5X Kinase Assay Buffer (SignalChem, Richmond, Canada, catalogue no. K03-09), supplemented with 0.25 mM DTT, 100 μM AMP and 200 μM ATP labeled with 4,1 kBq nmole^{-1} of [γ-^{32}P]ATP, in a final volume of 25 μl. Assays were initiated by addiction of 20 μM the purified ACA8 6His^{1}M-I^{116} and incubated at 25 °C controlled temperature for 2 h. Reactions were stopped by addiction of Laemmly buffer [Laemmly, 1970], and aliquots corresponding to 2-3 μg of purified substrate protein were loaded on to 18% polyacrylamide gel and subjected to SDS-PAGE and blotting as described in Luoni *et al.*, 2004. Radioactively labelled proteins were visualized by autoradiography.

For the kinase assay with CIPKs, purified ACA8 6His^{1}M-I^{116} (700 ng *per* sample) and strepII-tagged CIPK9 or CIPK14 proteins (60 ng *per* sample) were incubated for 30 min at 30 °C in 24 μl reactions that contained 66.7 mM Tris pH 8.0, 100 mM NaCl, 5 mM $MnSO_4$, 0.5 mM $CaCl_2$, 2 mM DTT, 10 μM ATP, and 4 μCi of [γ-^{32}P]ATP (3000 Ci/mmol). Reaction were stopped by addiction of 20 mM EDTA and then subjected to SDS-PAGE on a 16% polyacrylamide gel. SDS gels were fixed by Comassie staining and radioactively labelled proteins were visualized by autoradiography.

All experiments were repeated at least three times with similar results.

Results

ACA8 N-terminus region is phosphorylated in vitro by AMPK

ACA8 Ser 27 residue, one of the Ser residues involved in the regulative phosphorylation of ACA8 [Giacometti et al., 2012], is in a consensus motive for SnRKs [Nühse et al., 2004]. Plants SnRKs have their animal orthologue in the AMP-activated protein Kinase (AMPK); the aminoacidic conservation into this class of protein is 48% but if the focus is on the catalytic domain of the enzyme the conservation level arises till 60-65% [Poldge and Thomas, 2006]. It has furthermore been shown that plant SnRKs and animal AMPKs phosphorylate the same synthetic substrates, such as ALARA and syntide-2 peptides, with a high affinity [Hashimoto et al., 2012]. Moreover, AMPK was successfully used to phosphorylate plant substrates [Harthill et al., 2006; Lu et al., 2007].

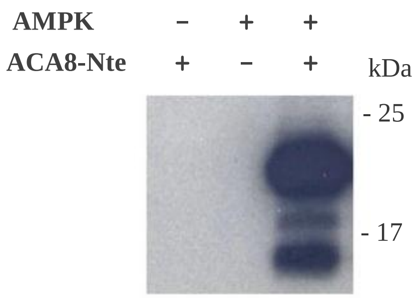

Fig. 1. Phosphorylation of the ACA8 N-terminus region by AMPK

The N-terminus of ACA8 (6His-^{1}M-I^{116}) was phosphorylated with a commercial AMPK as described in *Materials and methods*. Samples were solubilized and 2 μg of 6His-^{1}M-I^{116} were subjected to SDS-PAGE, blotting, and autoradiography. Results shown are from one experiment representative of three.

As a consequence of these observations, we decided to test the ability of a commercial AMPK to phosphorylate the N-terminus of ACA8, as a preliminary screening of the SnRK family. Figure 1 shows that the kinase was able to phosphorylate a 6His-tagged peptide corresponding to the sequence ^{1}M-I^{116} of ACA8.

Identification of CIPKs interacting with ACA8 by yeast two hybrid and BiFC experiments

The plant SnRKs family consists of three different subgroups, but only one is directly involved in Ca^{2+} sensing: the SnRK3 that groups the CBL Interacting Protein Kinases (CIPKs). Looking for a SnRK able to phosphorylate ACA8 we decided to perform a two hybrid screening using ACA8 N-terminus as bait and all the members of *Arabidopsis* CIPK family as prays. With this aim the DNA sequence codifying for the first 116 amino acids of ACA8 N-terminus (Nte) was cloned into the two-hybrid bait vector pGADT7. The resultant pGAD-ACA8Nte was used to co-transform the yeast strain PJ69-4A in combination with each of the pGBT9 pray vectors containing sequences codifying for the 26 CIPK isoforms. The co-transformation with pGAD-ACA8Nte/pGBT9 EV (empty vector) was used as a transactivation control; while the co-transformation with pGAD-CBL1/pGBT9-CIPK1 was used as a control of a positive interaction [D'Angelo et al., 2006]. As reported in figure 2, after 5 days on the SD-W-L 2,5 mM 3AT selective medium yeast cells transformed with the pGAD-ACA8Nte/pGBT9 EV combination did not grow, while the positive control grew as expected (white arrow). Only two of the 26 kinases, CIPK9 and CIPK14, showed interaction with ACA8 Nte: the growth of the respective co-transformants (gray arrows) is comparable with that of the positive control. To exclude the possibility that the growth of the two co-transformants could have been due to transactivation determined by the presence of the kinases themselves, we tested also pGBT9-CIPK9/pGAD EV, pGBT9-CIPK14/pGAD EV combinations: the results in figure 2 clearly show no growth for both controls.

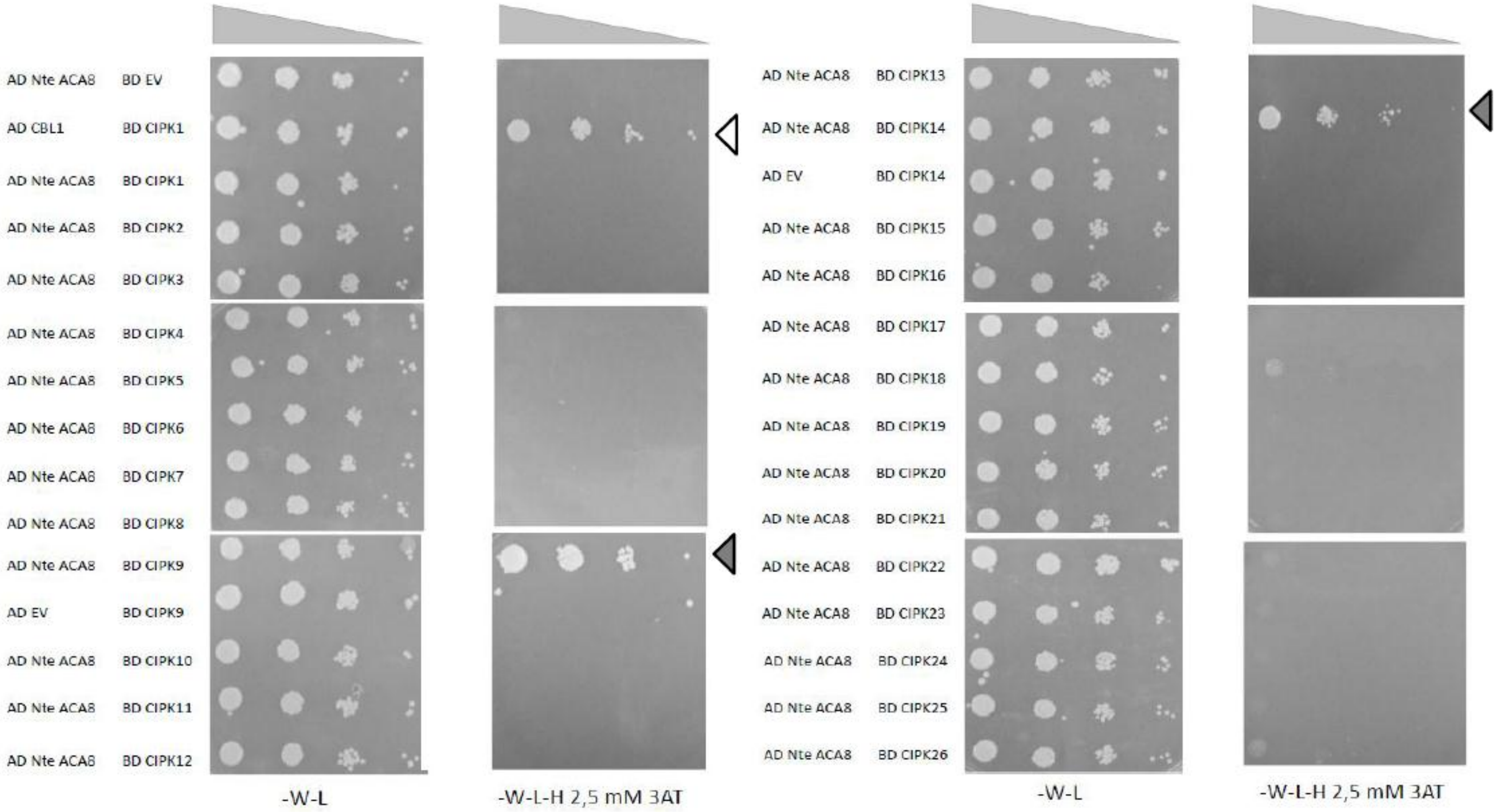
AD Nte ACA8 BD EV
AD CBL1 BD CIPK1
AD Nte ACA8 BD CIPK1
AD Nte ACA8 BD CIPK2
AD Nte ACA8 BD CIPK3
AD Nte ACA8 BD CIPK4
AD Nte ACA8 BD CIPK5
AD Nte ACA8 BD CIPK6
AD Nte ACA8 BD CIPK7
AD Nte ACA8 BD CIPK8
AD Nte ACA8 BD CIPK9
AD EV BD CIPK9
AD Nte ACA8 BD CIPK10
AD Nte ACA8 BD CIPK11
AD Nte ACA8 BD CIPK12
-W-L
-W-L-H 2,5 mM 3AT
AD Nte ACA8 BD CIPK13
AD Nte ACA8 BD CIPK14
AD EV BD CIPK14
AD Nte ACA8 BD CIPK15
AD Nte ACA8 BD CIPK16
AD Nte ACA8 BD CIPK17
AD Nte ACA8 BD CIPK18
AD Nte ACA8 BD CIPK19
AD Nte ACA8 BD CIPK20
AD Nte ACA8 BD CIPK21
AD Nte ACA8 BD CIPK22
AD Nte ACA8 BD CIPK23
AD Nte ACA8 BD CIPK24
AD Nte ACA8 BD CIPK25
AD Nte ACA8 BD CIPK26
-W-L
-W-L-H 2,5 mM 3AT

Fig 2. CIPK9 and CIPK14 interact with ACA8 N-terminus in yeast two hybrid. Serial of yeast PJ69-4A transformed with AD ACA8 N-terminus and each of the CIPKs in BD vectors. Positive control: transformation of yeast PJ69-4A with AD CBL1 and BD CIPK1 vectors (white arrow).
Growth on SD-W-L 2,5 mM 3AT indicates that ACA8 N-terminus interacts with CIPK9 and CIPK14 (gray arrows).

To confirm the interaction identified by yeast two-hybrid screening we decided to perform a BiFC experiment in *Nicotiana benthamiana* leaves cells using ACA8 FL protein. We preliminary checked the expression and the correct localization of ACA8 in the epidermal cells of *Nicotiana benthamiana* leaves after transient transformation with *Agrobacterium tumefaciens* bringing a GFP-ACA8 construct. In figure 3 the green florescence of GFP-ACA8 is clearly distributed along the periphery of the cells, indicating that the protein is expressed, it doesn't stuck in the ER and is not sequestered in other organelles. Moreover the pattern of signal distribution in two neighbour cells (indicated with the white arrow in the focus image) clearly shows PM localization.

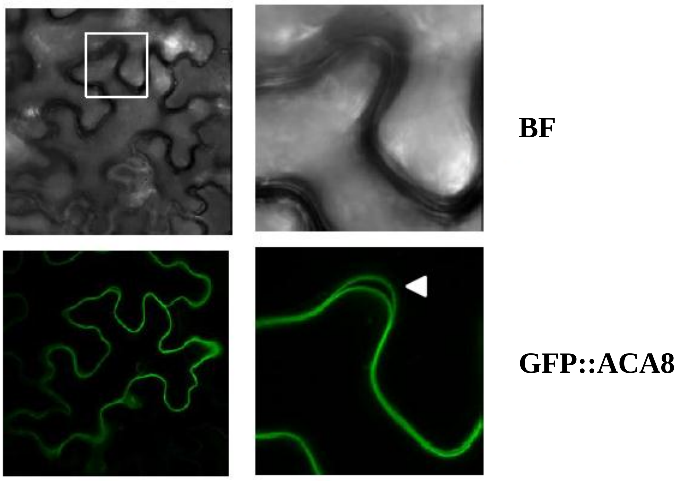

Fig 3. ACA8 correctly localises at the PM in epidermal cells of transiently transformed *N. benthamiana* leaves. Upper panels bright field (BF), bottom panels GFP fluorescence. Results, collected after 4 days from infiltration, are from one representative of four independent experiments. Scale bars: 40 µm; the focus images (on the right) are a 5-fold magnification of the left images.

The BiFC experiments were performed as described in *Materials and methods* using ACA8 FL protein fused to the C-terminal part of the YFP (YC::ACA8) and CIPK9 or CIPK14 fused to the N-terminal part of YFP (YN::CIPK9 and YN::CIPK14). The results are reported in Figure 4. Both for ACA8-CIPK9 and ACA8-CIPK14 a YFP fluorescence signal is present (left panels), indicating the formation of a complex between ACA8 and the kinase. Again the signal is at the periphery of the cells as expected for PM localization.

CIPKs are cytosolic proteins, which need to be targeted to the appropriate membrane by CBLs, in order to interact with their targets [Batistič et al., 2010; Kudla et al., 2010]. It is known that CIPK14 is localised at the tonoplast upon interaction with CBL2 and CBL3, and at the PM upon interaction with CBL8 [Batistič et al., 2010]. On the other hand, nothing is known so far about CBL-mediated targeting of CIPK9. Since ACA8 is localised at the PM, CIPK9 and CIPK14 interaction with the pump has to occur in that membrane compartment. To understand if CIPK9 and CIPK14 could be targeted at the PM by CBL1, a well characterized CBL exclusively localised on the PM, we decided to perform BiFC analysis using YN::CIPK9 and YN::CIPK14 each with YC::CBL1. The YFP signal present at the periphery of the cells in figure 4 (right panels) shows that both kinases are able to interact with CBL1 at the PM.

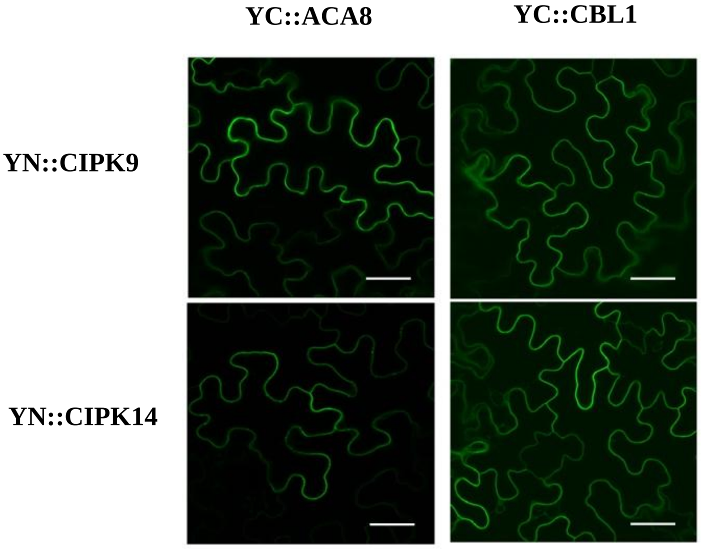

Fig 4. CIPK9 and CIPK14 interact with ACA8 FL and CBL1 in BiFC. Biomolecular fluorescence complementation (BiFC) analyses of YN::CIPK9 and YN::CIPK14 interactions with respectively YC::ACA8 (left panel) and YC::CBL1 (right panel) in transiently transformed *Nicotiana benthamiana* leaves. Both the kinases show interaction with ACA8 and CBL1 at the PM as indicated by the YFP signal (in green). Results, collected after 4 days from infiltration, are from one representative of at least three independent experiments. Scale bars: 40 μm

Phosphorylation of ACA8 N-terminus by CIPK9 and CIPK14

According to the yeast two-hybrid screen and BiFC results we decided to check whether CIPK9 and CIPK14 were able to phosphorylate the N-terminus of ACA8. We synthetized recombinant strepII-tagged CIPK9 and CIPK14 using the WG (wheat germ) *in vitro* transcription/translation system, already described as a successful method to produce suitable amount of active CIPKs [Hashimoto et al., 2012]; the His tagged peptide corresponding to the ^{1}M-I^{116} N-terminal sequence of ACA8 has been heterologously expressed in *E. coli* [Luoni et al., 2004]. Proteins were purified by affinity chromatography as described in *Materials and methods*. Figure 5 shows that both kinases, as expected [Hashimoto et al., 2012] are subjected to auto-phosphorylation (lane 1 and 4). Lane 2 and 5 shows that CIPK9 and CIPK14 are able to phosphorylate the His-tagged ACA8 N-terminus.

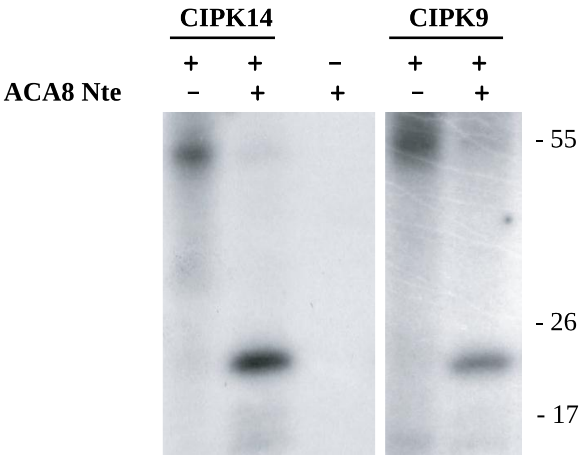

Fig 5. CIPK9 and CIPK14 phosphorylate ACA8 N-terminus *in vitro*. Results of *in vitro* phosphorylation assays using purified strepII-tagged CIPK9 (lane 4 and 5) or strepII-tagged CIPK14 (lane 1 and 2) without (lane 1 and 4) or in presence of 6His-^{1}M-I^{116}, performed as described in *Materials and methods*. Samples were solubilized and aliquots corresponding to 700 ng of 6His-^{1}M-I^{116} were subjected to SDS-PAGE, blotting and autoradiography. Results are from one experiment representative of three.

Conclusions and perspectives

ACA8 is one of the best biochemically characterized PM Ca^{2+} pump in plants. Recently we showed that phosphorylation of six different Ser residues in the N-terminal regulative region of ACA8 affects, at different degrees, the activity of the pump and its kinetic of interaction with CaM, suggesting that phospho-regulation of ACA8 may have important consequences on the characteristics of cytoplasmic Ca^{2+} waves and thus on the definition a stimulus-specific Ca^{2+} signature [Giacometti et al., 2012]. *In vitro* phosphorylation data indicate that CDPK16 is involved in phosphorylation of just two of these six Ser residues [Giacometti et al., 2012]. However there are no indications, by now, of which kinase(s) is involved *in vivo* in this short term regulation of ACA8 activity.

Here we show that the Ca^{2+} pump ACA8 interacts *in vivo* at the PM with two isoform of CIPKs, CIPK9 and CIPK14. Furthermore, we demonstrate that the N-terminal regulative region of ACA8 is phosphorylated *in vitro* by CIPK9 and CIPK14. These results indicate that ACA8 is a target of the CBL-CIPK signalling network, which is well known to have a crucial function in many biological processes like salt tolerance, potassium transport, nitrate sensing, and stomatal regulation [Kudla et al., 2010]. Our results open the possibility for a mechanism of ACA8 regulation mediated by CIPK-CBL complexes that can determine a rapid modulation of the activity of the pump in response to specific stimuli. Nevertheless, further work is needed to unravel the physiological role of CIPK-CBL mediated ACA8 phosphorylation and its correlation with Ca^{2+} signalling pathways.

A crucial aspect to be determined is if *in vivo* the reconstitution of CBL-CIPK-ACA8 phosphorylation complex has an effect on the cellular Ca^{2+} homeostasis. In order to answer to this question we are setting the conditions to perform a complementation test of *S. cerevisiae* mutant K616 [Cunningam and Finck, 1994]. This yeast strain is deprived of endogenous Ca^{2+}-ATPases; for this reason it is able to survive only in presence of high external Ca^{2+} concentration or if a constitutively active Ca^{2+} pump is heterologously expressed [Cunningam and Finck, 1994; Bonza and De Michelis, 2011]. The expression in *S. cerevisiae* K616 of an autoinhibited isoform of plant Ca^{2+}-ATPase, such as ACA8, is not able to complement the yeast phenotype; on the other hand the expression of deleted mutants of ACA8, like Δ74ACA8 that is constitutively active since it is deprived of the autoinhibitory domain, complements K616 phenotype [Bonza et al., 2004; Bækgaard et al. 2006; Fusca et al., 2009]. Thus, if the phosphorylation of ACA8 by CBL-CIPK complex activates the enzyme, the expression of these three proteins in K616 should complement its phenotype on selective medium.

As mentioned above, it was shown that phosphorylation influences ACA8 activity in a different way according to the Ser residue(s) involved in the phosphorylation event [Giacometti et al., 2012]. To understand the effect of CIPKs phosphorylation a very important thing that should be determined is the phosphorylation site of CIPK9 and CIPK14. With this aim we already tried to map the CIPKs phosphorylation site using single point mutant peptides corresponding to ^{1}M-I^{116} region, in which each of the six Ser residues involved in phosphorylation were mutated to Ala, for *in vitro* phosphorylation assays with both CIPK9 and CIPK14. Unfortunately the outcome of these experiments was not clear, probably as a result of phosphorylation on more than three Ser residues. Indeed, if the number of Ser residues subjected to phosphorylation is high, the difference between the level of phosphorylation of the WT and the level of phosphorylation of every single mutant peptide is too low to be clearly detected. Since this approach didn't allow us to map the phosphorylation site, to circumvent the problem we decided to subject the WT ACA8 N-terminus peptide to mass spectrometry analysis, after *in vitro* extensive phosphorylation. The set-up of the conditions to obtain an extensive *in vitro* phosphorylation is still in progress.

It has been demonstrated for CIPK1, CIPK23 and CIPK24 that CBLs have a role not only in targeting the kinase on the appropriate subcellular compartment [Batistič et al., 2010] but also in stimulating the kinase activity [Hashimoto et al., 2012]. According to these data would be very interesting to determine if the activity of CIPK9 and CIPK14 on ACA8 N-terminus could be stimulated by CBL1, a PM CBL which we showed to be able to interact with both kinases in BiFC experiments. With this aim we are performing *in vitro* phosphorylation experiments using of ACA8 N-terminus CIPK9 and CIPK14 in presence of CBL1.

References

Batistič O, Waadt R, Steinhorst L, Held K, and Kudla J (2010). CBL-mediated targeting of CIPKs facilitates the decoding of calcium signals emanating from distinct cellular stores. Plant Journal; **61**: 211–222.

Batistič O, Sorek N, Schültke S, Yalovsky S, Kudla J (2008). Dual fatty acyl modification determines the localization and plasma membrane targeting of CBL/CIPK Ca^{2+} signalling complexes in *Arabidopsis*. Plant Cell; **20(5)**:1346-62.

Benschop JJ, Mohammed S, O'Flaherty M, Heck AJR, Slijper M, Menke FLH (2007). Quantitative phosphoproteomics of early elicitor signalling in *Arabidopsis*. Molecular and Cellular Proteomics; **6**: 1198–1214.

Bonza MC and De Michelis MI (2011). The plant Ca^{2+}-ATPase repertoire: biochemical features and physiological functions. Plant Biology; **13**: 421–430.

Bonza, MC, Morandini P, Luoni L, Geisler M, Palmgren MG, De Michelis MI (2000). *At*-ACA8 encodes a plasma membrane-localized calcium-ATPase of *Arabidopsis* with a calmodulin-binding domain at the N terminus. Plant Physiol; **123**: 1495-1505.

Cerana M, Bonza MC, Harris R, Sanders D, De Michelis MI (2006). Abscisic acid stimulates the expression of two isoforms of plasma membrane Ca^{2+}-ATPase in *Arabidopsis thaliana* seedlings. Plant Biology; **8**: 572-578.

Chen Y, Hoehenwarter W, Weckwerth W (2010). Comparative analysis of phytohormone-responsive phosphoproteins in *Arabidopsis thaliana* using TiO2-phosphopeptide enrichment and mass accuracy precursor alignment. Plant Journal; **63**: 1–17.

Cunningham KW, and Fink GR (1994). Calcineurin-dependent growth control in *Saccharomyces cerevisiae* mutant lacking PMC1, a homolog of plasma membrane Ca^{2+}-ATPases. Journal of Cell Biology; **124**: 351-363.

D'Angelo C, Weinl S, Batistič O, Pandey GK, Cheong YH, Schültke S, Albrecht V, Ehlert B, Schulz B, Harter K, Luan S, Bock R, and Kudla J (2006). Alternative complex formation of the Ca^{2+}-regulated protein kinase CIPK1 controls abscisic acid-dependent and –independent stress responses in *Arabidopsis*. Plant Journal; **48**: 857–872.

Giacometti S, Marrano CA, Bonza MC, Luoni L, Limonta M and De Michelis MI (2012) Phosphorylation of serine residues in the N-terminus modulates the activity of ACA8, a plasma membrane Ca^{2+}-ATPase of *Arabidopsis thaliana*. Journal of Experimental Botany; **63**: 1215–1224.

Harthill JE, Meek SE, Morrice N, Peggie MW, Borch J, Wong BH, Mackintosh C (2006). Phosphorylation and 14-3-3 binding of *Arabidopsis* trehalose-phosphate synthase 5 in response to 2-deoxyglucose. Plant Journal; **47(2)**:211-23.

Hashimoto K, Eckert C, Anshütz U, Scholz M, Held K, Waadt R, Reyer A, Hippler M, Becker D, Kudla J (2012). Phosphorylation of calcineurin B-like (CBL) calcium sensor proteins by their CBL-interacting protein kinases (CIPKs) is required for full activity of CBL-CIPK complexes toward their target proteins. The Journal of Biological Chemistry; **287**: 7956-7968.

Hashimoto K and Kudla J (2011). Calcium decoding mechanism in plants. Biochimie; **93**: 2054-2059.

Jones AME, MacLean D, Studholme DJ, Sanz A, Andreasson E, Rathjen JP, Peck SC (2009). Phosphoproteomic analysis of nucleienriched fractions from *Arabidopsis thaliana*. Journal of Proteomics; **72**: 439–451.

Kudla J, Batistič O, Hashimoto K (2010). Calcium signals: the lead currency of plant information processing. Plant Cell; **22**: 541-63.

Lu CA, Lin CC, Lee KW, Chen JL, Huang LF, Ho SL, Liu HJ, Hsing YI and Su-May Yu (2007). The SnRK1A protein kinase plays a key role in sugar signaling during germination and seedling growth of rice. The Plant Cell; **19**: 2484–2499

Luoni L, Meneghelli S, Bonza MC, and De Michelis MI (2004). Auto-inhibition of *Arabidopsis thaliana* plasma membrane Ca^{2+}-ATPase involves an interaction of the N-terminus with the small cytoplasmic loop. FEBS Letters; **574**: 20-24.

McAinsh MR and Pittman JK (2009). Shaping the calcium signature. New Phytology; **181 (2)**: 275-294.

Meneghelli S, Fusca T, Luoni L, De Michelis MI (2008). Dual mechanism of activation of plant plasma membrane Ca^{2+}-ATPase by acidic phospholipids: evidence for a phospholipid binding site which overlaps the calmodulin-binding site. Molecular Membrane Biology; **25**:539-46.

Nakagami H, Sugiyama N, Mochida K, Daudi A, Yoshida Y, Toyoda T, Tomita M, Ishihama Y and Shirasu K (2010). Large-scale comparative phosphoproteomics identifies conserved phosphorylation sites in plants. Plant Physiology; **153**: 1161–1174.

Niittylä T, Fuglsang AT, Palmgren MG, Frommer WB and Schulze WX (2007). Temporal analysis of sucrose-induced phosphorylation changes in plasma membrane proteins of *Arabidopsis*. Molecular Cell Proteomics; **6 (10)**: 1711-1726.

Nühse TS, Bottrill A, Jones AME and Peck SC (2007). Quantitative phosphoproteomics analysis of plasma membrane proteins reveals regulatory mechanisms of plant innate immune responses. Plant Journal; **51**: 931–940.

Nühse TS, Stensballe A, Jensen ON, Peck SC (2004). Phosphoproteomics of the *Arabidopsis* plasma membrane and a new phosphorylation site database. Plant Cell; **16**: 2394–2405.

Nühse TS, Stensballe A, Jensen ON and Peck SC (2003). Large-scale analysis of in vivo phosphorylated membrane proteins by immobilized metal ion affinity chromatography and mass spectrometry. Molecular and Cellular Proteomics; **2**: 1234–1243.

Pandey GK, Cheong YH, Kim B, Grant JJ, Li L and Luan S (2007). CIPK9: a calcium sensor-interacting protein kinase required for low-potassium tolerance in *Arabidopsis*. Cell Research; **17**:411-421.

Polge C and Thomas M (2006). SNF1/AMPK/SnRK1 kinases, global regulators at the heart of energy control? Trends in Plant Science; **12(1)**: 20-28.

Reiland S, Messerli G, Baerenfaller K, Gerrits B, Endler A, Grossman J, Gruissem W and Baginsky S (2009). Large scale *Arabidopsis* phosphoproteomic profiling reveals novel choloroplast kinase substrates and phosphorylation networks. Plant Physiology; **150**: 889–903.

Romani G, Bonza MC, Filippini I, Cerana M, Beffagna N and De Michelis M.I. (2004). Involvement of the plasma membrane Ca^{2+}-ATPase in the short term response of *Arabidopsis thaliana* cultured cells to oligogalacturonides. Plant Biology; **6**:192-200.

Sanders D, Brownlee C and Harper JF (1999). Communicating with calcium. Plant Cell; **11**: 691-706.

Sanders D, Pelloux J, Brownlee C and Harper JF (2002). Calcium at the crossroads of signaling. Plant Cell; supplement: 401-417.

Schiǿtt M and Palmgren MG (2005). Two plant Ca^{2+} pump expressed in stomatal guard cells show opposite expression patterns during cold stress. Physiologia Plantarum; **124**: 278-283.

Spalding EP and Harper JF (2011) The ins and outs of cellular Ca^{2+} transport. Current Opininion in Plant Biology; **14**:715-20.

Sugiyama N, Nakagami H, Mochida K, Daudi A, Tomita M, Shirasu K and Ishihama Y(2008). Large-scale phosphorylation mapping reveals the extent of tyrosine phosphorylation in *Arabidopsis*. Molecular Systems Biology; **4**: article 193.

Waadt R, Schmidt LK, Lohse M, Hashimoto K, Bock R and Kudla J (2008). Multicolor bimolecular fluorescence complementation reveals simultaneous formation of alternative CBL-CIPK complexes *in planta*. Plant Journal; **56**: 505–516.

Whiteman S, Serazetdinova L, Jones AME, Sanders D, Rathjen J, Peck SC, Maathuis FJM (2008). Identification of novel proteins and phosphorylation sites in a tonoplast enriched membrane fraction of *Arabidopsis thaliana*. Proteomics; **8**: 3536–3547.